

8-2010

## Volumetric Modulated Arc Therapy Evaluation with the Radiological Physics Center Head and Neck Phantom

Kelly Kisling

Follow this and additional works at: [https://digitalcommons.library.tmc.edu/utgsbs\\_dissertations](https://digitalcommons.library.tmc.edu/utgsbs_dissertations)



Part of the [Medical Biophysics Commons](#)

---

### Recommended Citation

Kisling, Kelly, "Volumetric Modulated Arc Therapy Evaluation with the Radiological Physics Center Head and Neck Phantom" (2010). *The University of Texas MD Anderson Cancer Center UTHealth Graduate School of Biomedical Sciences Dissertations and Theses (Open Access)*. 70.  
[https://digitalcommons.library.tmc.edu/utgsbs\\_dissertations/70](https://digitalcommons.library.tmc.edu/utgsbs_dissertations/70)

This Thesis (MS) is brought to you for free and open access by the The University of Texas MD Anderson Cancer Center UTHealth Graduate School of Biomedical Sciences at DigitalCommons@TMC. It has been accepted for inclusion in The University of Texas MD Anderson Cancer Center UTHealth Graduate School of Biomedical Sciences Dissertations and Theses (Open Access) by an authorized administrator of DigitalCommons@TMC. For more information, please contact [digitalcommons@library.tmc.edu](mailto:digitalcommons@library.tmc.edu).

VOLUMETRIC MODULATED ARC THERAPY EVALUATION WITH THE RADIOLOGICAL  
PHYSICS CENTER HEAD AND NECK PHANTOM

by

Kelly D. Kisling, B.S.

APPROVED:

---

Rebecca Howell, Ph.D.  
Supervisory Professor

---

David Followill, Ph.D.

---

Geoffrey Ibbott, Ph.D.

---

Stephen Kry, Ph.D.

---

R. Allen White, Ph.D.

---

APPROVED:

---

Dean, The University of Texas  
Health Science Center at Houston  
Graduate School of Biomedical Sciences

VOLUMETRIC MODULATED ARC THERAPY EVALUATION WITH THE RADIOLOGICAL  
PHYSICS CENTER HEAD AND NECK PHANTOM

A  
THESIS

Presented to the Faculty of  
The University of Texas  
Health Science Center at Houston  
Graduate School of Biomedical Sciences  
and  
The University of Texas  
M. D. Anderson Cancer Center

in Partial Fulfillment

of the Requirements

for the Degree of

MASTER OF SCIENCE

by

Kelly D. Kisling, B.S.  
Houston, Texas

August 2010

## Acknowledgements

I would like to thank my advisor, Dr. Howell, for giving me guidance and great advice throughout this project and my graduate career. Also, I would like to thank my committee members for giving me direction and support: Dr. David Followill, Dr. Geoff Ibbott, Dr. Stephen Kry, and Dr. R. Allen White.

I would also like to acknowledge many other people who contributed to this project. The people at the RPC who were always there to help, including Carrie Amador, Paolo Alvarez, Nadia Hernandez, Andrea Molineu, the RPC students, and many others. Special thanks to Huy Duong at the RPC for sticking with me through a few dilemmas. Also, my fellow students and group members deserve thanks for helping me through school and this project: Sharmalee Randeniya, Laura Rechner, Sarah Scarboro, and Derek Yaldo.

I would also like to thank Dr. Jonas Fontenot at Mary Bird Perkins Cancer Center in Baton Rouge, LA, where part of my project was completed. I appreciate his willingness to take me under his wing and treat me just like one of his own graduate students.

Lastly, I would like to thank my family and friends: my parents, Doug and Karrie, my sisters, Amy and Kate, and Chris Malcolm. They were always interested in my research and asked about it despite not knowing what I was talking about. I also must thank them for giving me inspiration and encouragement and being fantastic role models. Without them, I could never be the person I am today.

VOLUMETRIC MODULATED ARC THERAPY EVALUATION WITH THE RADIOLOGICAL  
PHYSICS CENTER HEAD AND NECK PHANTOM

Publication No. \_\_\_\_\_

Kelly D. Kisling, B.S.  
Supervisory Professor: Rebecca Howell, Ph.D.

Validation of treatment plan quality and dose calculation accuracy is essential for new radiotherapy techniques, including volumetric modulated arc therapy (VMAT). VMAT delivers intensity modulated radiotherapy treatments while simultaneously rotating the gantry, adding an additional level of complexity to both the dose calculation and delivery of VMAT treatments compared to static gantry IMRT. The purpose of this project was to compare two VMAT systems, Elekta VMAT and Varian RapidArc, to the current standard of care, IMRT, in terms of both treatment plan quality and dosimetric delivery accuracy using the Radiological Physics Center (RPC) head and neck (H&N) phantom. Clinically relevant treatment plans were created for the phantom using typical prescription and dose constraints for Elekta VMAT (planned with Pinnacle<sup>3</sup> Smart Arc) and RapidArc and IMRT (both planned with Eclipse). The treatment plans were evaluated to determine if they were clinically comparable using several dosimetric criteria, including ability to meet dose objectives, hot spots, conformity index, and homogeneity index. The planned treatments were delivered to the phantom and absolute doses and relative dose distributions were measured with thermoluminescent dosimeters (TLDs) and radiochromic film, respectively. The measured and calculated doses of each treatment were compared to determine if they were clinically acceptable based upon RPC criteria of  $\pm 7\%$  dose difference and 4 mm distance-to-agreement. Gamma analysis was used to assess dosimetric accuracy, as well. All treatment plans were able to meet the dosimetric objectives set by the RPC and had similar hot spots in the normal tissue. The Elekta VMAT plan was more homogenous but less conformal than the RapidArc and IMRT plans. When comparing the measured and calculated doses, all plans met the RPC  $\pm 7\%/4$  mm criteria. The percent of points passing the gamma analysis for each

treatment delivery was acceptable. Treatment plan quality of the Elekta VMAT, RapidArc and IMRT treatments were comparable for consistent dose prescriptions and constraints. Additionally, the dosimetric accuracy of the Elekta VMAT and RapidArc treatments was verified to be within acceptable tolerances.

# TABLE OF CONTENTS

CHAPTER 1	INTRODUCTION .....	1
1.1	Statement of Problem .....	1
1.2	The Radiological Physics Center and Anthropomorphic QA Phantoms .....	7
1.3	Hypothesis and Specific Aims.....	9
CHAPTER 2	METHODS AND MATERIALS .....	10
2.1	VMAT Techniques Evaluated in This Study .....	10
2.1.1	<i>Elekta VMAT Planned with Pinnacle SmartArc.....</i>	<i>10</i>
2.1.2	<i>Varian RapidArc.....</i>	<i>11</i>
2.2	The RPC Anthropomorphic IMRT Head and Neck Phantom .....	13
2.3	Treatment Planning .....	15
2.3.1	<i>Phantom Imaging .....</i>	<i>15</i>
2.3.2	<i>Dose Prescription and Constraints .....</i>	<i>16</i>
2.3.3	<i>Volume Delineation.....</i>	<i>17</i>
2.3.4	<i>Treatment Plans.....</i>	<i>17</i>
2.4	Treatment Plan Quality Comparison .....	19
2.5	Dosimetric Accuracy Evaluation.....	20
2.5.1	<i>Phantom Irradiation.....</i>	<i>20</i>
2.5.2	<i>Dosimeters.....</i>	<i>23</i>
2.5.3	<i>Absolute Point Dose Analysis.....</i>	<i>28</i>
2.5.4	<i>Film, Plan, and Phantom Registration.....</i>	<i>29</i>
2.5.5	<i>Planar Dose Analysis .....</i>	<i>30</i>
2.5.6	<i>MLC Log File Analysis.....</i>	<i>34</i>
CHAPTER 3	RESULTS.....	35

3.1	Treatment Plan Quality Comparison .....	35
3.2	Dosimetric Accuracy Evaluation.....	38
3.2.1	<i>Absolute Point Dose Analysis</i> .....	38
3.2.2	<i>Planar Dose Analysis</i> .....	46
3.2.3	<i>MLC Log File Analysis</i> .....	62
CHAPTER 4	DISCUSSION.....	64
4.1	General Discussion.....	64
4.2	Conclusion.....	69
4.3	Future Work .....	69
CHAPTER 5	APPENDIX .....	71
5.1	Treatment Plan Isodose Distributions.....	71
5.2	Dose profiles.....	74
5.3	Gamma analysis.....	80
5.4	MLC Log File Results .....	98
CHAPTER 6	BIBLIOGRAPHY .....	100
VITA	.....	102



# LIST OF ILLUSTRATIONS

Figure 2-1 RPC IMRT head and neck phantom with dosimetry insert removed .....	13
Figure 2-2 Picture (left) and axial CT image (right) of phantom insert with the anterior edge on top	14
Figure 2-3 Contoured structures in Eclipse: primary PTV (blue), secondary PTV (yellow), and OAR (red) .....	17
Figure 2-4 Couch structure (purple) inserted for the IMRT and RapidArc plans .....	17
Figure 2-5 Beam angles entering body in 3D view of nine field IMRT treatment plan.....	18
Figure 2-6 Photograph of phantom on treatment table of the Varian Clinac iX linear accelerator .....	21
Figure 2-7 Setup of the RPC machine output check involving irradiating two TLD in a Lucite block mini-phantom .....	22
Figure 2-8 Dose response curve for the batch of EBT2 film used in this study.....	28
Figure 2-9 Area in axial plane where gamma analysis was performed with 5% dose difference and 3 mm DTA criteria .....	31
Figure 2-10 Area in sagittal plane where gamma analysis was performed with 5% dose difference and 3 mm DTA criteria .....	31
Figure 2-11 Area in axial plane where gamma analysis was performed with 7% dose difference and 4 mm DTA criteria .....	32
Figure 3-1 DVHs of the primary PTV (blue), secondary PTV (green), OAR (red), and normal tissue (brown) for the Elekta VMAT (solid), RapidArc (dotted), and IMRT (dashed) treatment plans .....	36
Figure 3-2 Lateral dose profile of the Elekta VMAT treatment.....	47
Figure 3-3 Lateral profile of the RapidArc treatment.....	48
Figure 3-4 Lateral dose profile of the IMRT treatment.....	49
Figure 3-5 Axial gamma analysis (5%/3mm) of third Elekta VMAT treatment delivery.....	52
Figure 3-6 Sagittal gamma analysis (5%/3mm) of third Elekta VMAT treatment delivery .....	53
Figure 3-7 Axial gamma analysis (5%/3mm) of first RapidArc treatment delivery .....	54

Figure 3-8 Sagittal gamma analysis (5%/3mm) of first RapidArc treatment delivery .....	55
Figure 3-9 Axial gamma analysis (5%/3mm) of second IMRT treatment delivery .....	56
Figure 3-10 Sagittal gamma analysis (5%/3mm) of second IMRT treatment delivery .....	57
Figure 3-11 Axial gamma analysis (7%/4mm) of third Elekta VMAT treatment delivery .....	59
Figure 3-12 Axial gamma analysis (7%/4mm) of first RapidArc treatment delivery .....	60
Figure 3-13 Axial gamma analysis (7%/4mm) of third IMRT treatment delivery .....	61
Figure 5-1 Isodose distribution of the Elekta VMAT treatment plan .....	71
Figure 5-2 Isodose distribution of the RapidArc treatment plan .....	72
Figure 5-3 Isodose distribution of the IMRT treatment plan .....	73
Figure 5-4 Posterior-to-anterior dose profile of the Elekta VMAT treatment .....	74
Figure 5-5 Inferior-to-superior dose profile of the Elekta VMAT treatment .....	75
Figure 5-6 Posterior-to-anterior dose profile of the RapidArc treatment .....	76
Figure 5-7 Inferior-to-superior dose profile of the RapidArc treatment .....	77
Figure 5-8 Posterior-to-anterior dose profile of the IMRT treatment .....	78
Figure 5-9 Inferior-to-superior dose profile of the IMRT treatment .....	79
Figure 5-10 Axial gamma analysis (5%/3mm) of first Elekta VMAT treatment delivery .....	80
Figure 5-11 Sagittal gamma analysis (5%/3mm) of first Elekta VMAT treatment delivery .....	81
Figure 5-12 Axial gamma analysis (5%/3mm) of second Elekta VMAT treatment delivery .....	82
Figure 5-13 Sagittal gamma analysis (5%/3mm) of second Elekta VMAT treatment delivery .....	83
Figure 5-14 Axial gamma analysis (5%/3mm) of second RapidArc treatment delivery .....	84
Figure 5-15 Sagittal gamma analysis (5%/3mm) of second RapidArc treatment delivery .....	85
Figure 5-16 Axial gamma analysis (5%/3mm) of third RapidArc treatment delivery .....	86
Figure 5-17 Sagittal gamma analysis (5%/3mm) of third RapidArc treatment delivery .....	87
Figure 5-18 Axial gamma analysis (5%/3mm) of first IMRT treatment delivery .....	88
Figure 5-19 Sagittal gamma analysis (5%/3mm) of first IMRT treatment delivery .....	89
Figure 5-20 Axial gamma analysis (5%/3mm) of third IMRT treatment delivery .....	90

Figure 5-21 Sagittal gamma analysis (5%/3mm) of third IMRT treatment delivery .....	91
Figure 5-22 Axial gamma analysis (7%/4mm) of first Elekta VMAT treatment delivery .....	92
Figure 5-23 Axial gamma analysis (7%/4mm) of second Elekta VMAT treatment delivery .....	93
Figure 5-24 Axial gamma analysis (7%/4mm) of second RapidArc treatment delivery.....	94
Figure 5-25 Axial gamma analysis (7%/4mm) of third RapidArc treatment delivery .....	95
Figure 5-26 Axial gamma analysis (7%/4mm) of first IMRT treatment delivery.....	96
Figure 5-27 Axial gamma analysis (7%/4mm) of second IMRT treatment delivery .....	97

## LIST OF TABLES

Table 2-1 Dimensions of structures in the phantom insert .....	14
Table 2-2 Dosimetric criteria set by the RPC and used for planning all treatments.....	16
Table 2-3 Irradiation of EBT2 film batch to generate a dose response curve for film calibration.....	27
Table 3-1 The values of each dosimetric objective for all three treatment plans, including prescriptions and dose constraints .....	35
Table 3-2 Maximum dose to the primary PTV, secondary PTV, OAR, and normal tissue structures with the percent of the prescription dose for each PTV shown in parenthesis .....	36
Table 3-3 Homogeneity indices (HI) of both PTVs calculated for all three treatment plans .....	37
Table 3-4 Doses measured by eight TLD in the phantom insert for three deliveries of the Elekta VMAT treatment .....	39
Table 3-5 Doses measured by eight TLD in the phantom insert for three deliveries of the RapidArc treatment .....	40
Table 3-6 Doses measured by eight TLD in the phantom insert for three deliveries of the IMRT treatment .....	41
Table 3-7 Treatment planning system calculation of the mean dose at eight TLD locations within the phantom insert .....	42
Table 3-8 Ratio of the measured TLD dose to the calculated TPS dose at eight locations in the phantom for three deliveries of the Elekta VMAT plan .....	43
Table 3-9 Ratio of the measured TLD dose to the calculated TPS dose at eight locations in the phantom for three deliveries of the RapidArc plan .....	44
Table 3-10 Ratio of the measured TLD dose to the calculated TPS dose at eight locations in the phantom for three deliveries of the IMRT plan .....	45
Table 3-11 Displacement (mm) of measurement from calculation of the posterior penumbra between the primary PTV and the OAR .....	50

Table 3-12 Percent of points passing gamma analysis with acceptability criteria of 5% dose difference and 3 mm DTA in the axial and sagittal planes bisecting the primary PTV .....	51
Table 3-13 Percent of points passing gamma analysis with acceptability criteria of 7% dose difference and 4 mm DTA in the axial plane bisecting the primary PTV .....	58
Table 3-14 The minimum, maximum, and range of the RMS values of leaf deviation (cm) for each moving leaf of both carriages for five deliveries of the first, clockwise arc of the RapidArc treatment .....	62
Table 3-15 The minimum, maximum, and range of the RMS values of leaf deviation (cm) for each moving leaf of both carriages for five deliveries of the second, counterclockwise arc of the RapidArc treatment.....	63
Table 5-1 The RMS values of leaf deviation (cm) for each moving leaf of both carriages for five deliveries of the first, clockwise arc of the RapidArc treatment .....	98
Table 5-2 The RMS values of leaf deviation (cm) for each moving leaf of both carriages for five deliveries of the second, counterclockwise arc of the RapidArc treatment.....	99

# Chapter 1 Introduction

## 1.1 Statement of Problem

Volume modulated arc therapy (VMAT) is a radiotherapy technique that delivers intensity modulated radiation therapy (IMRT) while simultaneously rotating the gantry. VMAT utilizes continuous gantry rotation, dynamic beam modulation, and variable dose rate to deliver conformal treatments.

VMAT evolved from a technique called intensity modulated arc therapy (IMAT), first proposed by Cedric Yu as an alternative to tomotherapy (1). IMAT was implemented on an existing linear accelerator (linac) and delivered treatments volumetrically, rather than slice by slice. Yu's technique used a multi-leaf collimator (MLC) to shape the beam dynamically while the gantry rotated and used multiple overlapping arcs. Each arc delivered one subfield of an intensity modulated treatment at each angle. IMAT was similar to the idea of step-and-shoot IMRT, which delivers two-dimensional intensity distributions from each static gantry position using several subfields. However, in IMAT, each subfield at a specific gantry angle would be delivered by separate arcs. The number of overlapping arcs depended on the complexity of the intensity distribution desired. Two to five arcs were typically required for clinical delivery of IMAT (2). Although Yu first proposed inverse planning for IMAT (1), forward planning was used for its actual implementation (2). During planning, arcs were approximated as multiple fixed fields at gantry angles separated by 5-10°. The plans mostly used three to five arcs and the final dose calculation approximated each arc as fixed fields at 10° gantry spacing.

Yu recognized that the forward planning techniques he implemented did not fully utilize the capabilities of IMAT to deliver conformal treatments. However, there were several challenges to developing effective planning and dose calculation techniques. Physical limitations of the linac,

including leaf travel speed, dose rate, and gantry rotation speed, complicated planning and affected the efficiency of treatments (1-3). Also, determining the optimal gantry spacing to approximate the arcs was a trade-off between optimization time, calculation time and accuracy (3).

In 2008, Karl Otto proposed the VMAT technique as a solution to the gantry angle sampling resolution problem for optimizations and dose calculations (3). A fine sampling improved the dose accuracy, but the limited MLC motion between small gantry angles restricted the optimization flexibility and increased the time of optimization. A coarser sampling allowed for greater MLC motion between gantry angles and, therefore, more freedom in the optimization, but provided a less accurate representation of the actual treatment. Otto's solution was to use an aperture-based optimization scheme in which sampling of gantry angle and MLC position was progressively increased. It began with a coarse sampling of static gantry positions and MLC aperture shapes and ended with a high resolution sampling to accurately model the dose delivered. MLC motion was more restricted as the number of samples increases, reducing the flexibility of the optimization, but increasing the accuracy of the dose calculation (3).

The concept of VMAT introduced by Otto led to the development of commercial VMAT treatment planning and delivery techniques, including Elekta VMAT (Elekta AB, Stockholm, Sweden), planning with Pinnacle<sup>3</sup> SmartArc (Philips Medical, Madison, WI), and Varian RapidArc™ with Eclipse treatment planning (Varian Medical Systems, Palo Alto, CA). To deliver conformal treatments, these VMAT techniques utilize continuously variable gantry position and speed, dose rate, and MLC aperture.

The VMAT techniques are marketed as delivering treatment plans equivalent to IMRT in a single arc while potentially requiring shorter treatment times and less monitor units (MU) than static gantry IMRT. For new techniques it is important for such claims be verified in practice prior to the technique's widespread use. The dose distributions achievable by VMAT techniques should be

compared to the standard of care for multiple treatment sites and geometries. Thorough comparisons of dose distributions achieved by treatments can help clinicians make decisions about patient radiotherapy treatments. If VMAT has plan quality that is equivalent to IMRT but with less MU and shorter treatment times, clinicians may choose VMAT to reduce the time a patient spends on the table and reduce the leakage radiation a patient receives as a result of fewer MU.

The claims about treatment delivery time and MU have been examined by several researchers. They have found that the treatment times for VMAT using one or two arcs are significantly reduced when compared to both 3D conformal and IMRT treatments (4-7). One study found that for head and neck cancers, one and two arc RapidArc treatments had an average reduction in MU of 59% from seven field sliding window IMRT (6). In this study, two arc treatments required 5% more MU than single arc treatments.

Plan quality of VMAT treatments has been compared with IMRT in several studies. In a planning study of twelve head and neck cancers, RapidArc one and two arc treatments were compared to seven field sliding window IMRT and was found to have similar sparing of organ at risk (OAR) (6). The homogeneity was best for two arc RapidArc and worst for single arc plans. These complex plans had two planning treatment volumes (PTV) treated to different prescriptions, a boost PTV and an elective PTV. In the boost PTV, the two arc RapidArc plan was significantly less conformal than IMRT. The authors concluded that two arc RapidArc treatment plans were similar to the IMRT dose distributions. It is important to note that in this study the versions of RapidArc planning used, preclinical Eclipse 8.2.16 and clinical Eclipse 8.2.22, did not allow simultaneous optimization of more than one arc, which is supported in current versions (6).

A different study compared RapidArc plans to IMRT for four virtual, water equivalent phantoms with variations of PTV and OARs (4). They found that RapidArc had better conformity and homogeneity and was better able to meet the plan objectives than five and nine field sliding



window IMRT. They also concluded that RapidArc plans with two arcs achieved better dose distributions than single arc plans (4).

Another planning study compared IMRT and Elekta VMAT planned with Pinnacle<sup>3</sup> SmartArc for six prostate and six head and neck patients (7). In this study, they concluded that the Elekta VMAT plans were comparable to IMRT in target coverage and critical structure sparing. The authors also noted that Elekta VMAT showed promise in complex head and neck cases (7).

Plan comparison studies are necessary to help clinicians determine which treatment techniques are best for specific treatment sites and geometries. However, the quality of treatment plans is subject to the abilities of the planner and the time spent on each plan. Thorough assessment of the treatment plans generated by a technique must be conducted by several planners in order to make clinicians fully aware of the quality of plans that VMAT techniques can achieve. We need more evidence that VMAT plans can be of comparable quality to IMRT, especially for more difficult, complex geometries, such as head and neck cancers, where there can be multiple, large treatment volumes with nearby critical structures. Additionally, no study has yet compared the various VMAT techniques directly to determine if the plan quality varies between the techniques.

In addition to studying the quality of dose distributions achieved by VMAT techniques in comparison with IMRT, the delivery accuracy of the dose calculated by treatment planning systems (TPS) has been investigated in several studies. For a new technique, verifying the accurate delivery of dose distributions is an important part of the quality assurance (QA) process prior to the technique's implementation. In one study, the accuracy of RapidArc dose calculation was evaluated by a Monte Carlo study of oropharynx radiotherapy (8). In this study, they compared Monte Carlo and the treatment planning calculation and determined that the accuracy of RapidArc dose calculation was adequate for clinical use when using a 2.5 mm dose grid.

Another study evaluated the accuracy of RapidArc dose delivery by patient specific verification for nine treatment plans for prostate and head and neck cancers (9). The plans were

delivered to a Scandidos Delta4® (Scandidos, Uppsala, Sweden), a cylindrical phantom with arrays of diodes, which was calibrated to an ionization chamber. The measured and calculated doses were compared using gamma analysis with 3% dose difference and 3 mm distance-to-agreement (DTA) criteria. They found that greater than 95% of the points passed in all cases and concluded that dose distributions delivered by RapidArc corresponded well with the planned treatments (9).

The accuracy of Elekta VMAT dose calculation for prostate and lung cancer plans was evaluated by measurements in a different study (5). One lung plan was delivered to a Delta4 phantom. Two prostate plans were delivered to a stack of Solid Water® (Gammex, Inc., Middleton, WI) and the dose was measured by an ionization chamber. One of the prostate plans was also delivered to the Delta4 phantom. For all tests, gamma analysis was used to evaluate dose delivery accuracy with 3% dose difference and 3 mm DTA criteria. For all treatments delivered to the Delta4 phantom, greater than 95% of the points passed. The dose measured by the ionization chamber in the Solid Water stack was less than 3% different from the calculated dose for both prostate treatments. The authors concluded that the measured and calculated dose distributions agreed well (5).

In another study the dose distributions of RapidArc plans for head and neck radiotherapy were measured in a QA phantom with GAFCHROMIC® EBT (International Specialty Products, Wayne, NJ) films in several coronal planes (6). The dose verification was evaluated using gamma analysis with 3% dose difference and 2 mm DTA criteria. For plans with one and two arcs, the average passing rate was greater than 97% and greater than 99%, respectively. In this study, one case compared single and two arc plans to IMRT and found that the two arc plan was the best with 99.1% of points passing. In comparison, IMRT had 96.4% passing. The authors noted that although EBT film provides good spatial resolution (0.3 mm), it is a less accurate and stable method of dosimetry than ionization chamber arrays. In conclusion, they determined that RapidArc treatments were accurately delivered (6).

The accurate delivery of calculated dose distributions was evaluated in another study for six prostate and six head and neck treatment plans created using Pinnacle<sup>3</sup> SmartArc for Elekta VMAT (7). The MatriXX<sup>TM</sup> 2D ionization chamber array in a MultiCube<sup>TM</sup> phantom (IBA Dosimetry Inc., Memphis, TN) was used for the plan QA. The gamma analysis was used to evaluate accuracy using a 3% dose difference and 3 mm DTA criteria. For the prostate and head and neck plans, the average passing rate was 98.9% and 98.3%, respectively. In comparison, the IMRT passing rates were 98.5% and 97.7%. The authors concluded that Elekta VMAT accurately delivered the planned treatments (7).

All of the dose delivery verifications have been similar to the type of dose verification employed for patient specific QA. Until now, no study has been conducted that uses a standardized and recognized method to verify that calculated doses are accurately delivered. Dose verification is necessary to assure physicists and clinicians of the accuracy with which patient treatments are delivered. This is especially important for complex treatments, such as in head and neck cancers, where conformal treatments need substantial intensity modulation to generate steep dose gradients.

In this project, we evaluated the plan quality of two VMAT techniques, Elekta VMAT planned with Pinnacle<sup>3</sup> SmartArc and Varian RapidArc, for a complex head and neck phantom radiotherapy treatment and compared the treatment plans to the current standard of care, IMRT. Additionally, the delivery accuracy of the calculated doses was evaluated using the protocol established by the Radiological Physics Center (RPC) for head and neck IMRT. This standardized protocol is used by the Radiation Therapy Oncology Group to credential institutions participating in clinical trials.

## **1.2 The Radiological Physics Center and Anthropomorphic QA Phantoms**

The Radiological Physics Center (RPC) was founded in 1968 as a National Cancer Institute (NCI) funded group with the mission to ensure that “institutions participating in clinical trials deliver prescribed radiation doses that are clinically comparable and consistent” (10). In multi-clinic studies, it is essential that radiation therapies delivered across all participating clinics are similar and that results are not skewed because of dosimetric differences between clinics. The RPC monitors the participating institutions by performing quality reviews through its on-site dosimetry review visits and off-site remote auditing techniques. The off-site auditing program includes:

- A mailable TLD program to verify machine output
- Comparison of the institutions’ dosimetry data with RPC standard dosimetry data
- Evaluation of reference or actual patient calculations to verify treatment planning algorithms
- Review of the institutions’ written QA procedures and records
- Mailed anthropomorphic phantoms to verify tumor dose delivery for special advanced treatment techniques such as IMRT, stereotactic radiosurgery, etc.
- Credentialing of institutions for participation in specific protocols
- Retrospective review of treatment records for patients entered into cooperative clinical trials.

The purpose of the anthropomorphic phantom audit process is to assess an institution’s ability to image the phantom, develop a specific treatment plan, and deliver the dose according to specific protocol guidelines or instructions. The phantom is treated as if it were an actual patient. The RPC currently has five anthropomorphic phantoms, a stereotactic radiosurgery head phantom, an IMRT head-and-neck phantom, a thorax phantom, a liver phantom, and a pelvic phantom. The basic design of each phantom is similar and consists of an outer plastic shell in the appropriate anatomical

shape. The shell is filled with water to represent soft tissue and has a compartment that houses the imageable targets and organs at risk where dosimeters are located. Radiochromic film and TLD are used for relative and absolute dose measurements, respectively. The films are located in two major planes and the TLD is used to normalize the film readings as well as measure the dose at a point. Once the phantom has been irradiated, it is returned to the RPC where the dosimeters are analyzed and compared to the institution's treatment planning system's dose calculations.

These phantoms are mailed to institutions that participate in cooperative clinical trials as a means to remotely evaluate their ability to plan and deliver dose within specific protocol criteria for field localization and dose delivery to targets and critical structures. Some radiation therapy clinics may be replacing IMRT with VMAT for certain treatment sites. In order to allow VMAT users in RTOG clinical trials involving IMRT, the RPC must ensure that VMAT treatments can deliver clinically comparable treatments to IMRT.

### **1.3 Hypothesis and Specific Aims**

We hypothesized that VMAT techniques generate treatment plans of comparable quality to IMRT and accurately deliver the calculated dose for complex head and neck treatments.

The hypothesis was tested by the following specific aims:

- 1) We created clinically relevant treatment plans for the RPC IMRT head and neck phantom from typical prescription and dose constraints for 1) Elekta VMAT planned with Pinnacle<sup>3</sup> SmartArc, 2) Varian RapidArc and 3) 6 MV IMRT.
- 2) We evaluated the plan quality of the two VMAT and one IMRT head and neck treatment plans to determine if they were clinically comparable.
- 3) We delivered the three planned treatments to the head and neck phantom and measured the dose distribution from each.
- 4) We compared the measured and calculated doses using clinically acceptable criteria of  $\pm 5\%$  dose difference and 3 mm DTA.

## Chapter 2 Methods and Materials

### 2.1 VMAT Techniques Evaluated in This Study

#### 2.1.1 Elekta VMAT Planned with Pinnacle SmartArc

The first VMAT technique evaluated in this study was a treatment plan generated using the SmartArc module in Pinnacle version 9 (Philips Medical, Madison, WI) and delivered using an Elekta Synergy linac (Elekta AB, Stockholm, Sweden). Pinnacle's VMAT treatment planning is based on work by Bzdusek, et al (11). It uses an inverse-planning approach based on dose-volume objectives that generates treatment plans with dynamic MLC and variable dose rate and gantry rotation speeds. The optimization takes into account the machine constraints in order to develop a deliverable plan.

First, the user sets up the arcs for optimization and inputs parameters such as arc length, collimator and couch angle, maximum arc delivery time, and final gantry spacing. Additionally, the TPS can generate additional arcs to be optimized simultaneously using the same parameters as the initial arc, but with opposite rotation direction. This is known as the dual arc feature. The initial optimization step generates fluence maps at a coarse resolution of  $24^\circ$  around each arc. Once this optimization has converged, each fluence map is converted to two to four MLC segments, depending on the extent of intensity modulation. Of these segments, the two with the most open leaf pairs are kept per initial angle. These segments are redistributed evenly around the arc. The MLC segments are now located every  $8^\circ$ . If the dual arc feature is employed, five MLC segments are generated per initial angle and two are kept per arc. In this case, the MLC segments are distributed in a manner that reduces leaf travel in each arc.

The next optimization step uses Pinnacle's Direct Machine Parameter Optimization (DMPO) on the existing control points. The MU and leaf positions for each control point and arc delivery time

are all variables included in the optimization. These variables are limited by the machine and user specified constraints, such as maximum and minimum dose rate and gantry rotation speed, maximum leaf speed, and maximum arc delivery time.

To improve the accuracy of the dose calculation during DMPO, the arc sampling resolution is reduced to the final gantry spacing by linearly interpolating leaf segments between the existing control points. The typical final gantry spacing is  $4^\circ$ , resulting in 91 control points. The interpolated control points are only used to improve the dose calculation accuracy and are not included in the DMPO. During optimization the dose is calculated using the Singular Value Decomposition (SVD) dose engine, a fast pencil beam algorithm that accounts for tissue heterogeneities in the primary beam. Once the machine parameters have been optimized, the jaw positions are determined.

The final dose is calculated using a convolution/superposition algorithm, either Adaptive Convolve or Collapsed-Cone Convolution, and each arc is approximated as 91 control points, assuming the typical final gantry spacing of  $4^\circ$  was selected by the user. In this study, we used the Adaptive Convolve dose calculation algorithm in Pinnacle. In flat areas, the dose grid is sampled at every fourth point and the dose in between is interpolated. The algorithm will switch to a full sampling if the dose grid cannot be interpolated accurately. The convolution/superposition algorithms in Pinnacle model the primary energy fluence and the head scatter and adjust for heterogeneities.

The control point information of the treatment plan, including MU and MLC aperture, is then transferred to the treatment machine. The control system of the linac, an Elekta Synergy in our study, determines the dose rate and gantry speed based on the plan information.

### **2.1.2**    *Varian RapidArc*

The second VMAT technique evaluated in this study was RapidArc, which was planned in Eclipse version 8.6 and delivered on a Varian Clinac iX linac (Varian Medical Systems, Palo Alto,



CA). Varian developed RapidArc based on the work of Otto and his novel optimization scheme, which Varian has termed their Progressive Resolution Optimizer (PRO) algorithm (3). Like Pinnacle's algorithm, it uses dose-volume objectives for an inverse-planning approach. The final plans have dynamic MLC, variable dose rate and variable gantry rotation speeds. The final dose is calculated using the Anisotropic Analytical Algorithm (AAA).

After the user has setup up the basic arc parameters, including arc length and collimator angle, the PRO begins optimizing each arc by modeling it as a small number of equally-spaced static control points with the same initial dose rate and MLC aperture conforming to the target shape. Then, the MLC aperture and dose rates are varied iteratively and the dose is calculated at each iteration point. The dose is calculated by first determining the fluence from the MLC aperture and dose rate and then converting it to dose using Eclipse's Multi-Resolution Dose Calculation (MRDC) algorithm, a fast convolution superposition algorithm that corrects for heterogeneities for the primary dose component. A cost function based on the dose-volume objectives set is used to determine if each variation should be kept. The algorithm then steps through various stages of resolution in which it adds control points to each arc progressively and continues to optimize all MLC shapes and dose rates. The final resolution level finishes with 177 control points per arc, which leads to control points approximately every  $2^{\circ}$  for a  $360^{\circ}$  arc.

Once the optimization has finished, Eclipse uses the AAA to calculate dose, with each arc approximated as 177 static control points. AAA models the treatment beam as beamlets of multiple sources: the primary photons generated in head and secondary sources scattered from the linac head, including the extra-focal photons and the contaminating electrons. The AAA dose engine also accounts for tissue heterogeneities.

## 2.2 The RPC Anthropomorphic IMRT Head and Neck Phantom

The phantom used throughout this study was an anthropomorphic head and neck phantom designed and constructed by the RPC for credentialing of institutions participating in RTOG head and neck protocols involving IMRT. The phantom, shown in Figure 2-1, was designed to mimic the geometry of this treatment site and to hold radiation dosimeters for measuring the dose delivered to the phantom. The phantom was constructed of materials that are tissue-equivalent.

The phantom consists of a plastic outer shell shaped like a human head and neck. The water-tight shell is hollow except for a polystyrene insert and can be filled with water to simulate the human tissue surrounding the insert (12). There are plugs in the bottom of the phantom through which water can be filled and drained from the phantom.

The removable dosimetry insert, seen next to the phantom in Figure 2-1, contains the treatment volumes and places to insert radiation dosimeters. It is 13 cm in height, 10.5 cm wide, and 7.5 cm long (12). The dosimetry insert has two halves that can be separated for the insertion and removal of dosimeters. Figure 2-2

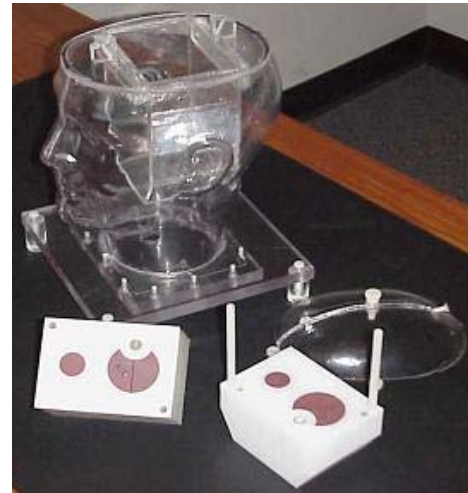


**Figure 2-1 RPC IMRT head and neck phantom with dosimetry insert removed**

shows the superior half of the insert next to an axial CT image of a cross-section of the insert. The structures simulated in the insert are indicated in Figure 2-2 and include two solid water PTVs and an acrylic OAR representing the spinal cord. The primary PTV represents an oropharyngeal tumor and the secondary PTV represents the peripheral nodes. The densities of the materials in the insert are sufficiently different so they are readily visualized on CT images without having a significant effect on the treatment fields. The difference in atomic number of the materials is also insignificant for treatment. The secondary PTV and OAR are cylinders with their axes in the superior-inferior

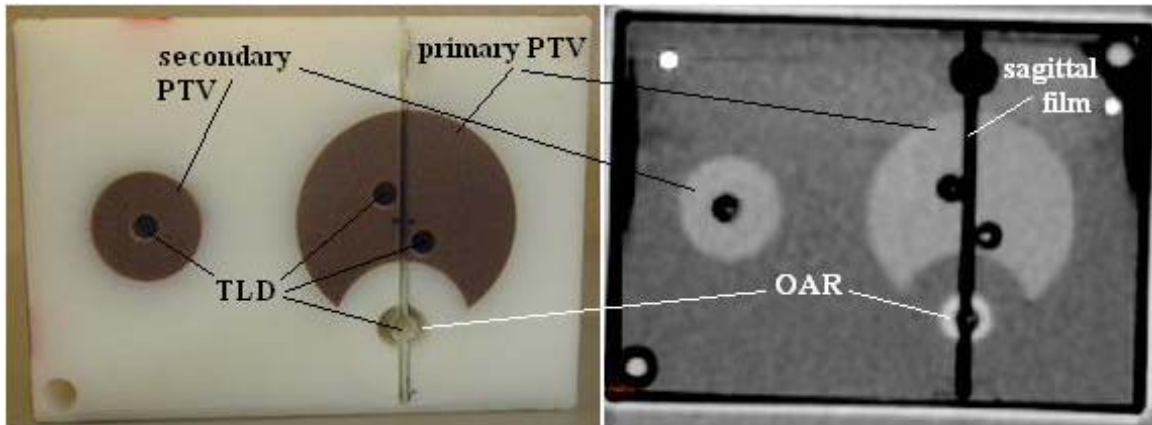


**Figure 2-2 Picture (left) and axial CT image (right) of phantom insert with the anterior edge on top**

direction and the dimensions shown in Table 2-1 (12). The primary PTV is in the shape of a cylinder oriented in the same direction as the other structures, but with a portion cut out on its posterior side where it wraps around the abutting OAR volume.

**Table 2-1 Dimensions of structures in the phantom insert**

Structure	Diameter (cm)	Length (cm)
Primary PTV	4	5
Secondary PTV	2	5
Organ at risk	1	13

As shown in Figure 2-2, the inner side of each insert half has four holes drilled for holding thermoluminescent dosimeter (TLD) capsules to measure absolute dose in eight locations. The TLD capsules are placed in pairs, with one TLD in the superior half of the insert and another in the same location in the inferior half. There are two pairs of TLD in the primary PTV offset from the center (a posterior and an anterior pair) and a pair in the center of both the secondary PTV and the OAR.

There are three radiochromic films placed in the insert to measure the dose distribution in the axial and sagittal planes. There is one film in the axial plane where the two halves of the insert meet and two films in the sagittal plane bisecting the primary PTV, one in each half of the insert. The gap

for the sagittal film in the superior half of the insert is shown in Figure 2-2. The sagittal films have a cutout where the TLDs in the OAR are located.

On the axial face of the inferior insert, pins are located in three of the corners to poke holes in the film. Additionally, there are five tiny holes drilled in the outer left side of the insert through which a small tool can be inserted to pierce the sagittal films. The holes left by piercing the film are useful for registering the film to the treatment plan later. More details are provided in section 2.5.4 Film, Plan, and Phantom Registration for more details about film and treatment plan registration.

## **2.3 Treatment Planning**

To determine if the two VMAT techniques evaluated in this study were clinically comparable to IMRT for head and neck radiotherapy, we created clinically relevant treatment plans for the RPC IMRT head and neck phantom from common prescription and dose constraints for each technique evaluated in this study: Elekta VMAT planned with Pinnacle<sup>3</sup> SmartArc, Varian RapidArc and 6 MV IMRT.

### **2.3.1 Phantom Imaging**

We performed a CT simulation of the phantom to acquire images of the phantom for treatment planning. We positioned the phantom supine and “head-first” on the table and used the lasers to place external radiopaque markers on the phantom. Next, we placed masking tape where the lasers crossed on the left and right sides and face of the phantom and drew crosshairs to mark the treatment isocenter. We then took a scout image of the phantom and set the scan extent to include enough margin superior and inferior of the phantom insert to include the effects of scatter in the dose calculation.

For the Elekta VMAT treatments, we simulated the phantom using a GE LightSpeed® RT 16-slice CT scanner (GE Healthcare, Waukesha, WI). The CT simulation used the parameters

specified by the protocol for a stereotactic head and neck patient at Mary Bird Perkins Cancer Center. The protocol generated 1.25 mm thick images. CT data were imported into the Pinnacle<sup>3</sup> TPS for the Elekta VMAT treatment planning.

For the IMRT and RapidArc treatments, we simulated the phantom using a Philips Brilliance 64-slice CT scanner (Philips Healthcare, Andover, MA) and the AcQSim workstation. The CT simulation used the parameters specified by the MD Anderson protocol for a head and neck patient, but with the slice thickness reduced from 2.5 mm to 1.5 mm to better visualize the TLDs in the phantom. The CT data for the IMRT and RapidArc treatments were imported into the Eclipse TPS for planning.

### 2.3.2 Dose Prescription and Constraints

The same treatment planning objectives were used for all treatment plans and were based on RPC specifications. These criteria were derived from a head and neck prescription for the RTOG protocol 0022: 66 Gy to the primary PTV (the tumor) and 54 Gy to the secondary PTV (the peripheral node). However, these high doses are out of the useful range for GafChromic® EBT2 film and have been scaled down by a factor of ten for the RPC phantom test case resulting in a primary prescribed dose of 6.6 Gy and secondary dose of 5.4 Gy. At least 95% of the primary PTV volume must receive its prescription dose ( $D_{95\%} \geq 6.6$  Gy). Also, 95% of the secondary PTV must receive at least 5.4 Gy ( $D_{95\%} \geq 5.4$  Gy). The OAR simulates the spinal cord, so it was not allowed to receive more than 4.5 Gy, one-tenth of the 45 Gy dose limit for the spine.

**Table 2-2 Dosimetric criteria set by the RPC and used for planning all treatments**

Structure	Dosimetric Criteria
Primary PTV	$D_{95\%} \geq 6.60$ Gy
	$D_{99\%} \geq 6.14$ Gy
Secondary PTV	$D_{95\%} \geq 5.40$ Gy
	$D_{99\%} \geq 5.03$ Gy
Normal tissue	max dose $\leq 7.26$ Gy
Organ at risk	max dose $< 4.50$ Gy

Additional treatment planning criteria included minimizing the hot spots and that 99% of each target

volumes must receive more than 93% of that target's prescription dose. These criteria are summarized in Table 2-2.

### 2.3.3 Volume Delineation

Using the image segmentation tools in each corresponding TPS, we contoured the two PTVs and the OAR without any expansions (see Figure 2-3). A total body structure was generated, automatically in Eclipse and manually in Pinnacle. We created a normal tissue structure by subtracting the two PTV volumes from the total body structure. We also contoured each of the eight TLD. In the Eclipse TPS, the TLD had to be converted to high resolution segments before adequate contouring was possible.

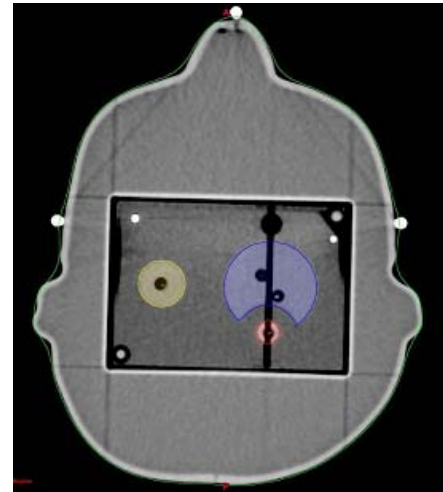


**Figure 2-3 Contoured structures in Eclipse: primary PTV (blue), secondary PTV (yellow), and OAR (red)**

### 2.3.4 Treatment Plans

In the TPS, we localized the plans to the radiopaque external fiducials indicating the simulation isocenter, which can be seen on the CT image shown in Figure 2-3. We placed the treatment isocenter at the geometric center of the two PTV structures. To do this, we made a single structure from both the primary and secondary PTVs. We determined the couch shifts necessary to

move from the simulation isocenter to the treatment isocenter.

The treatment couch for each of the three treatment plans was defined as follows. For the SmartArc plan, we removed the simulation couch. For the RapidArc and IMRT

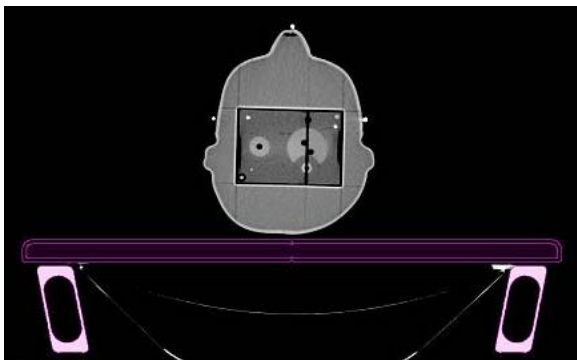


**Figure 2-4 Couch structure (purple) inserted for the IMRT and RapidArc plans**

plans, we added the Exact® couch top with flat panel structure with the rails in the out position. This couch is shown in Figure 2-4 and represents the actual linac couch on which the corresponding treatments were delivered.

The treatments were planned based on the typical clinical head and neck radiotherapy parameters of the institution in which the treatments were delivered. Both VMAT plans consisted of two full coplanar 6 MV arcs. The Elekta VMAT plan (planned with Pinnacle SmartArc) used a 45° collimator for both arcs and the RapidArc plan had a collimator offset of  $\pm 15^\circ$  (345° and 15°). The IMRT plan used nine coplanar, equally-spaced 6 MV beams (200°, 240°, 280°, 320°, 0°, 40°, 80°, and 160° seen in Figure 2-5) and a 0° collimator was set. The couch was set at 0° for all plans.

We set the final gantry spacing of the Pinnacle SmartArc plan to 4°. All plans were initially optimized until the planning criteria set by the RPC were met. More optimization attempts were made to improve the homogeneity and conformity of the dose distributions. We attempted to reduce

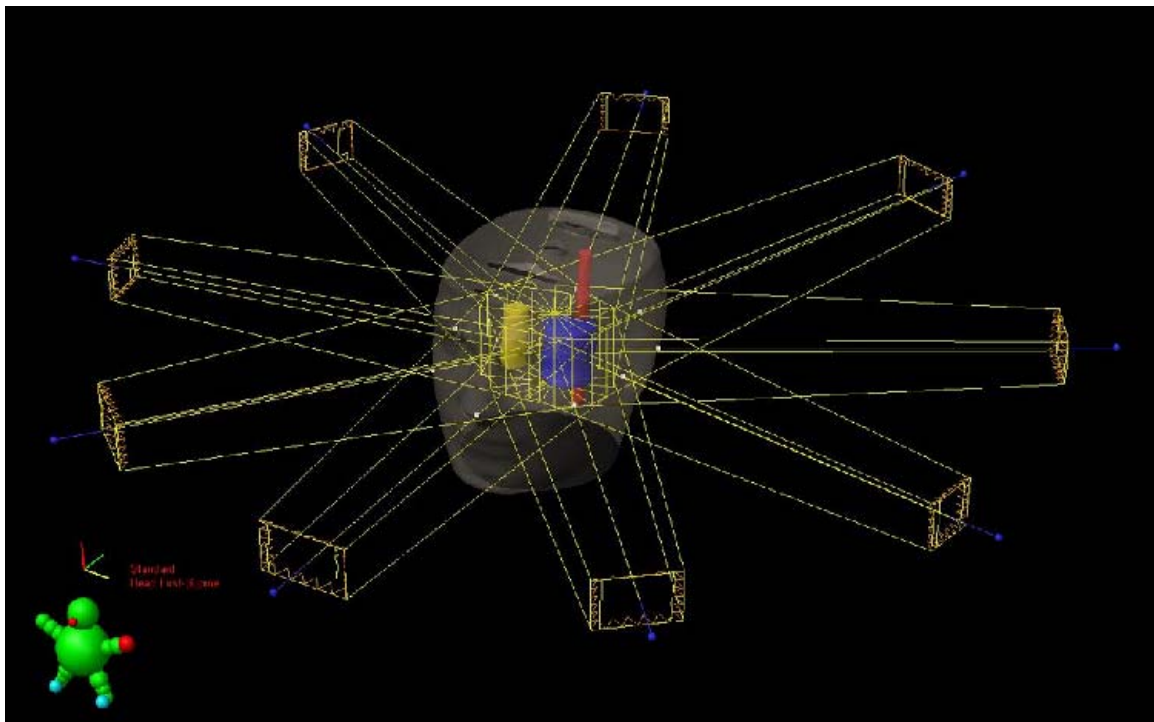


**Figure 2-5 Beam angles entering body in 3D view of nine field IMRT treatment plan**

the hot spots in the PTVs and make the dose in these structures as homogenous as possible. We created additional structures, such as volume expansions, rings and avoidance structures, to conform the prescription dose to the PTVs as much as possible.

The final dose for the SmartArc plan was calculated with the Adaptive Convolve dose engine. The RapidArc and IMRT plans were calculated with the AAA dose engine. All plans were calculated using a 4 mm calculation grid and were normalized to approximately 95% of the primary PTV receiving 6.6 Gy. The Elekta VMAT, RapidArc, and IMRT plans had a total of 1491, 2494, and 2274 MU, respectively. The total number of MU for each arc of an individual delivery of the Elekta VMAT and RapidArc plans were high and the treatments were splits into three and two fractions, respectively. The dose per fraction was reduced correspondingly to achieve the full 6.6 Gy prescription. The final treatments were delivered in three fractions of 2.2 Gy for Elekta VMAT and two fractions of 3.3 Gy for RapidArc.

## **2.4 Treatment Plan Quality Comparison**

We evaluated the plan quality of the two VMAT and one IMRT head and neck treatment plans to determine if they were clinically comparable. First, we evaluated each plan's ability to achieve the dose objectives set by the RPC, outlined in Table 2-2. To qualitatively evaluate the quality of each treatment plan, we generated and examined dose-volume histograms (DVH).

To compare the plans on their ability to minimize hot spots and to keep doses to normal tissues low we recorded the maximum doses in each PTV, the OAR, and normal tissue. The maximum dose was taken as the dose to the hottest 0.1 cc from the DVH. Additionally, the percentage of the secondary PTV receiving its prescription dose, its PTV coverage, was compared for all plans. The primary PTV coverage was not compared because the plans were normalized to the



prescription dose covering 95% of the primary PTV. The secondary PTV coverage indicated the plans ability to give adequate dose to a secondary volume while maintaining primary PTV coverage.

We quantified how well the prescription dose conformed to the primary PTV using the conformity index (CI) expressed in equation 2-1. The CI evaluated a plan's ability to spare normal tissue from the high doses delivered to treatment volume. In equation 2-1,  $V_{prescrip}$  was the total volume of tissue receiving the prescription dose, 6.6 Gy.  $V_{PTV}$  was the volume of the primary PTV structure.

$$CI = \frac{V_{prescrip}}{V_{PTV}} \quad \text{Eq. 2-1}$$

Since optimal plans have uniform doses in their treatment volumes, the homogeneity of each PTV was evaluated. We used the homogeneity index (HI), described in equation 2-2 below, to characterize the homogeneity.  $D_{5\%}$  was the dose delivered to the hottest 5% of PTV structure and  $D_{95\%}$  was the minimum dose received by 95% of the PTV structure, both taken from the plan's DVH.

$$HI = \frac{D_{5\%}}{D_{95\%}} \quad \text{Eq. 2-2}$$

## 2.5 Dosimetric Accuracy Evaluation

To determine if the dosimetric accuracy of the VMAT techniques was clinically acceptable, we delivered each of the three planned treatments to the RPC IMRT head and neck phantom and measured the dose distribution with TLDs and radiochromic film.

### 2.5.1 Phantom Irradiation

We delivered the Elekta VMAT plan on an Elekta Synergy® linac at Mary Bird Perkins Cancer Center in Baton Rouge, LA. The Synergy was equipped with an MLCi2 which had 10 mm

leaf width and forty leaves per bank. The linac was calibrated following the TG-51 protocol to 1 cGy/MU in muscle at  $d_{\max}$  under reference conditions of 100 cm SSD and 10 cm by 10 cm field size.

We delivered the RapidArc and IMRT plans on a Varian Clinac iX linac. The MLC system was the Varian Millennium 120 which had sixty leaves per bank. The central 40 leaves were 5 mm in width and the peripheral leaves were 10 mm in width. The linac was calibrated following the TG-51 protocol to 1 cGy/MU in muscle at  $d_{\max}$  under reference conditions of 100 cm SSD and 10 cm by 10 cm field size.

Prior to the delivery, we measured the machine output for 6 MV x-rays using the monthly QA protocol of the linac's institution. After the machine output was verified, we positioned the phantom on the treatment table in the same manner as the simulation: head-first supine, and lined up to the simulation isocenter indicated by the initial crosshair marks (see Figure 2-6). Then, we shifted the couch to the treatment isocenter and drew new crosshairs on the top and sides of the phantom.



**Figure 2-6 Photograph of phantom on treatment table of the Varian Clinac iX linear accelerator**

We delivered each treatment as specified by its treatment plan and delivered all fractions. Each irradiation of the Elekta VMAT plan and RapidArc plan involved delivering three and two fractions, respectively (refer to section 2.3.4 Treatment Plans for explanation). The treatment deliveries and measurements were repeated three separate times. We loaded new TLD and radiochromic films into the phantom prior to each irradiation. Between each irradiation, we had to remove the insert to unload the previous treatment's dosimeters and

replace with new ones. The setup was confirmed prior to each irradiation and the phantom adjusted as necessary to align the phantom to the treatment isocenter.

We performed an additional output check following a standardized RPC protocol that involves irradiating two TLDs in 4.4 cm by 4.4 cm square blocks of PMMA under conditions specified by the RPC. These blocks, known as mini-phantoms, were 3 cm tall with the TLDs located in the middle at 1.5 cm depth. The field size was 10 cm by 10 cm and the source-to-surface distance (SSD) was set to 100 cm to the top of the block. 300 MU of 6 MV photons were delivered to the TLDs, which were at the  $d_{\text{max}}$  for 6 MV. The TLD block and setup are shown in Figure 2-7.

The doses to the TLDs were subsequently read-out by the RPC and corrections were applied to determine the machine output. The purpose of this check was to compare the machine output with the nominal dose for 300 MU under



**Figure 2-7 Setup of the RPC machine output check involving irradiating two TLD in a Lucite block mini-phantom**

reference conditions. We used this value later to correct our measurements for machine output variations from the nominal output used to calculate dose (see section 2.5.3 Absolute Point Dose Analysis).

All plans were delivered using the record and verify system, Mosaiq, and treated in QA mode.

### **2.5.2 Dosimeters**

TLD and radiochromic film are radiation dosimeters that are used extensively by the RPC in their credentialing process. The dosimeters measure radiation dose passively and are ideal for remote audits where the phantom is mailed to an institution, irradiated, and then mailed back to the RPC for analysis. In this study, TLD and radiochromic film were used to measure absolute point doses and relative dose distributions, respectively.

#### **2.5.2.1 Thermoluminescent Dosimetry**

Thermoluminescent (TL) dosimetry is based upon the thermoluminescence process in which light is emitted from a material upon heating. These materials, known as TL phosphors, are crystal structures that contain imperfections, known as traps. These traps hold electrons or their holes in an electric potential well. When the crystal is heated, these electrons and holes can recombine at luminescence centers. When this occurs, a light photon is released. The intensity of this light released can be measured.

Some of these TL phosphors can perform as dosimeters if the energy deposited by radiation causes an ionization event that raises electrons to the traps. If the number of electron-hole pairs in traps is approximately proportional to the energy deposited by radiation, then the radiation dose received by the crystal material can be determined from the intensity of light released.

The RPC uses lithium fluoride powder doped with magnesium and titanium impurities to provide traps, a TL phosphor, as the sensitive material in their TLD. This material is also known as TLD-100. The sensitive part of the dosimeter is housed in a high-impact polystyrene cylindrical capsule, 15 mm tall and 4 mm in diameter. There are two separate packets of powder in each capsule, about 20 mg each, that yield two measurements.

The radiation dose received by the powder is determined by heating each packet of powder individually and measuring the amount of light emitted by a photomultiplier tube. The reading is

adjusted by several correction factors to obtain absorbed dose to muscle,  $D$ , as seen in Equation 2-3 below.

$$D = M \times S \times E \times L \times F \quad \text{Eq. 2-3}$$

$M$  is the TL response per mass of powder measured.  $S$  is the system calibration factor, absorbed dose per system response, which is found by measuring the TL response of TLD irradiated to known doses by Co-60 under standard conditions.  $E$  is an energy correction that is applied since the TL material response varies with energy slightly differently than tissue. Also,  $L$  is a linearity correction factor that is applied because the TL response is not exactly linear with dose and becomes supra-linear at higher doses. Lastly,  $F$ , a fading correction factor is applied that is dependent on the time elapsed from the irradiation to the reading. The reading fades at a rate that decreases exponentially with time because the trapped electrons and holes are not completely stable. The fading rate is dependent on the depth of the trap (energy required to excite electron sufficiently to enable recombination). Shallower, more unstable traps fade faster. By about ten days post irradiation, the fading becomes relatively constant (13). Therefore, the RPC waits a minimum ten days to measure the TL response to allow the most unstable traps to recombine and reduce the uncertainty of the measurement due to uncertainty of the exact time elapsed since irradiation.

The RPC determines the energy response, dose linearity, and fading corrections for each batch of TLD they use. A single batch was used for this study and corresponding corrections were applied. The TLD were all read at least 14 days post-irradiation. This TLD system has been shown to agree with ionization chamber measurements within  $\pm 4\%$  at a 90% confidence level (13). The precision of the TLD measurement system is 3%.

#### 2.5.2.2 Radiochromic Film Dosimetry

Radiochromic film is a radiation dosimeter that measures planar radiation dose distributions. Unlike radiographic film, it is self-developing and requires no processing post-irradiation. It has

good spatial resolution ( $< 0.1$  mm) which makes it ideal for measuring high dose gradients (14). The particular radiochromic film used in this study was GafChromic® EBT2 (International Specialty Products, Wayne, NJ) which is designed for use in external beam radiation therapy applications.

EBT2 film is nearly tissue equivalent ( $Z_{\text{eff}} = 6.84$  according to the manufacturer) and has low energy-dependence in the energy range of therapeutic radiation and its scatter. Its response reported by the manufacturer is about 10% different at 60 keV from 6 MV. A more recent study has found that the response varies only about 4.5% from energies of 75 kVp to 18 MeV (14). EBT2 is designed for measurement of doses ranging from 1 cGy to 40 Gy.

The active component of the film is a 30 micron thick layer of material that develops a blue polymer upon exposure to ionizing radiation. The active layer also contains a yellow dye that reduces the light sensitivity of the film and causes the film to appear to turn dark green with exposure. Irradiation causes the film to absorb light at 636 nm and 585 nm peaks. The reduced transmission of light, the optical density (OD), is related to the dose received.

Three films were cut from a template for each phantom irradiation. The two sagittal films, superior and inferior, were cut to fit into the slots in the insert and had a cutout for the OAR TLD. The axial film was cut to the approximate shape of the insert and sandwiched between the two halves of the insert. The films were marked along the edges to maintain the correct orientation.

The recommendations by AAPM Task Group 55 for radiochromic film handling and dosimetry were followed in this study (15). We read all films at least 10 days post-irradiation to allow the film to fully develop and reduce uncertainties caused by the density increase, which is proportional to the logarithm of time. The films were kept in consistent conditions of low humidity and room temperature and were stored in dark, light-blocking envelopes. An un-exposed piece of film was stored with each set of film to measure background radiation.

We measured the OD distribution of the EBT2 film using a transmission densitometer, the CCD100 Microdensitometer (Photoelectron Corporation, Lexington, MA). This system consisted of

placing the films on a light box with light-emitting diodes (LED) and measuring the light transmitted through the films with a charge-coupled device (CCD) camera. The LEDs emissions were centered at 665 nm, which is close to the primary absorption peak of irradiated EBT2 film. The system was enclosed in a light-tight closet to prevent outside light contaminating the measurement. We set the camera to the optimal focal distance from the film, based on the size of area to be measured, 150 mm by 150 mm in the center of the densitometer, and subsequently checked the focus. Outside of this focal area, we covered the densitometer with a black mask to block the light. The resolution of the CCD camera was 512 by 512 pixels, resulting in pixel sizes of about 0.3 mm.

Next we imaged a blank piece of film from the same batch covering the entire imaging area. This image was stored as a 'flat field' to correct for scanner variations in the subsequent readings. Then we set a spatial calibration by imaging a 10 mm by 10 mm grid. After the scanner was calibrated, we measured the optical densities of the experimental films, maintaining the same film orientation during reading. We imaged the axial film by itself and the two sagittal films together, allowing for a small separation between the superior and inferior films. The measurements were saved as .FIT files.

To generate a dose response curve that correlated OD to radiation dose for our specific batch of EBT2 film, we performed a calibration of the film batch. We cut nine 3 cm by 3 cm squares of film and marked them to maintain their orientation. All film squares were placed on the center of 9 cm slabs of solid water on a linac table and covered with a 1.5 cm slab of solid water. The pieces were oriented approximately 1 cm apart. We set a 100 cm SSD to the top of the solid water stack and centered it in a 35 cm by 35 cm field. We then irradiated the film squares with 6 MV photons at the  $d_{\text{max}}$  depth, 1.5 cm. We delivered a specified number of MU, removed a single square of film, repositioned the setup, and delivered another specified number of MU until all nine squares of film had been irradiated to a different total number of MU. The total number of MU delivered to each square of film can be seen below in Table 2-3. The dose delivered to each square of film was calculated by

multiplying the total delivered MU by the output factor for a 35 cm by 35 cm field, 1.095, and are also shown in Table 2-3. The film squares were exposed to doses ranging from 0.55 Gy to 14.78 Gy.

**Table 2-3 Irradiation of EBT2 film batch to generate a dose response curve for film calibration**

<b>square #</b>	<b>Total MU</b>	<b>Dose (Gy)</b>
1	50	0.55
2	150	1.64
3	250	2.74
4	350	3.83
5	550	6.02
6	750	8.21
7	950	10.40
8	1150	12.59
9	1350	14.78

We imaged each square of film using the same method described above and measured the OD over a region of interest in the center of each square three times. A background square of film that was stored with the calibration film squares was also measured and the value subtracted from the average OD of each square. We plotted the net optical densities against the calculated dose delivered and fit a third-order polynomial to the data (see Figure 2-8). We used the equation of the fit, equation 2-4, to convert the OD of our experimental films,  $x$ , to dose,  $D$ , in Gy. The OD of the corresponding background film was measured and subtracted from the OD of the experimental films before converting to dose.

$$D = 38.289x^3 - 20.793x^2 + 7.0476x \quad \text{Eq. 2-4}$$



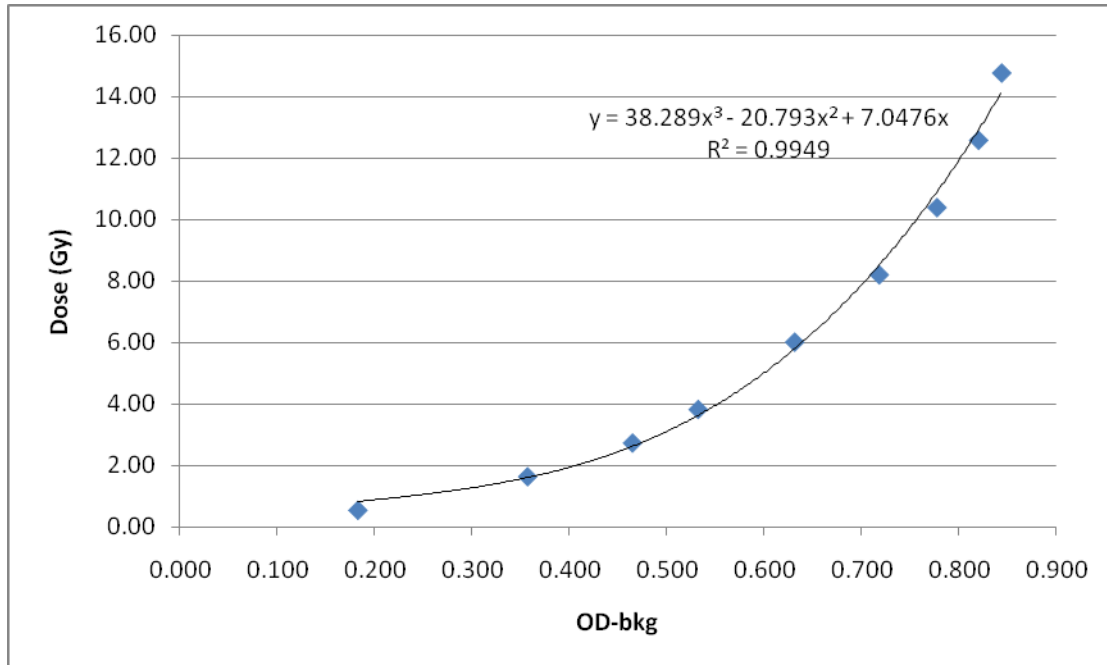


**Figure 2-8 Dose response curve for the batch of EBT2 film used in this study**

### 2.5.3 Absolute Point Dose Analysis

The absolute dose delivered to each of the eight TLDs in the phantom insert was measured using the RPC method described in 2.5.2.1

Thermoluminescent Dosimetry. The output of the machine was determined from the pairs of TLD irradiated in the mini-phantoms during the same sessions as the head and neck phantom irradiations. To ensure a true comparison of the calculated dose to delivered dose without the effects of machine output variation, we normalized the measured dose to the measured machine output. We then compared these corrected measured doses to the doses predicted by the TPS, which were the mean doses in the TLD structures recorded from the TPS. We found the ratio of the corrected measured dose to the TPS calculated dose for each TLD site. To comply with RPC standards, the measured point doses of the primary PTV and secondary PTV must be within  $\pm 7\%$  of the calculated dose; the ratio must be within 0.93 to 1.07.

#### **2.5.4** *Film, Plan, and Phantom Registration*

To facilitate comparing measured dose distributions to the calculation of the treatment planning systems, the films and treatment plan data had to be registered to a single coordinate system. We exported the plans, CT images, and dose distributions from Pinnacle and Eclipse in the DICOM-RT format. We then imported them into the Computational Environment for Radiotherapy Research (CERR) (J.O. Deasy and Washington University, St. Louis, MO). This software was developed for the MATLAB® language (The MathWorks, Inc., Natick, MA) to view and analyze treatment plans in a standard format. In this software, we were able to register the treatment plan to the actual phantom coordinates by selecting specified points on the treatment planning CT images that correspond to known locations in the phantom.

In an additional program developed for MATLAB, called `rpcfilm`, we opened the .FIT files containing the OD information of the films. We used the holes pierced in the film, which were visible in the film images, to register the film to the phantom coordinates of the actual pins and converted from OD using the dose response curve we generated (see Figure 2-8). We accounted for the OD of the background film piece.

To allow a comparison of absolute dose, the film dose was normalized to the corresponding dose measured by the TLDs in the primary PTV. In several locations, the ratio of the TLD-measured dose to the film-measured dose was determined. For the axial film, the average of the superior and inferior TLD doses were used to determine the ratios of dose at the locations on the film corresponding to the sets of anterior and posterior TLD. For the sagittal films, we determined the ratios of the locations corresponding to all four TLDs in the primary PTV: anterior superior, anterior inferior, posterior superior and posterior inferior. For each film plane measurement, axial or sagittal, we used the average of its TLD/film measurement ratios to correct the film to absolute dose.

### 2.5.5 Planar Dose Analysis

In the rpcfilm program, the film measurements were compared to the registered treatment plan dose distribution. We measured profiles of the dose taken through the center of the primary PTV in each orthogonal direction. We took the anterior-posterior and lateral profiles from the axial film and the superior-inferior profile from the sagittal films. The film measurements were sampled at a 0.3 mm resolution. We smoothed the profiles by using a moving average over eleven data points, or 3 mm. We visually compared the film profiles to the treatment plan calculated profiles to determine if any major shifts from the planned setup had occurred.

The dose fall-off between the posterior edge of the primary PTV and the anterior edge of the OAR was evaluated based on DTA. We performed a linear regression of the penumbra on the smoothed anterior-posterior profile from the axial film and of the penumbra of the corresponding treatment plan profile. We evaluated three points along each linear regression at 25%, 50% and 75% of the difference between the maximum and minimum dose levels. The maximum and minimum doses were taken as the average of a relatively flat region in the primary PTV and in the OAR, respectively. The distance between these doses along the measured and calculated dose profile was measured. We calculated the average value of these three distances for each treatment delivery for each treatment type and compared it to the RPC acceptability criterion: 4 mm for the penumbra between the primary PTV and the OAR.

The planar doses measured were also compared to the TPS calculated doses in rpcfilm using gamma analysis as described by Low, et al (16). We used this test to evaluate how well our measured and calculated dose distributions agree. First, we used acceptability criteria of  $\pm 5\%$  dose difference and 3 mm DTA with 95% of the points passing being clinically acceptable. These criteria are the typical values used by the RPC for IMRT credentialing with anthropomorphic phantoms and are common clinical criteria, as well. However, the RPC currently does not include gamma analysis in

credentialing for head and neck IMRT. We evaluated an area covering both PTVs and the OAR in both the axial and sagittal planes, shown in Figure 2-9 and Figure 2-10, respectively.



**Figure 2-9 Area in axial plane where gamma analysis was performed with 5% dose difference and 3 mm DTA criteria**

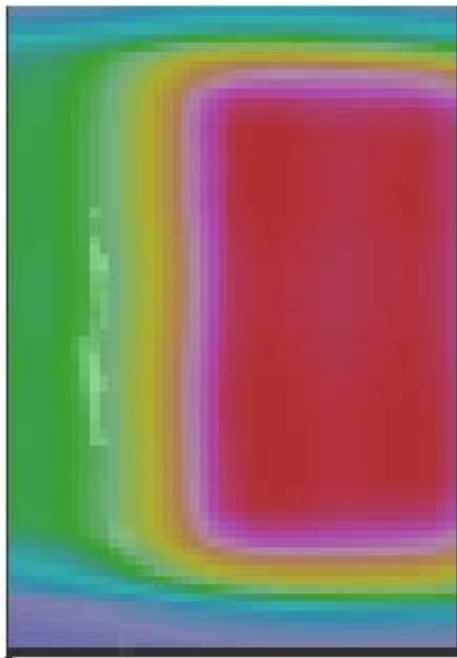


**Figure 2-10 Area in sagittal plane where gamma analysis was performed with 5% dose difference and 3 mm DTA criteria**

Although the RPC does not use gamma analysis for their head and neck IMRT credentialing, they have been collecting data using a  $\pm 7\%$  dose difference and 4 mm DTA criteria over a region

defined in the axial plane, shown in Figure 2-11. Therefore, we performed a second gamma analysis using  $\pm 7\%$  dose difference and 4 mm DTA criteria in a region around the primary PTV in the axial plane. We compared the percent of points passing with data collected from 452 institutions that have

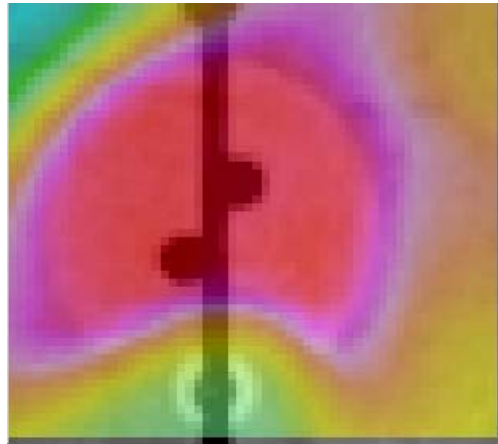


**Figure 2-11 Area in axial plane where gamma analysis was performed with 7% dose difference and 4 mm DTA criteria**

undergone the RPC credentialing process for head and neck IMRT.

#### 2.5.5.1 Gamma Analysis

Gamma analysis is a quantitative evaluation of how well two dose distributions agree (16). It incorporates two different criteria to evaluate the agreement of two dose distributions into a single value, the  $\gamma$ -index. The criteria compare points based on the dose difference between the two distributions at a point and the distance to a point in the other distribution of the same dose (distance-to-agreement, DTA). This analysis involves setting the acceptable dose difference and DTA criteria and determining how many points are in agreement.

The purpose of using two measures to evaluate how well dose distributions agree is to provide for high and low dose gradients. In high dose gradients, the dose is changing rapidly from point to point, and small spatial errors may cause large differences in dose. However, the distance between two points of the same dose may be small. In low dose gradient regions, where the dose is

more homogenous, small discrepancies in dose value may cause the distance between two points of the same dose to be very far away, even if the difference in dose from nearby points is small.

The first step in gamma analysis is determining the value of  $\Gamma(r_m, r_c)$  for every measurement and calculation point, which is described by equation 2-5 below, where  $r_m$  is a single measurement point, and  $r_c$  is a spatial point in the calculated dose distribution.  $\Delta d_m$  is the preset DTA criterion and  $\Delta D_m$  is the preset dose difference criterion.

$$\Gamma(r_m, r_c) = \sqrt{\frac{r^2(r_m, r_c)}{\Delta d_m^2} + \frac{\delta^2(r_m, r_c)}{\Delta D_m^2}} \quad \text{Eq. 2-5}$$

where,

$r(r_m, r_c) = |r_m - r_c|$ , the DTA and

$\delta(r_m, r_c) = D_c(r_c) - D_m(r_m)$ , the dose difference

$\Gamma(r_m, r_c)$  forms an ellipse when it is set equal to one with the major axes being DTA,  $r(r_m, r_c)$ , and dose difference,  $\delta(r_m, r_c)$ . A  $\Gamma(r_m, r_c)$  of less than or equal to one passes the acceptance criteria set. The  $\gamma$ -index is the minimum value of the term,  $\Gamma(r_m, r_c)$ , for a single measurement point,  $r_m$ . If the  $\gamma$ -index is less than or equal to one, then that point in the measured dose distribution passes the acceptance criteria. The  $\gamma$ -index can be found for every point in a measured distribution and the total percent of points passing can be determined (16).

The software rpcfilm, which we used to perform gamma analyses, has a tool to mask certain areas of the film image. This was used to exclude areas beyond the film edge and the pin prick marks that were included in the evaluation areas. The mask nullifies the area in the gamma analysis, not counting it as passing or failing.

### **2.5.6**    *MLC Log File Analysis*

In order to better understand patterns we found in the results, we recorded the dynalog files for repeated deliveries of the RapidArc plan. The dynalog files are Varian's MLC log files and record the error in the MLC position, counted every 50 milliseconds, relative to the expected MLC position as defined by the treatment plan. The errors are reported in two ways. The first is the root mean square (RMS) of the deviation of each leaf over the whole treatment. The other is a histogram of the magnitude of the errors of each count. The files were recorded separately for five deliveries of each arc and the variation of the RMS leaf deviation was evaluated for the repeated deliveries of the RapidArc plan.

## Chapter 3 Results

### 3.1 Treatment Plan Quality Comparison

To determine the TPS ability to generate treatment plans that can achieve typical prescriptions and constraints for the RPC head and neck phantom, each plan was evaluated on its ability to meet the RPC constraints, which were presented in Table 2-2. The results of this analysis are shown below in Table 3-1.

**Table 3-1 The values of each dosimetric objective for all three treatment plans, including prescriptions and dose constraints**

Structure	Dosimetric Criteria	Elekta VMAT	RapidArc	IMRT
Primary PTV	$D_{95\%} \geq 6.60 \text{ Gy}$	6.58 Gy	6.60 Gy	6.59 Gy
	$D_{99\%} \geq 6.14 \text{ Gy}$	6.37 Gy	6.35 Gy	6.42 Gy
Secondary PTV	$D_{95\%} \geq 5.40 \text{ Gy}$	5.43 Gy	5.43 Gy	5.41 Gy
	$D_{99\%} \geq 5.03 \text{ Gy}$	5.40 Gy	5.28 Gy	5.32 Gy
Normal tissue	$\text{max dose} \leq 7.26 \text{ Gy}$	6.76 Gy	6.89 Gy	6.82 Gy
Organ at risk	$\text{max dose} < 4.5 \text{ Gy}$	4.14 Gy	4.09 Gy	4.10 Gy

The data in the first row of Table 3-1 defines the prescription for the primary target volume. The treatment plans were normalized to meet this objective (6.6 Gy to 95% of the primary PTV volume). However, the actual values of primary PTV coverage resulting from the normalization are slightly less than 6.60 Gy for 95% of the primary PTV volume. Since this is a result of the treatment plan normalization, it was not considered in the analysis of each plan's ability to comply with the RPC dose objectives. All plans passed all of the other dosimetric criteria.

Next, we qualitatively compared the DVHs of the three different treatment plans. The DVHs are shown in Figure 3-1. The slopes of the DVHs of both PTVs for the Elekta VMAT plans are steeper than the other plans, indicating more uniform PTV dose. The RapidArc plan had slightly less



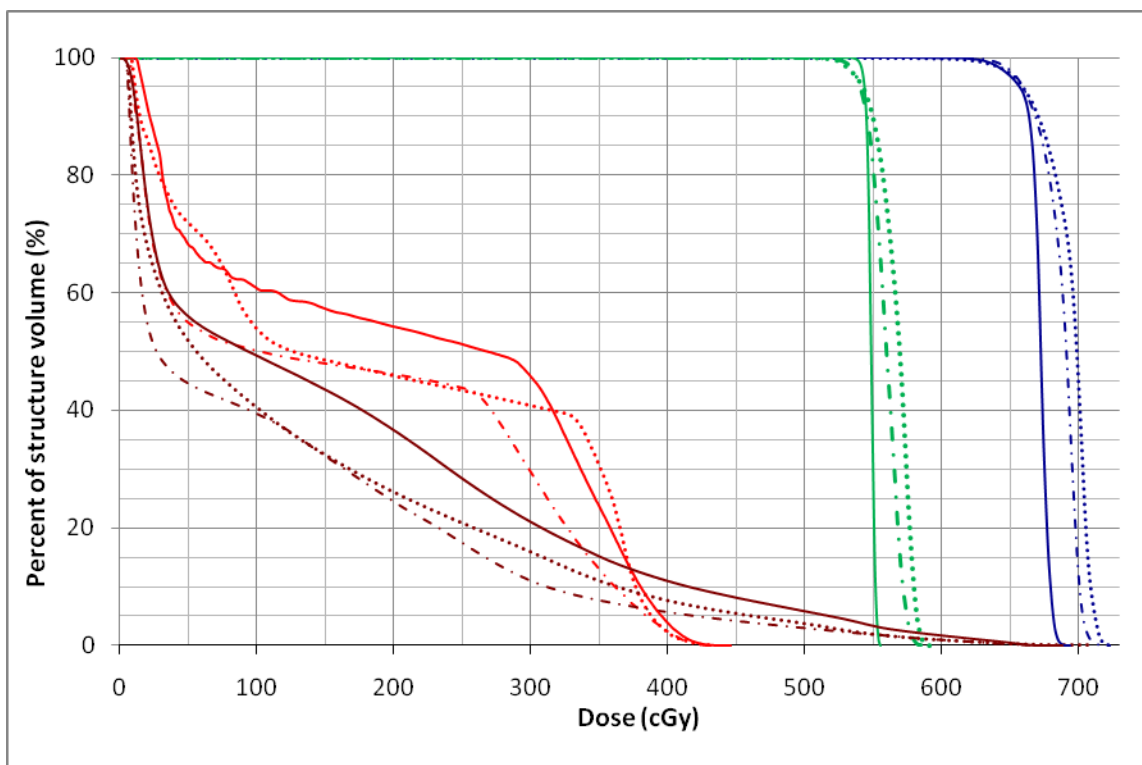


**Figure 3-1 DVHs of the primary PTV (blue), secondary PTV (green), OAR (red), and normal tissue (brown) for the Elekta VMAT (solid), RapidArc (dotted), and IMRT (dashed) treatment plans**

steep dose than the IMRT plan, as well. However, the normal tissue dose was generally higher for the Elekta VMAT plan in comparison to the RapidArc and IMRT plans.

The maximum doses in both PTVs, the OAR and the normal tissue were compared to see how well the treatment plans could reduce the magnitude of the hot spots. The maximum doses for each plan are reported in Table 3-2. The hot spots in the PTVs were lowest for the Elekta VMAT plan. The maximum doses of the OAR and normal tissue were similar for all plans.

**Table 3-2 Maximum dose to the primary PTV, secondary PTV, OAR, and normal tissue structures with the percent of the prescription dose for each PTV shown in parenthesis**

Structure	Elekta VMAT	RapidArc	IMRT
Primary PTV	688 cGy (104%)	719 cGy (109%)	714 cGy (108%)
Secondary PTV	553 cGy (102%)	587 cGy (109%)	581 cGy (108%)
OAR	4.14 Gy	4.09 Gy	4.10 Gy
Normal tissue	6.76 Gy	6.89 Gy	6.82 Gy

The percentage of each treatment volume covered by the prescription dose for the secondary PTV was determined for all treatment plans. The values obtained for the Elekta VMAT, RapidArc, and IMRT plans were 99.2%, 96.0%, and 95.7%, respectively. The Elekta VMAT plan was able to achieve greater prescription dose coverage of the secondary PTV.

The conformity index (CI) was calculated using equation 2-1 for the primary PTV for all treatment plans. Generally, lower values of CI indicate better conformity and a perfectly conformal dose would have a CI of 0.95. The resulting CI were 1.08, 1.02, and 1.01 for the Elekta VMAT, RapidArc, and IMRT plans respectively. The Elekta VMAT treatment plan had the highest CI, indicating that it had a less conformal dose distribution than the RapidArc and IMRT treatment plans. This is consistent with the higher normal tissue doses seen in the DVH of the Elekta VMAT treatment (brown solid line) in Figure 3-1.

The homogeneity index (HI) was calculated using equation 2-2 for both the primary and secondary PTVs for all treatment plans. Lower values of HI indicate more uniform dose in the treatment volumes. The results are reported in Table 3-3. The RapidArc and IMRT treatment plans had the highest HI, indicating that those plans had less uniform dose in the treatment volumes. These results are consistent with the DVHs shown in Figure 3-1, where the slopes of the primary and secondary PTV DVHs (blue and green solid lines, respectively) are steepest for the Elekta VMAT plan.

**Table 3-3 Homogeneity indices (HI) of both PTVs calculated for all three treatment plans**

<b>Structure</b>	<b>Elekta VMAT</b>	<b>RapidArc</b>	<b>IMRT</b>
Primary PTV	1.04	1.08	1.07
Secondary PTV	1.02	1.07	1.06

Isodose distributions for all three treatment plans can be found in the Appendix in Figure 5-1, Figure 5-2, Figure 5-3.

## **3.2 Dosimetric Accuracy Evaluation**

### **3.2.1 *Absolute Point Dose Analysis***

The doses at eight locations in the phantom were measured using TLD capsules. All of the actual dose values measured are reported in the in Table 3-4 for the Elekta VMAT treatment, Table 3-5 for the RapidArc treatment, and Table 3-6 for the IMRT treatment. The doses are listed in cGy for each TLD measurement for each treatment delivery. The average and percent standard deviation of the three deliveries are also shown. Each measurement point is identified by the position of the TLD in the phantom. The TLD position is described by the structure the TLD it is located within and its placement within that structure (superior versus inferior and, when applicable, anterior versus posterior). The greatest percent standard deviation of TLD measurements at a single point for the Elekta VMAT, RapidArc, and IMRT treatments were 1.22%, 1.45%, 1.82%, respectively. At most measurement locations the percent standard deviation is less than 1% indicating that there is little variation in the TLD measurements across treatment deliveries. Table 3-7 shows the mean dose calculated for each TLD structure by the TPS for each plan.

**Table 3-4 Doses measured by eight TLD in the phantom insert for three deliveries of the Elekta VMAT treatment**

TLD position	1	Delivery 2	3	Average	Percent standard deviation
Primary PTV Superior Anterior	644	644	647	645	0.27%
Primary PTV Inferior Anterior	643	650	646	646	0.51%
Primary PTV Superior Posterior	635	641	647	641	0.89%
Primary PTV Inferior Posterior	643	641	649	644	0.72%
Secondary PTV Superior	527	534	525	528	0.88%
Secondary PTV Inferior	517	527	529	524	1.22%
OAR Superior	259	261	260	260	0.48%
OAR Interior	253	257	256	256	0.78%

**Table 3-5 Doses measured by eight TLD in the phantom insert for three deliveries of the RapidArc treatment**

TLD position	1	Delivery 2	3	Average	Percent standard deviation
Primary PTV Superior Anterior	724	737	737	732	1.01%
Primary PTV Inferior Anterior	745	742	736	741	0.68%
Primary PTV Superior Posterior	728	734	738	733	0.71%
Primary PTV Inferior Posterior	735	744	751	744	1.08%
Secondary PTV Superior	591	604	608	601	1.45%
Secondary PTV Inferior	621	622	622	622	0.04%
OAR Superior	357	357	358	357	0.06%
OAR Interior	355	361	362	359	1.01%

**Table 3-6 Doses measured by eight TLD in the phantom insert for three deliveries of the IMRT treatment**

TLD position	1	Delivery 2	3	Average	Percent standard deviation
Primary PTV Superior Anterior	704	715	708	709	0.73%
Primary PTV Inferior Anterior	711	704	708	708	0.48%
Primary PTV Superior Posterior	714	713	719	715	0.49%
Primary PTV Inferior Posterior	713	708	714	712	0.41%
Secondary PTV Superior	599	598	590	596	0.89%
Secondary PTV Inferior	599	590	591	593	0.87%
OAR Superior	299	295	306	300	1.82%
OAR Interior	301	293	300	298	1.50%

**Table 3-7 Treatment planning system calculation of the mean dose at eight TLD locations within the phantom insert**

TLD position	Elekta VMAT	RapidArc	IMRT
Primary PTV Superior Anterior	671	694	689
Primary PTV Inferior Anterior	671	700	690
Primary PTV Superior Posterior	677	697	685
Primary PTV Inferior Posterior	681	701	689
Secondary PTV Superior	550	575	569
Secondary PTV Inferior	551	578	569
OAR Superior	321	346	306
OAR Inferior	317	353	302

The ratios of the measured TLD dose to the calculated dose of the corresponding TLD structure in the TPS are reported in Table 3-8, Table 3-9, and Table 3-10 for the Elekta VMAT, RapidArc, and IMRT treatments, respectively. The six measurement points in the PTVs were evaluated to determine if they met the RPC absolute dose criterion of  $\pm 7\%$ . The dose of the OAR is not included in this analysis since it is generally a steep dose gradient and small errors in position may cause larger errors in dose.

The ratios at these six locations in the phantom are within 0.93 to 1.07 for all three deliveries of all three treatment plans and, therefore, pass the RPC criterion. In the PTVs, where the dose is relatively uniform, the IMRT treatment had the best agreement, and the RapidArc treatment had the worst agreement. However, in the OAR, where there is a steep dose gradient, the RapidArc treatment had the best agreement, and the Elekta VMAT had the worst agreement. Also, the Elekta VMAT

treatment plans consistently underestimated the dose while the RapidArc and IMRT treatment plans mostly overestimated the dose, with the exceptions occurring in the OAR dose.

**Table 3-8 Ratio of the measured TLD dose to the calculated TPS dose at eight locations in the phantom for three deliveries of the Elekta VMAT plan**

TLD position	Delivery			Average
	1	2	3	
Primary PTV Superior Anterior	0.97	0.97	0.98	0.98
Primary PTV Inferior Anterior	0.97	0.98	0.98	0.98
Primary PTV Superior Posterior	0.95	0.96	0.97	0.96
Primary PTV Inferior Posterior	0.96	0.95	0.97	0.96
Secondary PTV Superior	0.97	0.98	0.97	0.98
Secondary PTV Inferior	0.95	0.97	0.97	0.97
OAR Superior	0.82	0.83	0.82	0.82
OAR Interior	0.81	0.82	0.82	0.82



**Table 3-9 Ratio of the measured TLD dose to the calculated TPS dose at eight locations in the phantom for three deliveries of the RapidArc plan**

TLD position	Delivery			Average
	1	2	3	
Primary PTV Superior Anterior	1.02	1.04	1.04	1.03
Primary PTV Inferior Anterior	1.04	1.04	1.03	1.04
Primary PTV Superior Posterior	1.02	1.03	1.04	1.03
Primary PTV Inferior Posterior	1.03	1.04	1.05	1.04
Secondary PTV Superior	1.01	1.03	1.03	1.02
Secondary PTV Inferior	1.05	1.05	1.05	1.05
OAR Superior	1.01	1.01	1.01	1.01
OAR Interior	0.99	1.00	1.00	1.00

**Table 3-10 Ratio of the measured TLD dose to the calculated TPS dose at eight locations in the phantom for three deliveries of the IMRT plan**

TLD position	Delivery			Average
	1	2	3	
Primary PTV Superior Anterior	1.00	1.02	1.01	1.01
Primary PTV Inferior Anterior	1.01	1.00	1.00	1.00
Primary PTV Superior Posterior	1.02	1.02	1.03	1.02
Primary PTV Inferior Posterior	1.01	1.01	1.01	1.01
Secondary PTV Superior	1.03	1.03	1.01	1.02
Secondary PTV Inferior	1.03	1.01	1.02	1.02
OAR Superior	0.96	0.95	0.98	0.96
OAR Interior	0.98	0.95	0.97	0.97

### 3.2.2 *Planar Dose Analysis*

#### 3.2.2.1 Dose profile comparison

The measured and calculated dose profiles for the Elekta VMAT, RapidArc, and IMRT treatments are reported in Figure 3-2 through Figure 3-4 and in the Appendix in Figure 5-4 through Figure 5-9. Figure 3-2 through Figure 3-4 show the lateral profiles taken from the axial film through the center of the primary PTV. Figure 5-4 through Figure 5-9 show the posterior-to-anterior profile measured from the axial film and the inferior-to-superior profile measured from the sagittal films, both through the center of the primary PTV. In each figure, the corresponding calculation is shown along with the measurements of all three treatment deliveries of each plan.

In general, the measured dose profiles were lower than calculation for the Elekta VMAT treatment deliveries (Figure 3-2, Figure 5-4, and Figure 5-5), which corresponds with the TLD measurements where the ratios of measured to calculated doses was less than one. For the RapidArc (Figure 3-3, Figure 5-6, and Figure 5-7) and IMRT treatments (Figure 3-4, Figure 5-8, and Figure 5-9), the measured dose profiles were greater than calculation. This trend was also seen in the TLD measurement to calculation ratios, which were mostly greater than one for both the RapidArc and IMRT treatment deliveries. All treatments had difficulty with the posterior-to-anterior dose profile in the region of the dose falloff between the primary PTV and the OAR. The Elekta VMAT had the greatest deviation between the measured and calculated penumbra in this region (Figure 5-4). This corresponds with the large difference between the measured TLD dose in the OAR and calculation for the Elekta VMAT treatment, as shown in Table 3-8. The gap in the measurements shown in the inferior-to-superior dose profiles (Figure 5-5, Figure 5-7, and Figure 5-9) corresponds to the location of the gap between the two sagittal films used to measure these profiles.

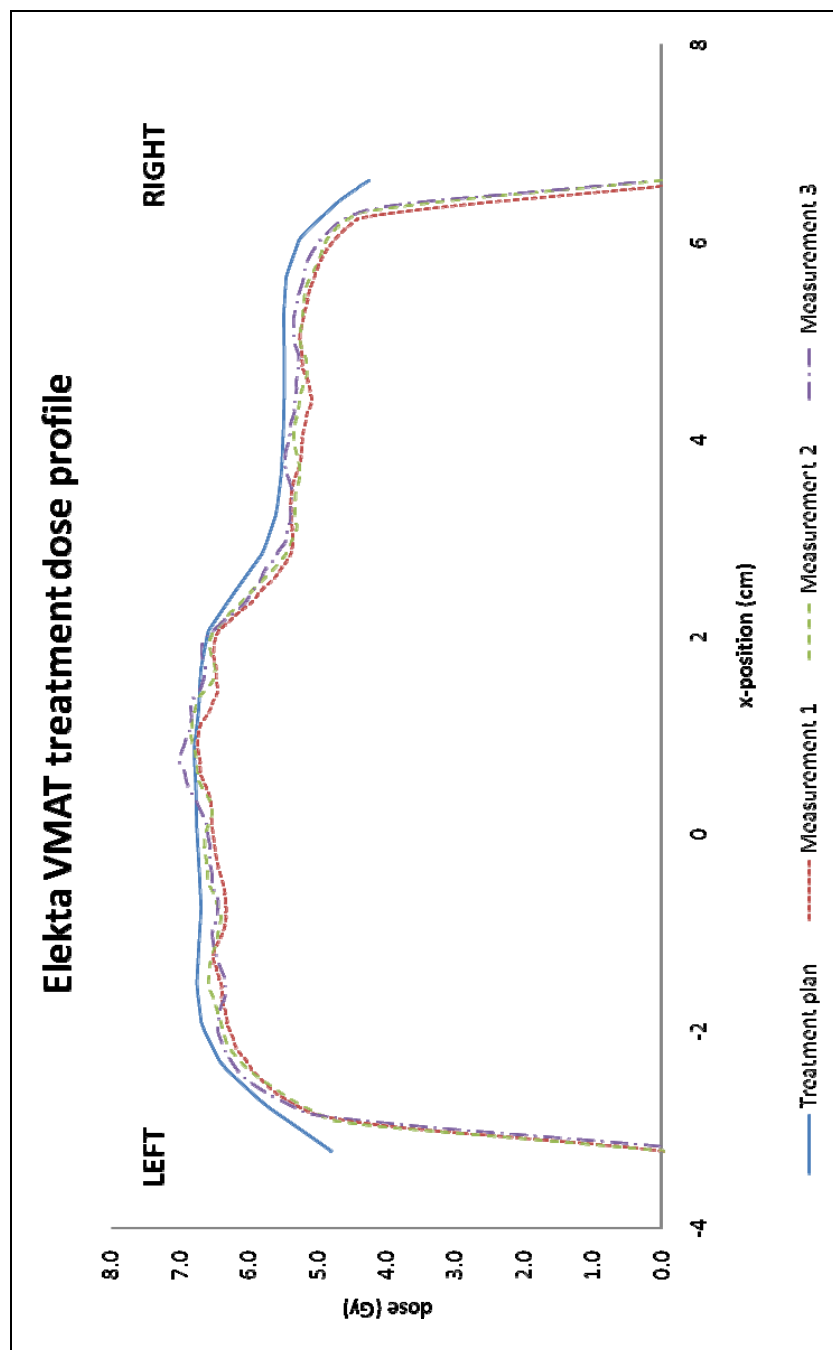


Figure 3-2 Lateral dose profile of the Elekta VMAT treatment

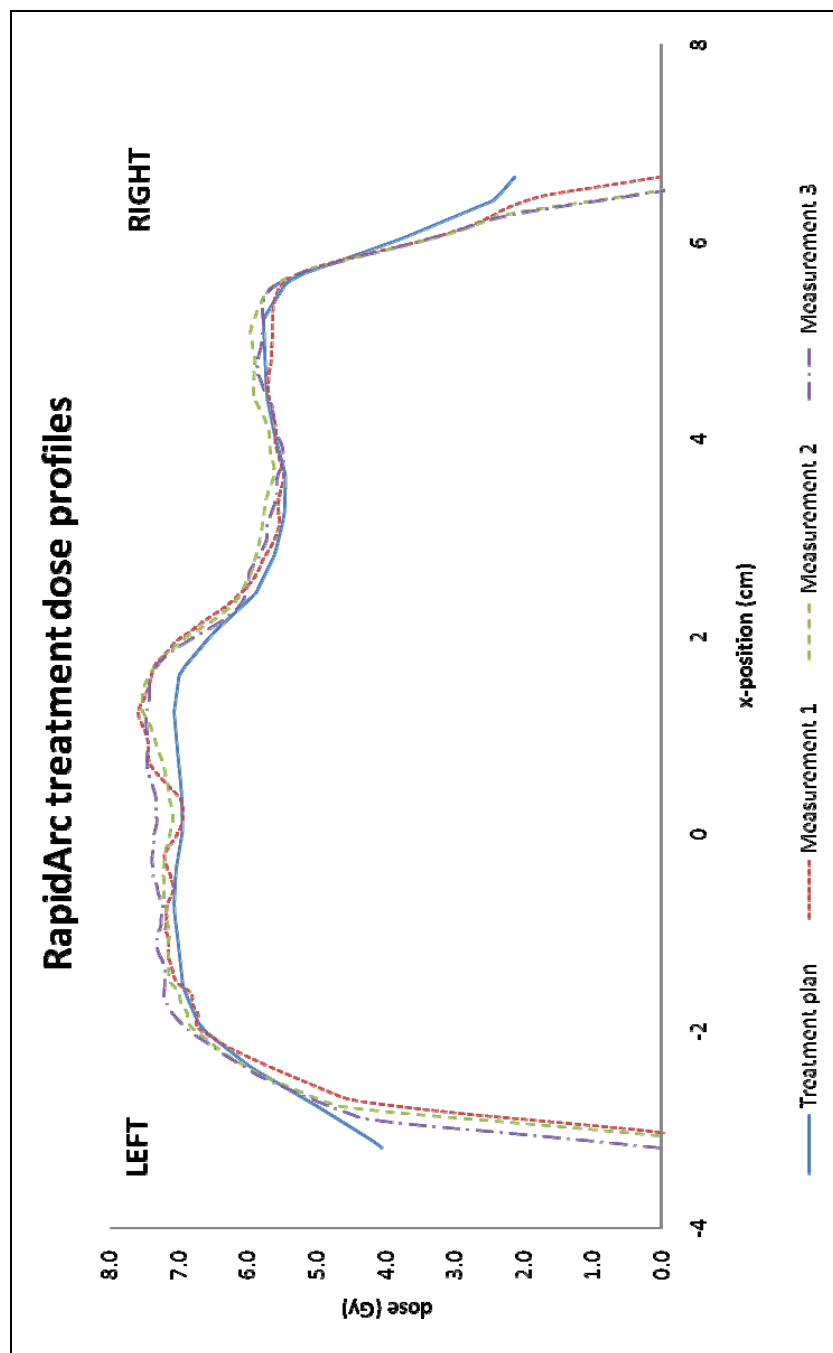


Figure 3-3 Lateral profile of the RapidArc treatment

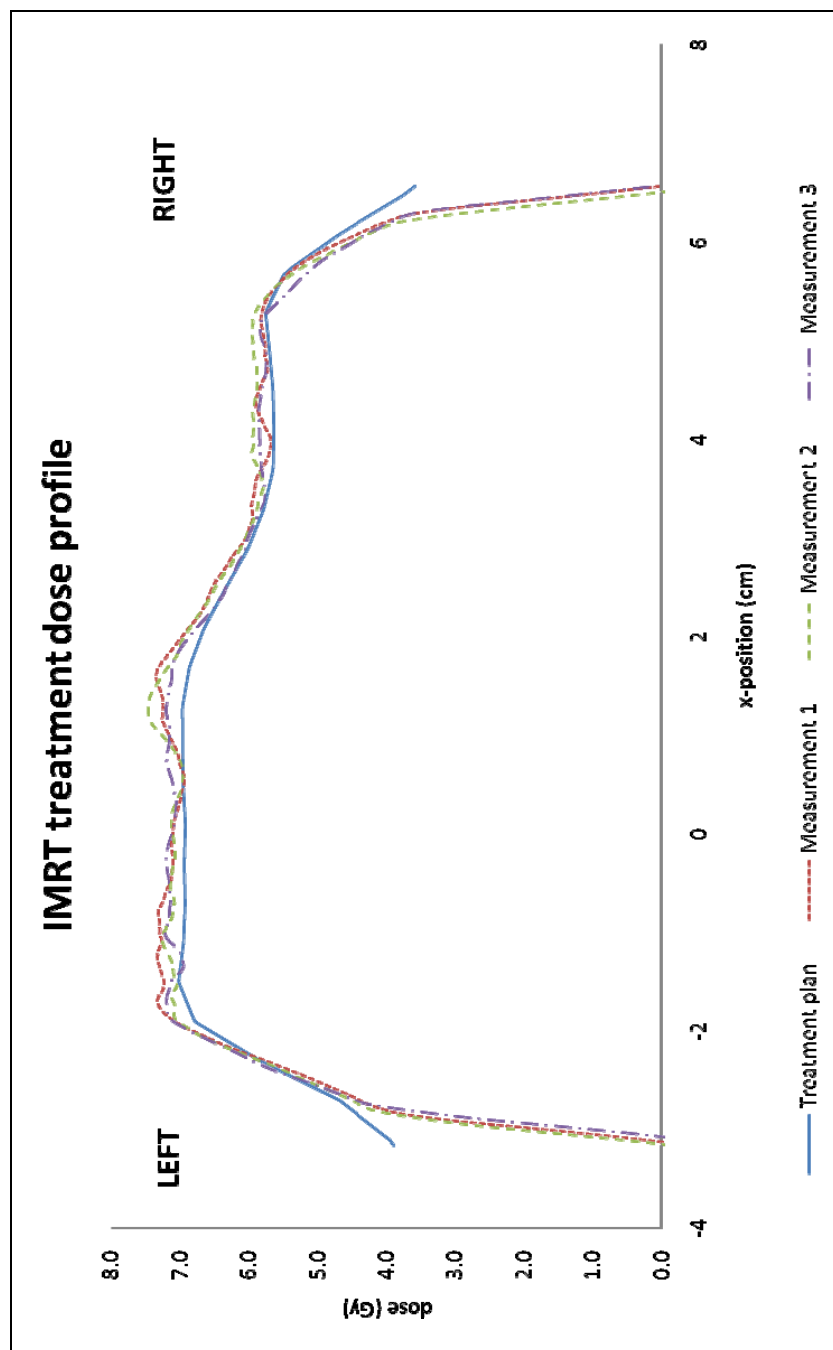


Figure 3-4 Lateral dose profile of the IMRT treatment

The results of the displacement of the measured posterior penumbra from calculation are shown in Table 3-11 in millimeters for all treatment deliveries. All deliveries met the 4 mm DTA criterion specified by the RPC. The displacement of the penumbra measured from the Elekta VMAT treatments is by far the largest, which corresponds with the large deviation seen in the posterior-to-anterior dose profile measured (Figure 5-4). The displacement of the RapidArc and IMRT treatments was no more than 2.0 mm in all cases.

**Table 3-11 Displacement (mm) of measurement from calculation of the posterior penumbra between the primary PTV and the OAR**

Treatment	Delivery			Average
	1	2	3	
Elekta VMAT	3.4	3.5	3.2	3.4
RapidArc	1.2	1.3	1.7	1.4
IMRT	2.0	1.9	1.5	1.8

#### 3.2.2.2 Gamma analysis

The agreement of the axial and sagittal film measurements to the corresponding treatment plans was evaluated using gamma analysis. The spatial distribution of the gamma analyses' results for all treatments and deliveries are shown in Figure 5-10 through Figure 5-27 in the Appendix, and representative examples are shown here in Figure 3-5 through Figure 3-13. The gamma analyses shown in these figures did not use the masking feature and, therefore, the entire area, including the areas off the film edge, was included in the analyses shown. Consequently, the results of the gamma analysis reported in the figures represent artificially lower percent of points passing.

The first evaluation used acceptability criteria of  $\pm 5\%$  dose difference and 3 mm DTA in both the axial and the sagittal planes. The resulting percent of points passing with masking used per treatment delivery are reported in Table 3-12. The average percent of points passing for each plane evaluated for each treatment technique are shown in the table, as well. The IMRT treatment had the highest average percent of points passing (85.7% and 85.4% in the axial and sagittal planes,

**Table 3-12 Percent of points passing gamma analysis with acceptability criteria of 5% dose difference and 3 mm DTA in the axial and sagittal planes bisecting the primary PTV**

Treatment	Film plane	Delivery			Average
		1	2	3	
Elekta VMAT	axial	70.6%	74.2%	84.0%	76.2%
	sagittal	76.1%	76.6%	79.0%	77.2%
RapidArc	axial	84.5%	80.7%	74.8%	80.0%
	sagittal	82.2%	68.7%	75.2%	75.4%
IMRT	axial	80.1%	86.9%	90.0%	85.7%
	sagittal	84.4%	88.5%	83.2%	85.4%

respectively) and the Elekta VMAT treatment had the lowest average percent of points passing in the axial plane (76.2%) while the RapidArc treatment had the lowest average percent of points passing in the sagittal plane (75.4%). We also noted greater variation between deliveries of the Elekta VMAT and RapidArc plans than the IMRT plan. The Elekta VMAT results ranged from 70.6% to 84.0% and the RapidArc results ranged from 68.7% to 84.5%, while the range of percent passing for the IMRT treatment was 80.1% to 90.0%.

Figure 3-5 through Figure 3-10 show the axial and sagittal film results of one delivery of each treatment technique. Most plans failed in regions of sharp dose falloff, such as in the region between the primary PTV and the OAR. Some plans also had difficulties meeting the acceptability criteria in the high dose regions inside the primary PTV.



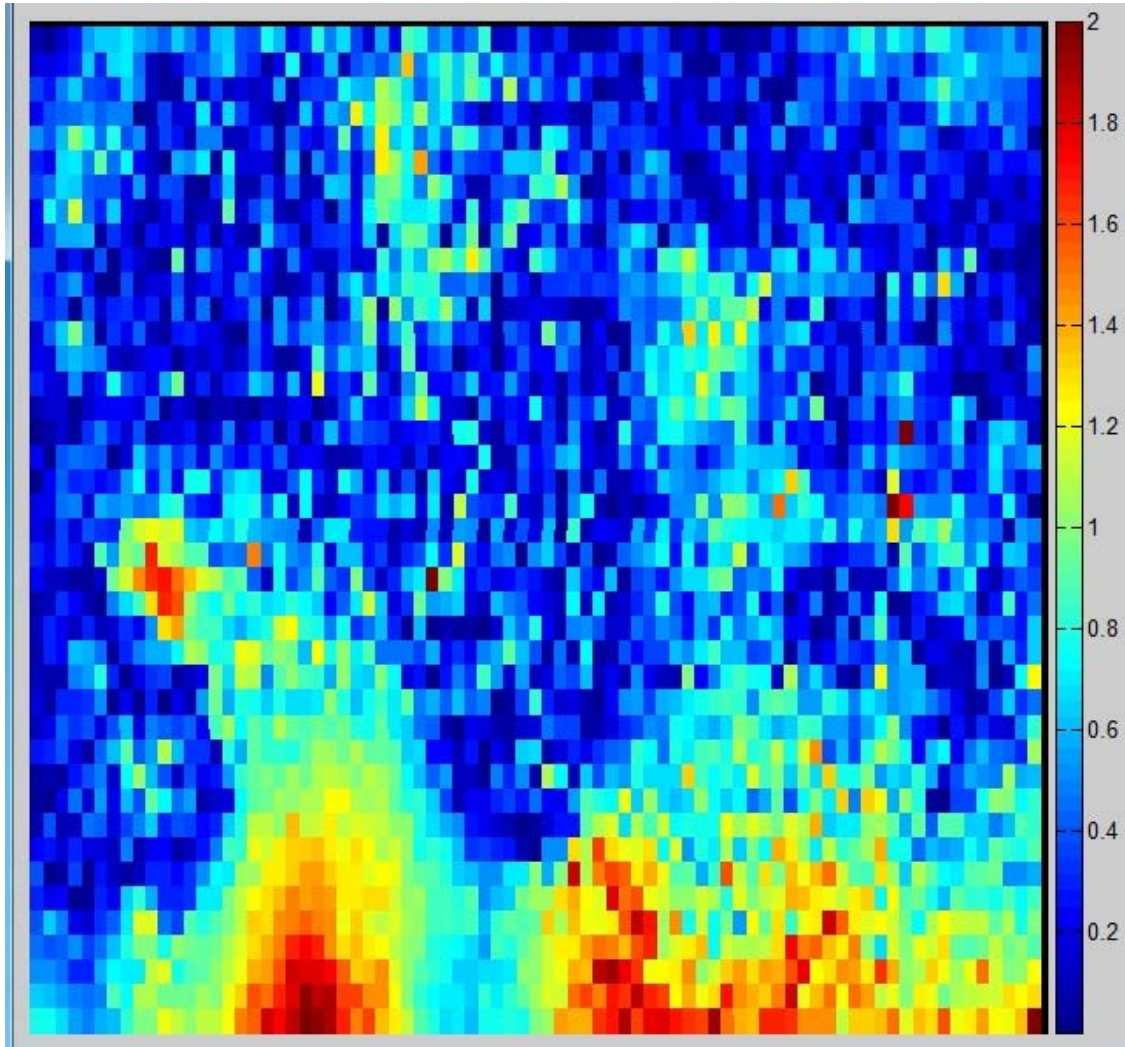
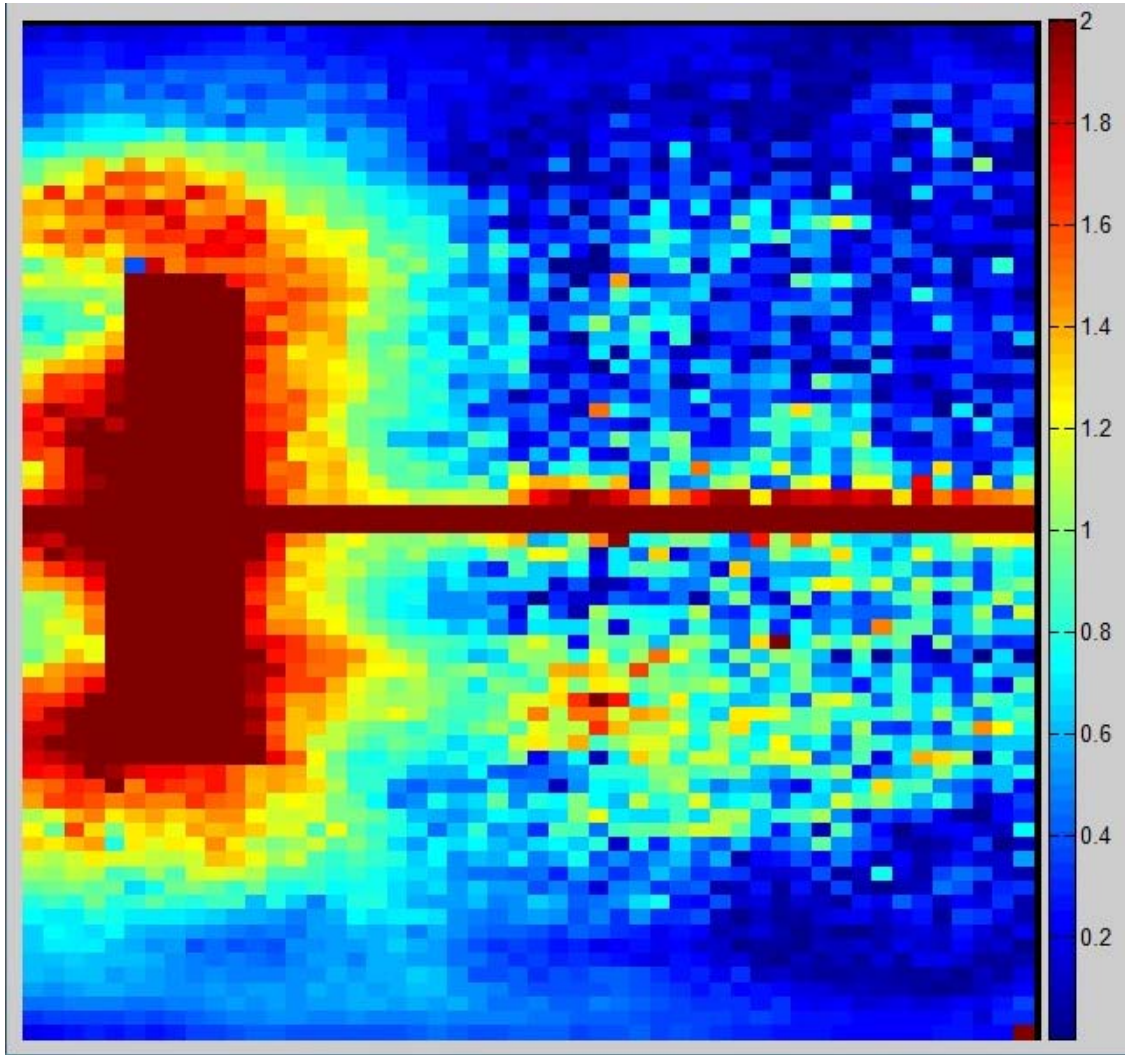


Figure 3-5 Axial gamma analysis (5%/3mm) of third Elekta VMAT treatment delivery



**Figure 3-6 Sagittal gamma analysis (5%/3mm) of third Elekta VMAT treatment delivery**

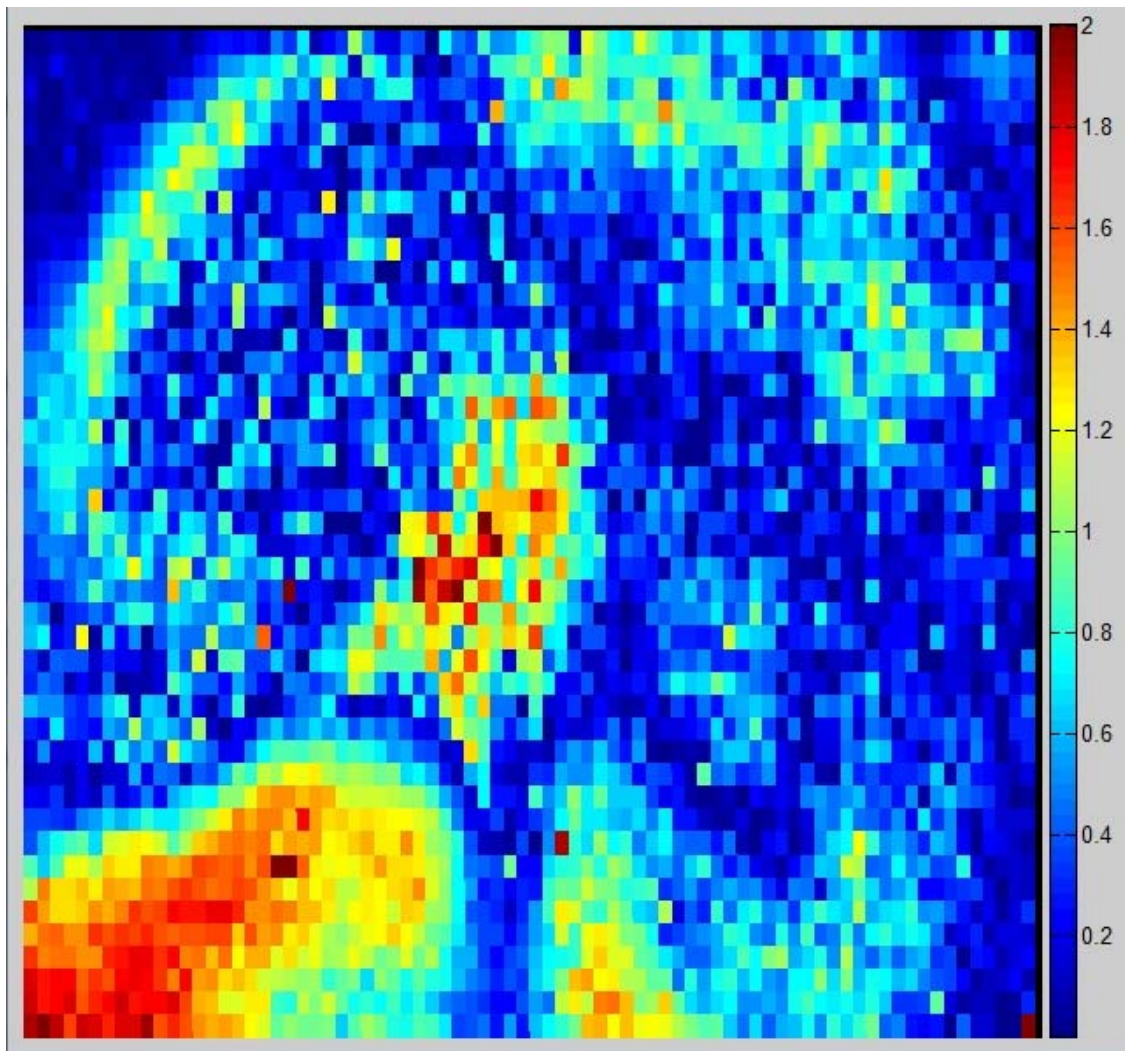


Figure 3-7 Axial gamma analysis (5%/3mm) of first RapidArc treatment delivery



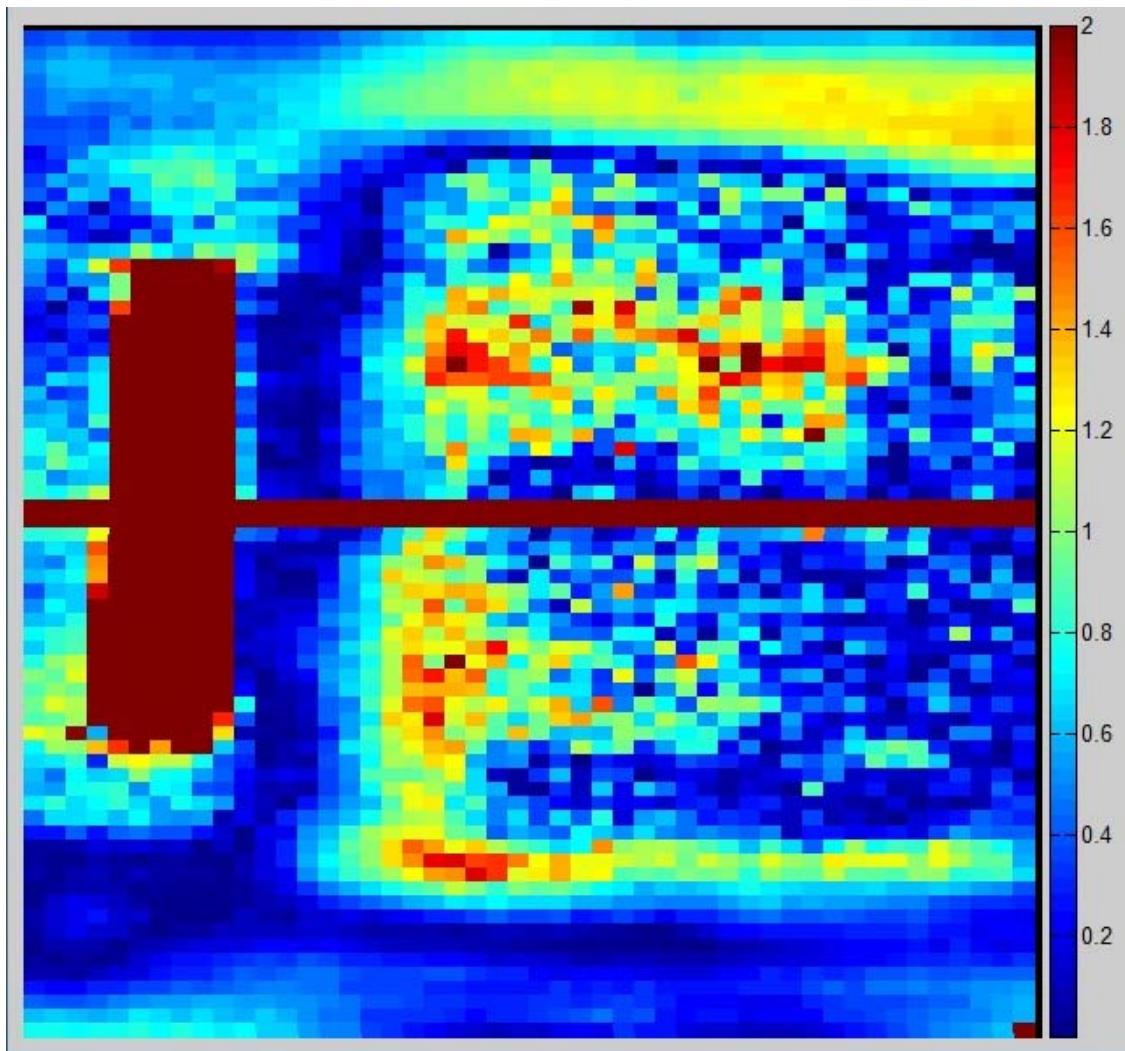
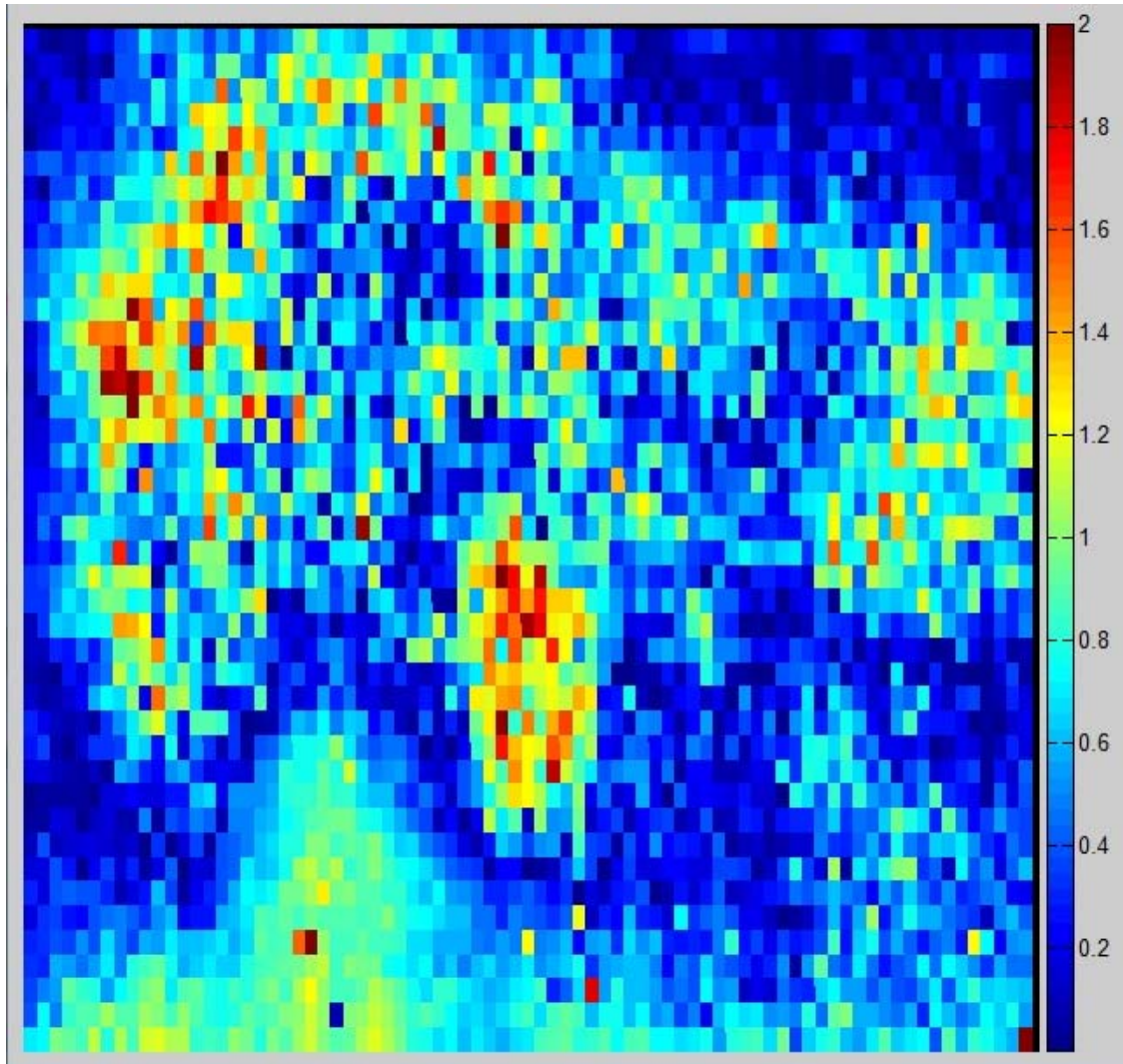


Figure 3-8 Sagittal gamma analysis (5%/3mm) of first RapidArc treatment delivery



**Figure 3-9 Axial gamma analysis (5%/3mm) of second IMRT treatment delivery**

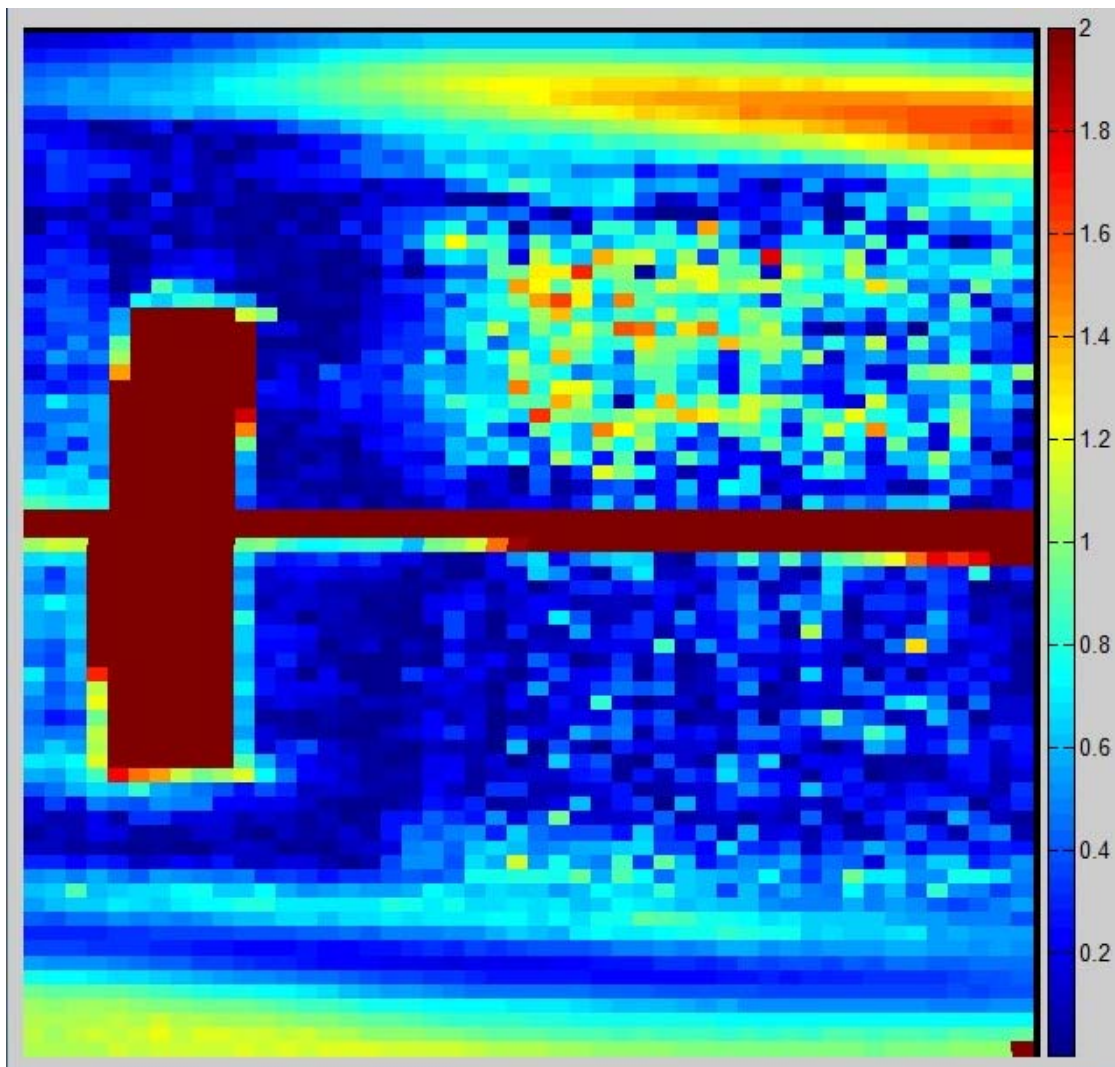


Figure 3-10 Sagittal gamma analysis (5%/3mm) of second IMRT treatment delivery

The second gamma analysis used acceptability criteria of  $\pm 7\%$  dose difference and 4 mm DTA. The results are reported in Table 3-13. These values were compared with data collected by the RPC. As of May 27, 2010, the average percent of points passing gamma analysis was 87% for all 452 institutions evaluated and 93% for the 365 institutions that were successfully credentialed by the RPC (17). The results of most irradiations of each treatment compare favorably with the national average. Only the first delivery of the Elekta VMAT treatment was lower than the national average. Only the IMRT treatment had all deliveries performing better than the national average of institutions successfully credentialed.

**Table 3-13 Percent of points passing gamma analysis with acceptability criteria of 7% dose difference and 4 mm DTA in the axial plane bisecting the primary PTV**

Treatment	Delivery			Average
	1	2	3	
Elekta VMAT	83.7%	89.4%	92.1%	88.4%
RapidArc	91.5%	91.0%	87.3%	89.9%
IMRT	94.2%	96.9%	98.0%	96.4%

For the less stringent acceptability criteria, the percent of points passing the gamma analysis improved for all treatment deliveries. The IMRT treatments still had the highest average percent of points passing at 96.4%, while the Elekta VMAT and RapidArc had the lowest at 88.4% and 89.9%, respectively. The Elekta VMAT treatment still exhibited large variations between deliveries with the less stringent acceptability criteria.

Representative examples of the spatial distribution of the gamma analyses for one delivery of each treatment technique can be seen in Figure 3-11 through Figure 3-13. For the  $\pm 7\%$  dose difference and 4 mm DTA acceptability criteria, the regions that failed were mostly concentrated in the steep dose gradient between the primary PTV and the OAR, with some areas around the periphery of the primary PTV still having difficulty.



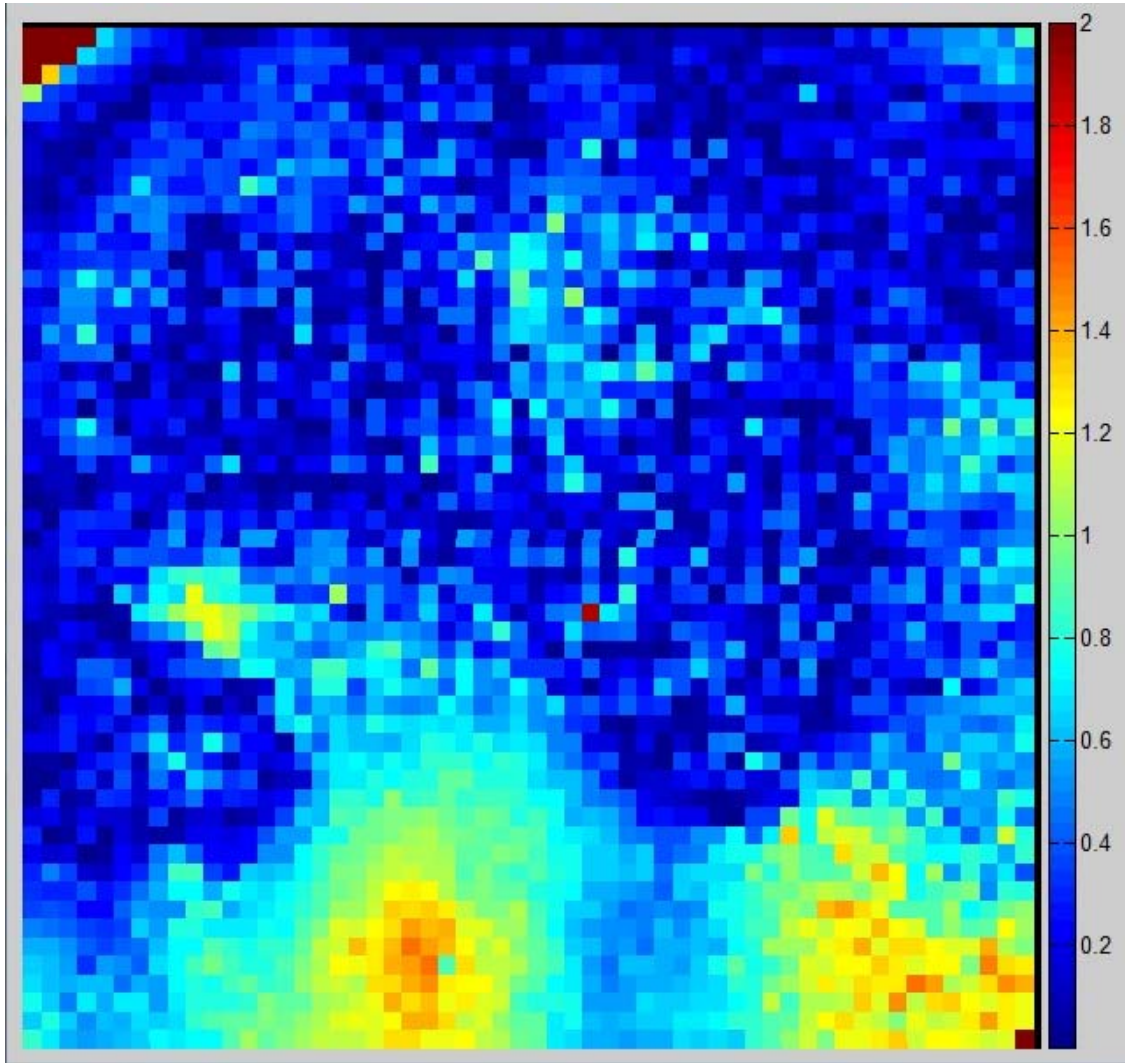


**Figure 3-11 Axial gamma analysis (7%/4mm) of third Elekta VMAT treatment delivery**



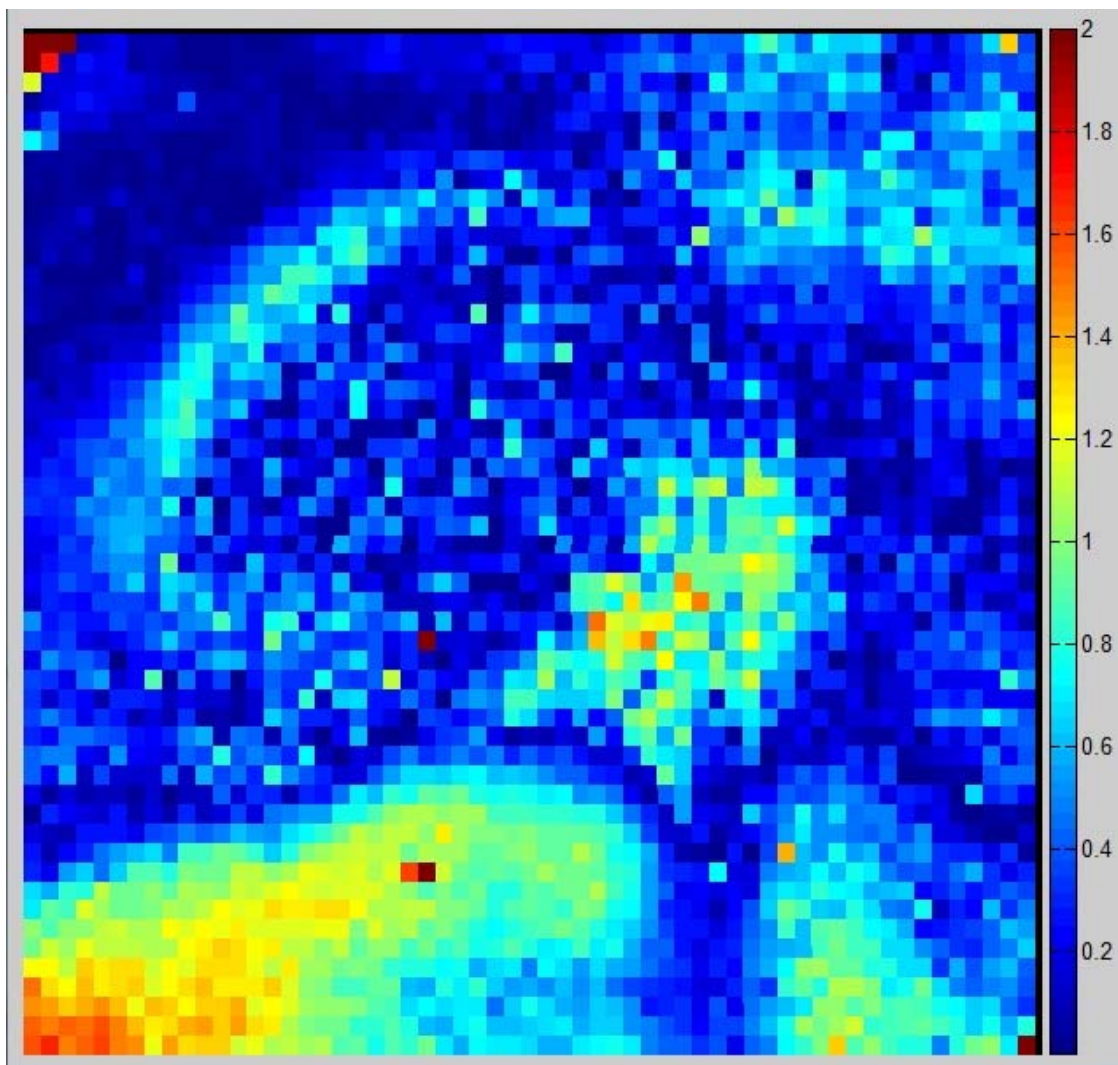


**Figure 3-12 Axial gamma analysis (7%/4mm) of first RapidArc treatment delivery**

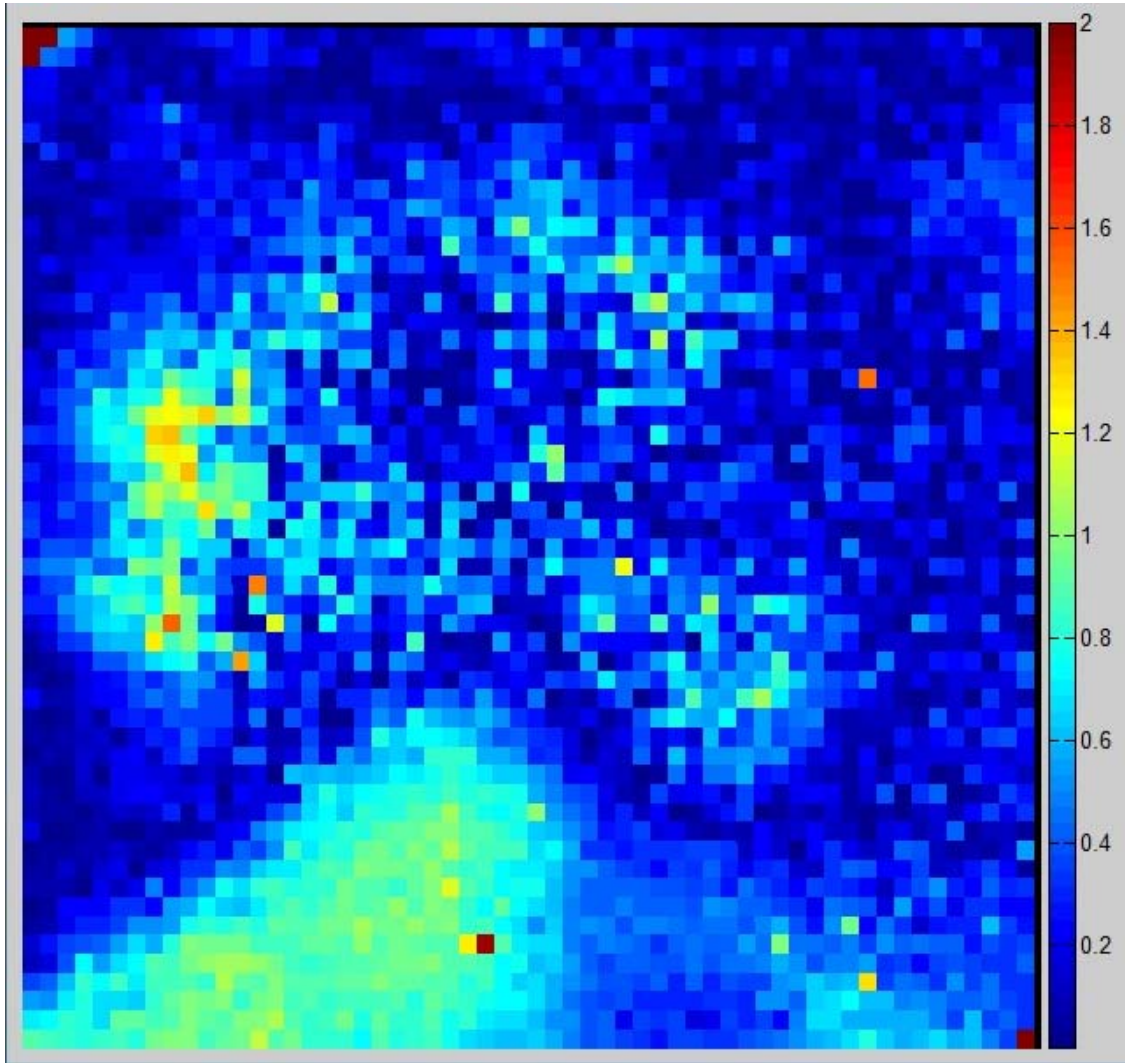


**Figure 3-13 Axial gamma analysis (7%/4mm) of third IMRT treatment delivery**

### 3.2.3 MLC Log File Analysis

The MLC dynalog files for repeated RapidArc deliveries were analyzed to explore the variation in the gamma analysis results across five treatment deliveries of the same plan. Table 3-14 and Table 3-15 show the minimum, maximum, and range of the RMS values of each moving leaf for the five treatment deliveries. Table 3-14 shows the results of the first, clockwise arc, and Table 3-15 shows the second, counterclockwise arc. Only the results of the moving leaves are shown, which included the central sixteen leaves. The RMS values of leaf deviation for the peripheral leaves were zero. The results of each carriage are shown separately.

**Table 3-14 The minimum, maximum, and range of the RMS values of leaf deviation (cm) for each moving leaf of both carriages for five deliveries of the first, clockwise arc of the RapidArc treatment**

Leaf	Carriage A			Carriage B		
	Minimum	Maximum	Range	Minimum	Maximum	Range
23	0.026	0.027	0.001	0.024	0.024	0
24	0.043	0.044	0.001	0.041	0.041	0
25	0.051	0.051	0	0.038	0.038	0
26	0.043	0.043	0	0.041	0.041	0
27	0.046	0.047	0.001	0.043	0.044	0.001
28	0.044	0.044	0	0.037	0.037	0
29	0.043	0.044	0.001	0.038	0.038	0
30	0.043	0.043	0	0.046	0.046	0
31	0.046	0.046	0	0.051	0.051	0
32	0.036	0.037	0.001	0.044	0.045	0.001
33	0.035	0.035	0	0.04	0.041	0.001
34	0.038	0.038	0	0.047	0.048	0.001
35	0.04	0.041	0.001	0.052	0.052	0
36	0.031	0.031	0	0.045	0.045	0
37	0.031	0.031	0	0.043	0.043	0
38	0.023	0.024	0.001	0.023	0.024	0.001

**Table 3-15 The minimum, maximum, and range of the RMS values of leaf deviation (cm) for each moving leaf of both carriages for five deliveries of the second, counterclockwise arc of the RapidArc treatment**

Leaf	Carriage A			Carriage B		
	Minimum	Maximum	Range	Minimum	Maximum	Range
23	0.021	0.022	0.001	0.024	0.024	0
24	0.036	0.037	0.001	0.051	0.051	0
25	0.035	0.035	0	0.044	0.044	0
26	0.041	0.041	0	0.051	0.051	0
27	0.048	0.048	0	0.051	0.051	0
28	0.043	0.043	0	0.052	0.052	0
29	0.049	0.049	0	0.056	0.057	0.001
30	0.043	0.043	0	0.047	0.048	0.001
31	0.049	0.049	0	0.04	0.04	0
32	0.044	0.044	0	0.048	0.049	0.001
33	0.046	0.046	0	0.04	0.041	0.001
34	0.051	0.051	0	0.031	0.032	0.001
35	0.046	0.046	0	0.034	0.034	0
36	0.047	0.047	0	0.032	0.032	0
37	0.041	0.042	0.001	0.03	0.031	0.001
38	0.028	0.028	0	0.026	0.027	0.001

The RMS values of the individual leaf variation remained mostly constant across all deliveries. The RMS leaf deviation varied at most 0.01 mm across all deliveries. The RMS values of leaf deviation for the moving leaves for each treatment delivery are shown in the Appendix in Table 5-1 and Table 5-2.

## **Chapter 4    Discussion**

### **4.1    General Discussion**

Our results indicate that the two VMAT techniques evaluated in this study have the ability to generate plans of comparable quality as IMRT while delivering the calculated dose distributions within acceptable tolerances for complex treatments, such as head and neck radiotherapy. Clinics may choose to use these VMAT techniques in lieu of IMRT for various treatment sites in order to reduce the total time of treatment for the patient and potentially reduce the MU necessary for some treatment sites (4-7). However, each clinic should make treatment decisions based on their specific requirements and should perform their own thorough QA of whichever treatment technique they choose. Also, because of the differences in the TPS, thorough treatment planning studies should be conducted to determine what treatment is best for their specific clinic and even for specific patient cases.

In treatment planning studies, it is important to remember that they are not entirely objective. The results are influenced by several factors, including the abilities of the person planning treatments, the techniques used, the treatment site and geometry, and the time spent on a plan. As a result, plans of varying quality can be generated for the same patient using the same treatment planning system. These subjectivities of treatment planning confound the investigation of TPS performance.

Although treatment planning studies are partially subjective, the treatment planning differences in conformity and uniformity seen between the plans may be attributed to the planning objectives available in each TPS. In Pinnacle<sup>3</sup>, where the dose distribution was more uniform in the treatment volumes, the target dose objectives can be set to achieve uniform dose at a specified prescription. In Eclipse, there is no uniform dose objective, just a minimum dose objective. In order to increase the uniformity of the target dose, a maximum dose objective can be specified. Eclipse

also has a normal tissue objective which attempts to improve the dose falloff from the target volume, but Pinnacle<sup>3</sup> does not. These differences in dose objective specification may explain the tradeoff between uniformity and conformity in the treatment plans produced by Pinnacle<sup>3</sup> and Eclipse, respectively; however, this needs to be verified through further testing.

As for the dosimetric accuracy results, the measured doses delivered by the Elekta VMAT and RapidArc techniques were consistent with the calculated doses, however the IMRT measurements corresponded to their calculation better overall. The DTA agreement of the posterior penumbra of the primary PTV as measured from the film was greater for the Elekta VMAT treatment. Also, the percent of points passing the gamma analysis was lower for both the Elekta VMAT and RapidArc treatments. Additionally, there appeared to be greater variation between treatments in the results of the gamma analyses at the  $\pm 5\%$  dose difference and 3 mm DTA level. The simultaneous gantry rotation with varying speeds and dynamic MLC motion may be the cause of the reduced agreement. Although the MLC deviations did not seem to vary between treatments, the additional uncertainty of the gantry position, gantry rotation speed and MLC positions are compounded in VMAT treatments and could be the cause of the differences in the dose delivery from treatment to treatment. The plans evaluated in this study involved a high degree of modulation, which may have caused the linacs to utilize more MLC motion and gantry rotation speed variation than plans with less modulation. The effects of these complex motions and their uncertainties need to be fully understood for QA and should be further investigated.

The literature, for the most part, is in agreement with the findings of these studies. Several planning studies have been conducted for VMAT techniques utilizing two arcs and found that they were equivalent to IMRT. One study by Rao, et al. has found that Elekta VMAT planned with Pinnacle<sup>3</sup> SmartArc generated plans that were comparable in target coverage and critical structure sparing to IMRT for six prostate and six head and neck patient cases (7). A study by Verbakel, et al.

has concluded that RapidArc was similar to seven field sliding window IMRT for twelve head and neck treatments that, like our study, had a primary and secondary PTV prescription (6). They found that the sparing of the OAR was similar, but that the RapidArc plans were significantly less conformal. In their study, they used an older version of Eclipse that could not simultaneously optimize two arcs, which could explain why our results found consistent conformality between RapidArc and IMRT.

One study found that RapidArc performed better than both five and nine field sliding window IMRT (4). In this study by Oliver, et al. that investigated virtual phantoms of varying geometries, they found that the RapidArc plans had better conformity and uniformity and were better able to meet the dose objectives than the IMRT plans. As mentioned before, planning studies are subjective and this could explain the different findings.

As for dosimetric accuracy, the literature has found consistently that the accuracy of VMAT treatments is clinically acceptable. In studies of Elekta VMAT, it was found in two separate studies that greater than 95% of points passed gamma analysis with criteria of 3% dose difference and 3 mm DTA (5, 7). The study by Bedford and Warrington investigated prostate and lung plans using a diode array. However, they planned their treatment using in-house TPS and transferred the plans to be calculated in Pinnacle<sup>3</sup> (5). Rao, et al. evaluated prostate and head and neck cases with a two-dimensional ion chamber array and, similarly to this study, planned their treatments with Pinnacle<sup>3</sup> SmartArc (7).

RapidArc accuracy was evaluated in a Monte Carlo study by Gagne, et al. and found to be adequate for clinical use when a 2.5 mm grid was used to calculate dose in Eclipse (8). Two additional studies used measurement to verify RapidArc delivery (6, 9). In one, Korreman, et al. found that greater than 95% of points passed 3% dose difference and 3 mm DTA criteria when prostate and head and neck treatments were measured with a diode array calibrated to an ion chamber (9). The other study by Verbakel, et al. used EBT films to measure the dose of a head and

neck plan in several coronal planes and found that greater than 99% of the points passed a gamma analysis with 3% dose difference and 2 mm DTA criteria (6). In fact, both of these studies found that RapidArc performed better than IMRT.

The literature agrees with the conclusions of this study that the accuracy of VMAT techniques is acceptable. However, each study using gamma analysis has found a higher percent of points passing for stricter criteria (3% dose difference and 3 mm DTA or less). Also, some studies found, upon comparison with IMRT, that RapidArc performed better. There may be several explanations for this discrepancy. The simplest is that plans that are more challenging may affect the accuracy of treatment techniques differently. For example, in order to deliver the degree of modulation of dose necessary for more complex plans, VMAT treatments may need to utilize more gantry rotation speed variation. This variation may add additional uncertainty to the treatment. An IMRT plan would only need to increase the MU and number of segments at a static gantry angle. Furthermore, the actual behavior of the linac rotation may vary from what the TPS expects in order to deliver the plan. The plans in this study were very complex with a high degree of modulation and may yield different results for different treatment techniques.

Other reasons for the discrepancy may involve the technique of measurement. For studies involving an ion chamber or diode array, the spatial resolution is limited (5, 7, 9). In order to perform a gamma analysis, they must interpolate between measurement points, which can affect the results. For example, two studies used the Delta4 phantom, which has a spatial resolution of 5 mm in the central 6 cm by 6 cm area and 10 mm at the periphery (5, 9).

In another example, the ion chamber array used in the study by Rao, et al. had a spatial resolution of 7.6 mm and measurements were linearly interpolated to 1 mm spatial resolution. Measurements in this study were analyzing at a 3 mm DTA criterion. They noted that film measurements would be able to detect a greater degree of modulation (7). Ion chamber arrays have a



volume averaging affect that can smooth the measurements, as well. The volume of the chamber in the MatriXX array used in this study was  $0.08 \text{ cm}^3$  (7).

Our analysis used EBT2 film that was not smoothed before performing the gamma analysis. The inherent noise of these measurements may have affected the accuracy. Also, this technique has a much higher spatial resolution and does not need to interpolate measurements. Therefore, it can detect greater dose modulation.

The normalization technique used in each study may also affect the accuracy found. Many studies do not mention how they calibrate or normalize their measurements. Film is known to be a less accurate method of dosimetry and is often used for relative dose accuracy evaluation. In this study, we normalized our film measurements to TLD measurements, following RPC protocol. Absolute measurements, like ours, are more strenuous. In the study by Verbakel, et al., they used two pieces of EBT film in each measurement plane. This technique can be used to reduce the uncertainty of inhomogenous film construction (18). However, they did not mention their normalization technique, nor if they smoothed their film before comparing it to the treatment plan (6). For these reasons, it makes it difficult to compare the results of different QA measurement techniques.

Our study followed the RPC protocol to determine if the plans were delivered within acceptable accuracy tolerances. This well established protocol assesses absolute dose measurements and has been used for years to evaluate institutions internationally. Additionally, it evaluates the VMAT techniques in an extreme situation. The plans evaluated were very complex with steep dose gradients and multiple target volumes with different prescriptions. Also, it was the first study to compare different VMAT techniques head to head and offered new insight in how they perform in similar situations. The VMAT techniques we chose to evaluate involved linacs, the Varian Clinac iX and Elekta Synergy, and TPS, Pinnacle<sup>3</sup> and Eclipse, that are established and prevalent in the US.

Although this study has many strengths, there are a few limitations. The plans were generated for a phantom simulating real head and neck geometry. However, human anatomy is more

complex and diverse. This study has shown that VMAT techniques can develop plans of IMRT quality, but they may not always do so in all patient cases. Additionally, this was only a planning study and cannot fully predict patient outcomes. Prospective clinical trials are needed to determine if the effects of treatments are actually the same when VMAT is used in place of IMRT.

Overall, this study has contributed to the body of knowledge on the treatment planning capabilities of two VMAT techniques and, for the first time, has compared them. Clinicians now have more information to decide if VMAT is an appropriate treatment for their patients. It may be used to help reduce the discomfort of long treatment times and help increase throughput in a clinic (4-7). Additionally, it assures them that the treatments can be delivered with acceptable accuracy.

## **4.2 Conclusion**

In conclusion, our hypothesis that the VMAT techniques evaluated would generate plans of comparable quality to IMRT and accurately deliver the calculated dose for complex head and neck treatments was supported by the results. All treatment plans performed similarly across all metrics used to evaluate treatment plan quality with the exception of a tradeoff between dose conformity to and uniformity in the treatment volumes. The Elekta VMAT treatment, planned with Pinnacle<sup>3</sup> Smart Arc, had more uniform target dose but less conformal plans than the RapidArc and IMRT treatments, planned with Eclipse. Additionally, all deliveries of all treatments passed the RPC credentialing criteria. When compared to the average percent of points passing gamma analysis for all institutions passing head and neck IMRT credentialing, the three treatment techniques evaluated compared favorably on average.

## **4.3 Future Work**

There are many questions left about the clinical impact of VMAT treatments. The shorter treatment times, greater spreading of lower doses, and potentially fewer MU involved with VMAT

may have radiobiological and clinical effects. These should be studied for their effects on cell kill, tumor control, patient morbidity, late effects, and overall survival.

The complicated combination of the variable gantry rotation speed and dynamic MLC motion should be further investigated to fully understand their uncertainties. Similarly, the ability of the TPS to predict the gantry motion should be examined to potentially improve the dose calculation accuracy.

Lastly, there are several VMAT products available, including linacs capable of delivering VMAT treatments and TPS for VMAT planning and dose calculation, and some can be used with multiple vendors. Many combinations of these products should be investigated to encompass the full range of systems available.

## Chapter 5 Appendix

### 5.1 Treatment Plan Isodose Distributions

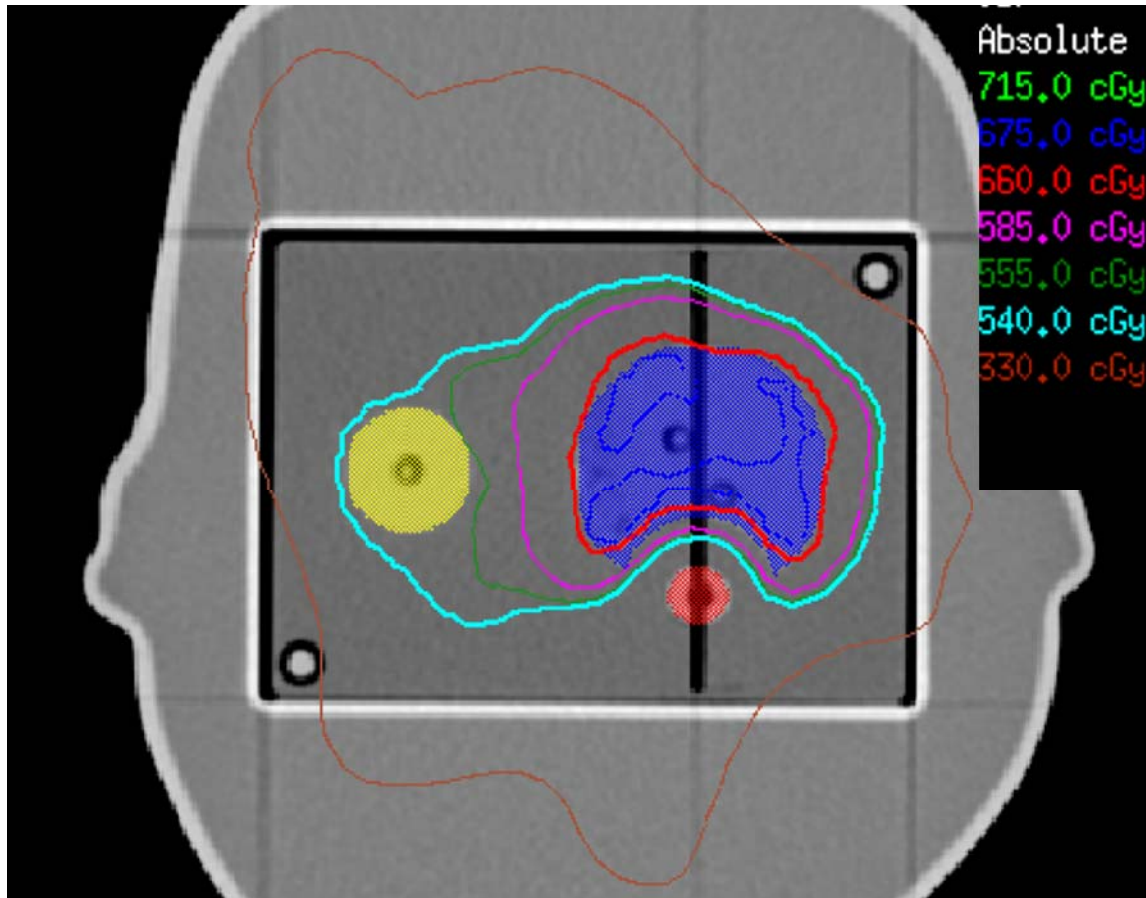


Figure 5-1 Isodose distribution of the Elekta VMAT treatment plan

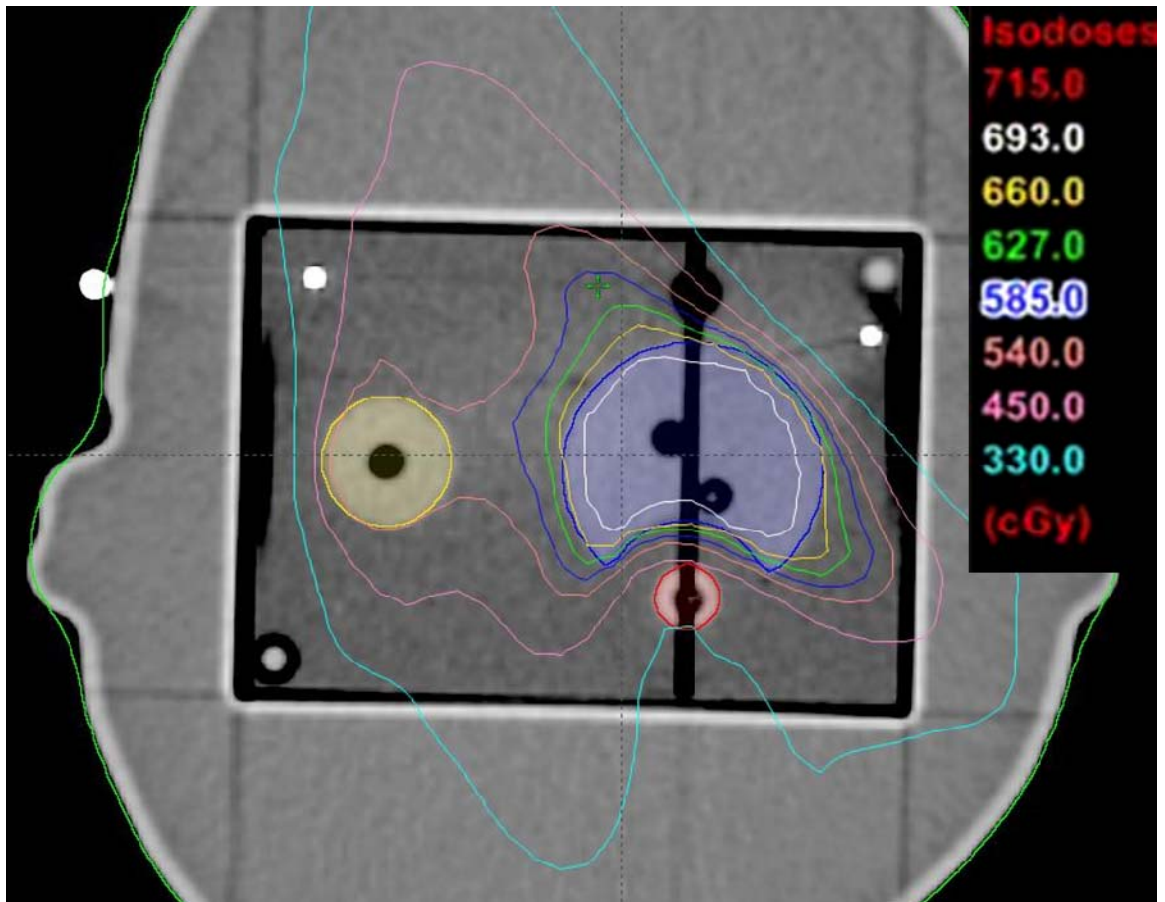


Figure 5-2 Isodose distribution of the RapidArc treatment plan

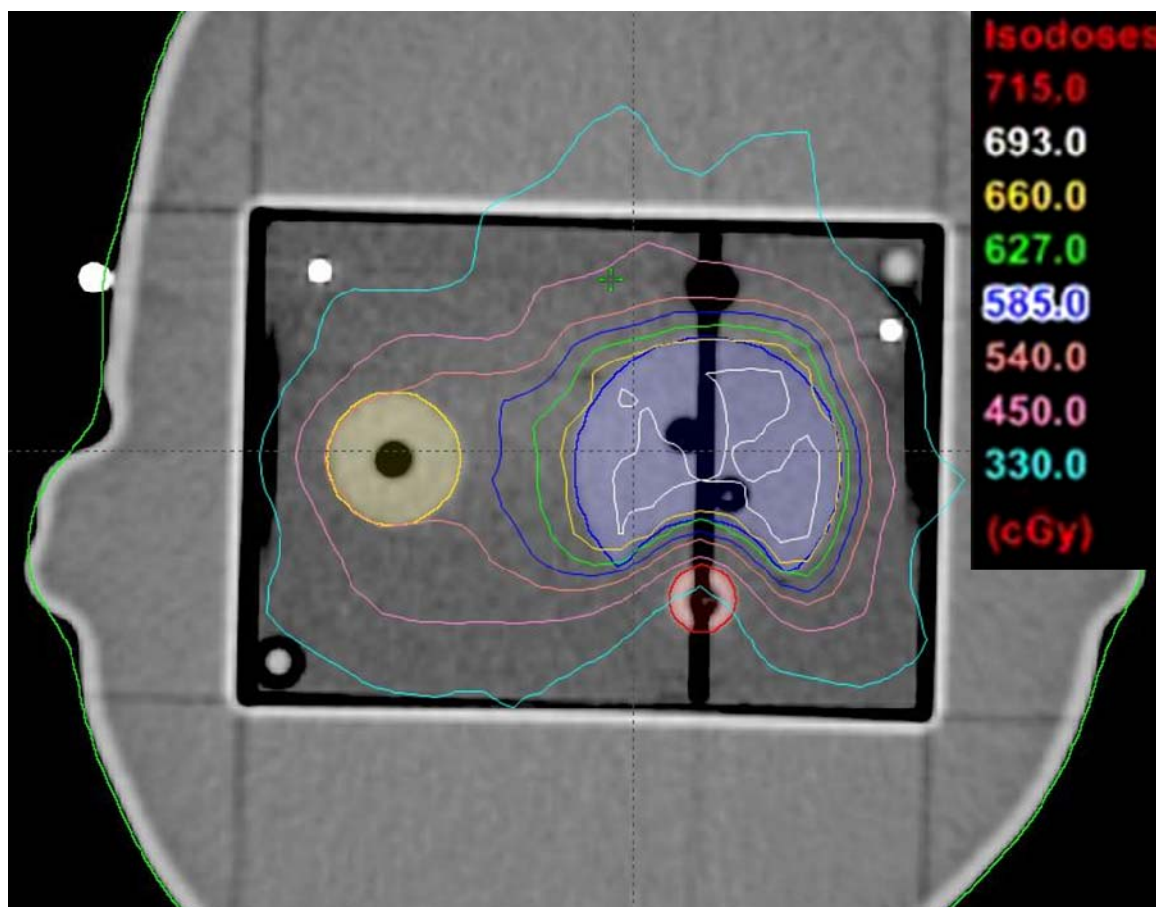


Figure 5-3 Isodose distribution of the IMRT treatment plan

5.2 Dose profiles

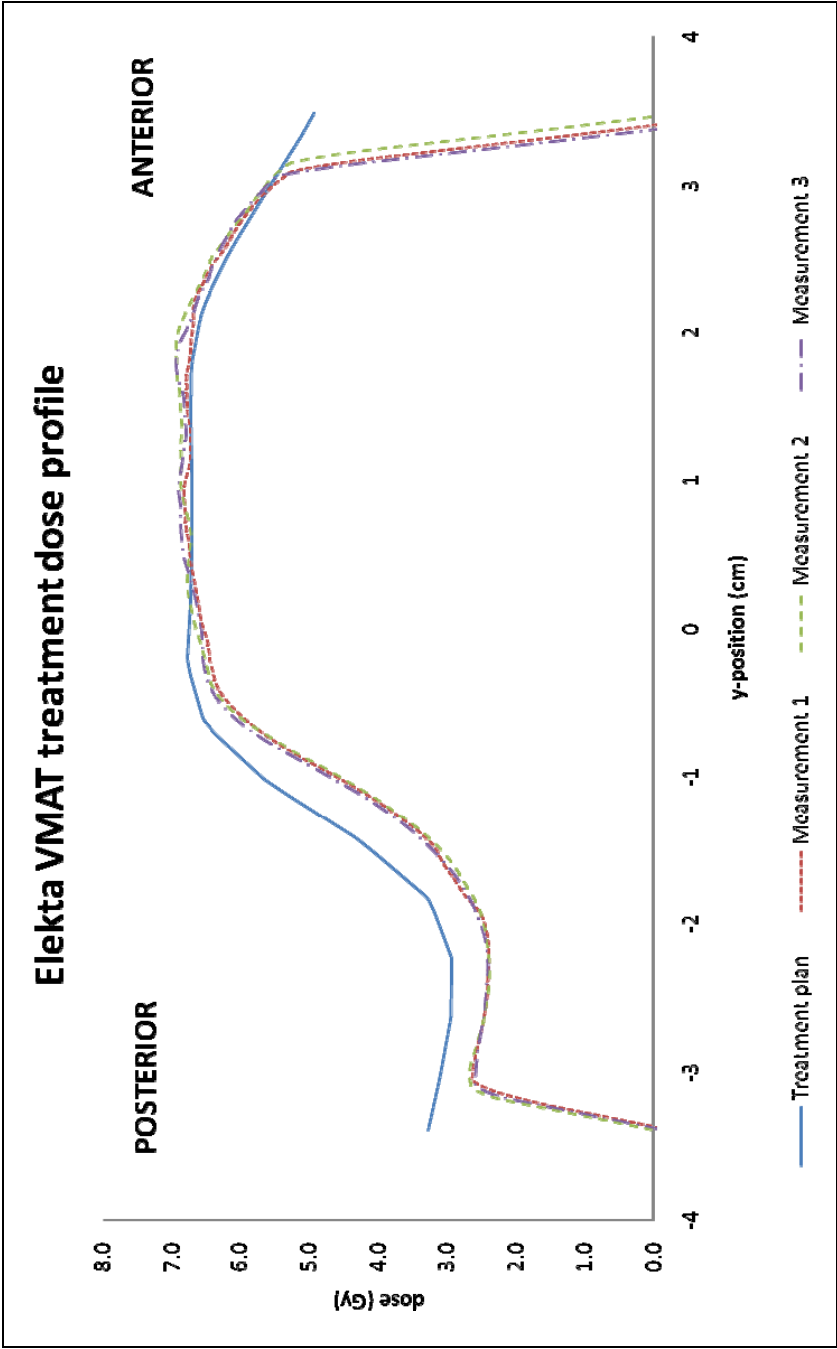


Figure 5-4 Posterior-to-anterior dose profile of the Elekta VMAT treatment

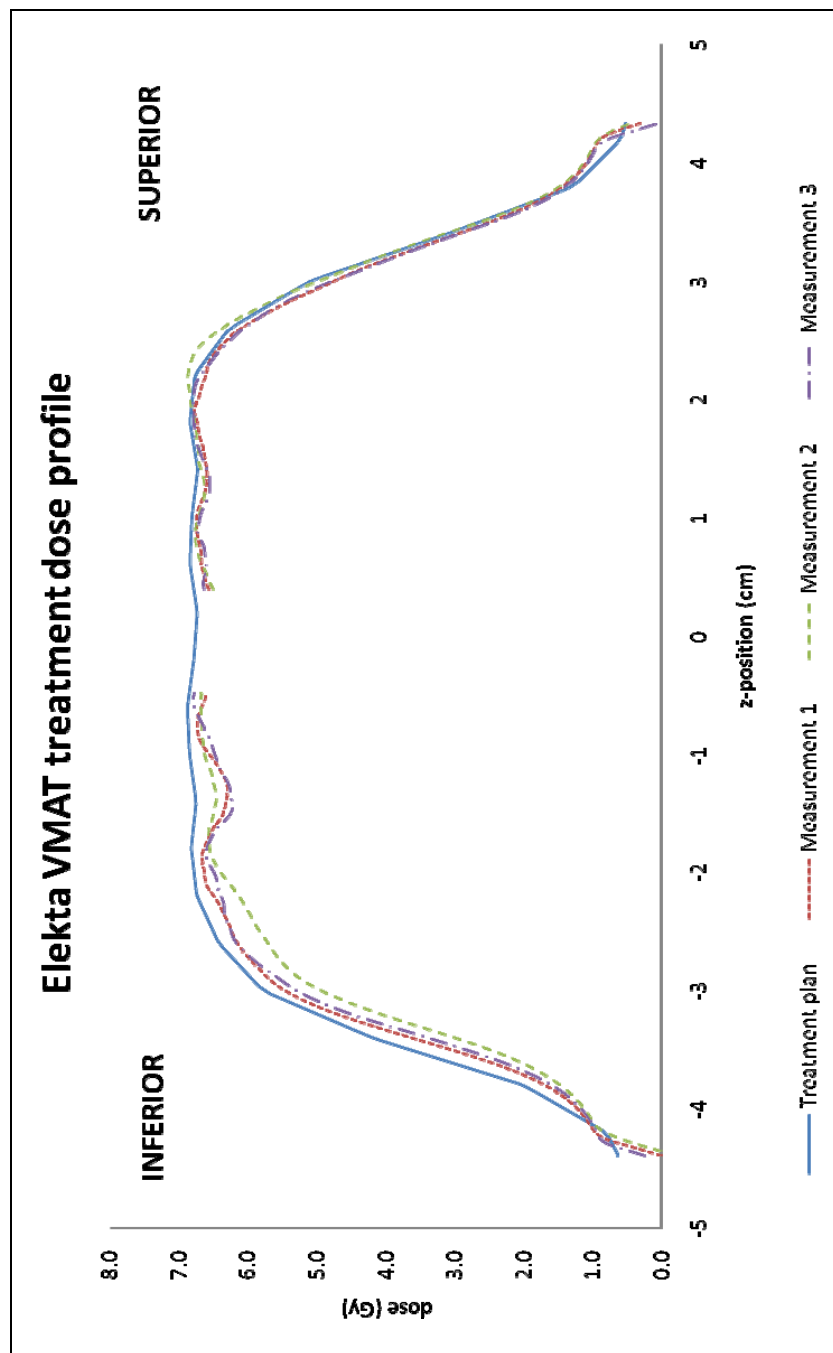


Figure 5-5 Inferior-to-superior dose profile of the Elekta VMAT treatment



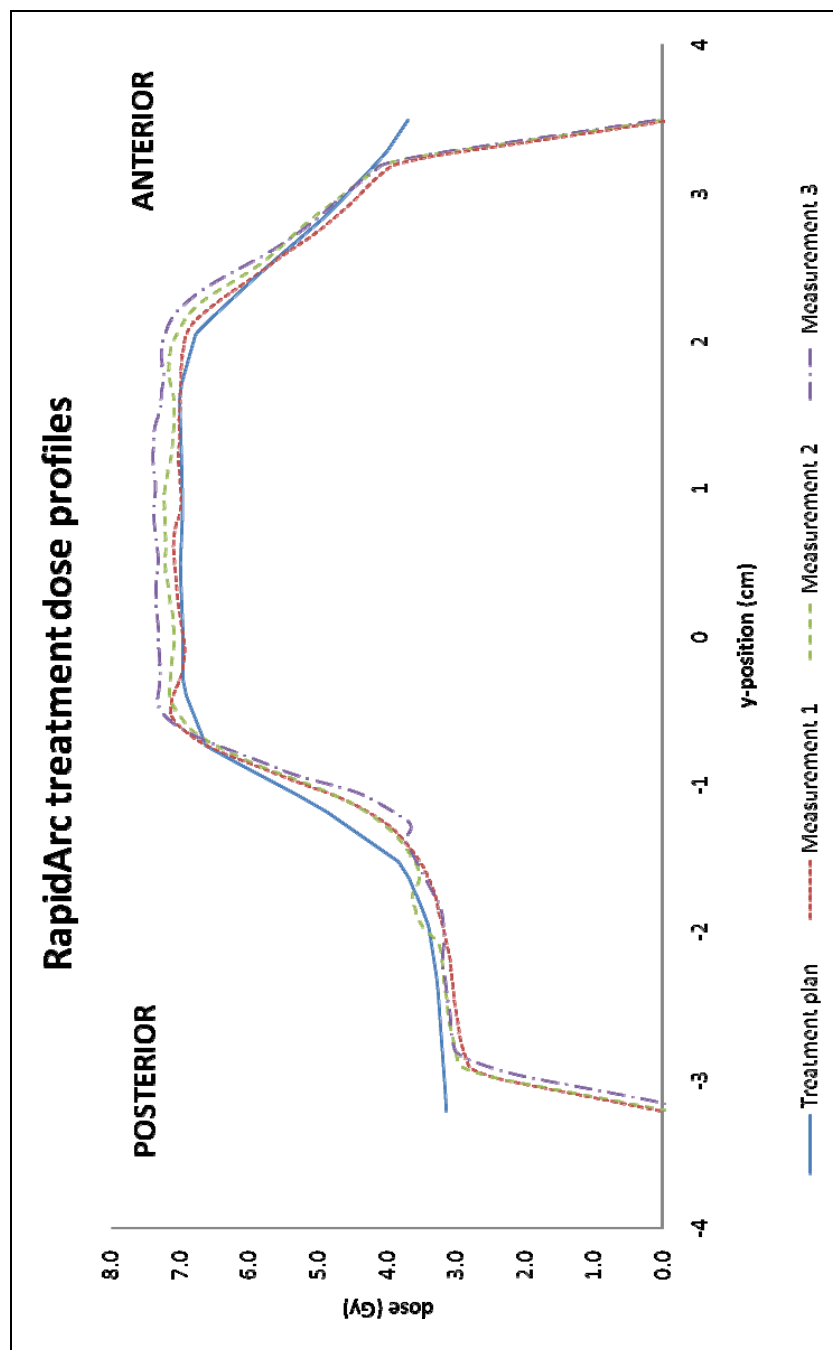


Figure 5-6 Posterior-to-anterior dose profile of the RapidArc treatment

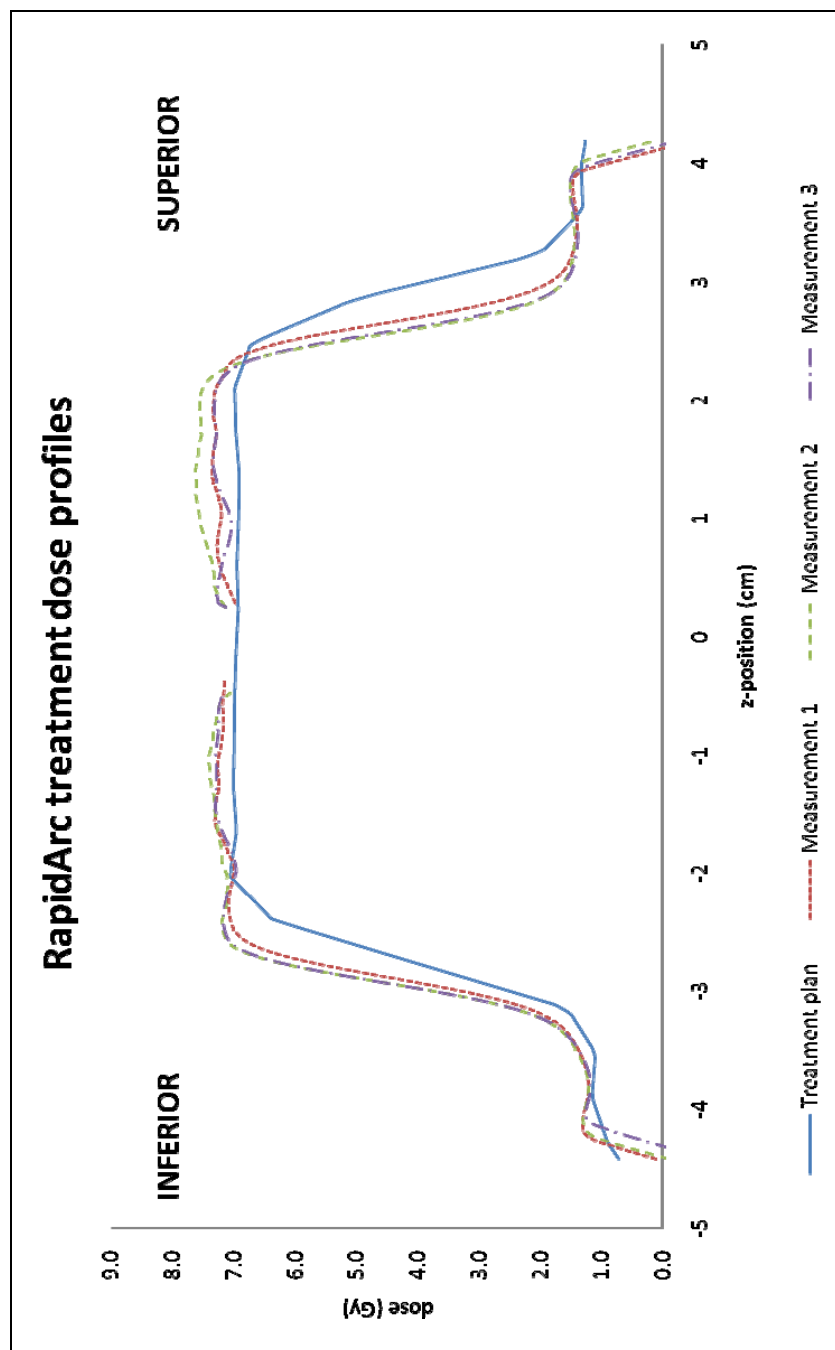


Figure 5-7 Inferior-to-superior dose profile of the RapidArc treatment

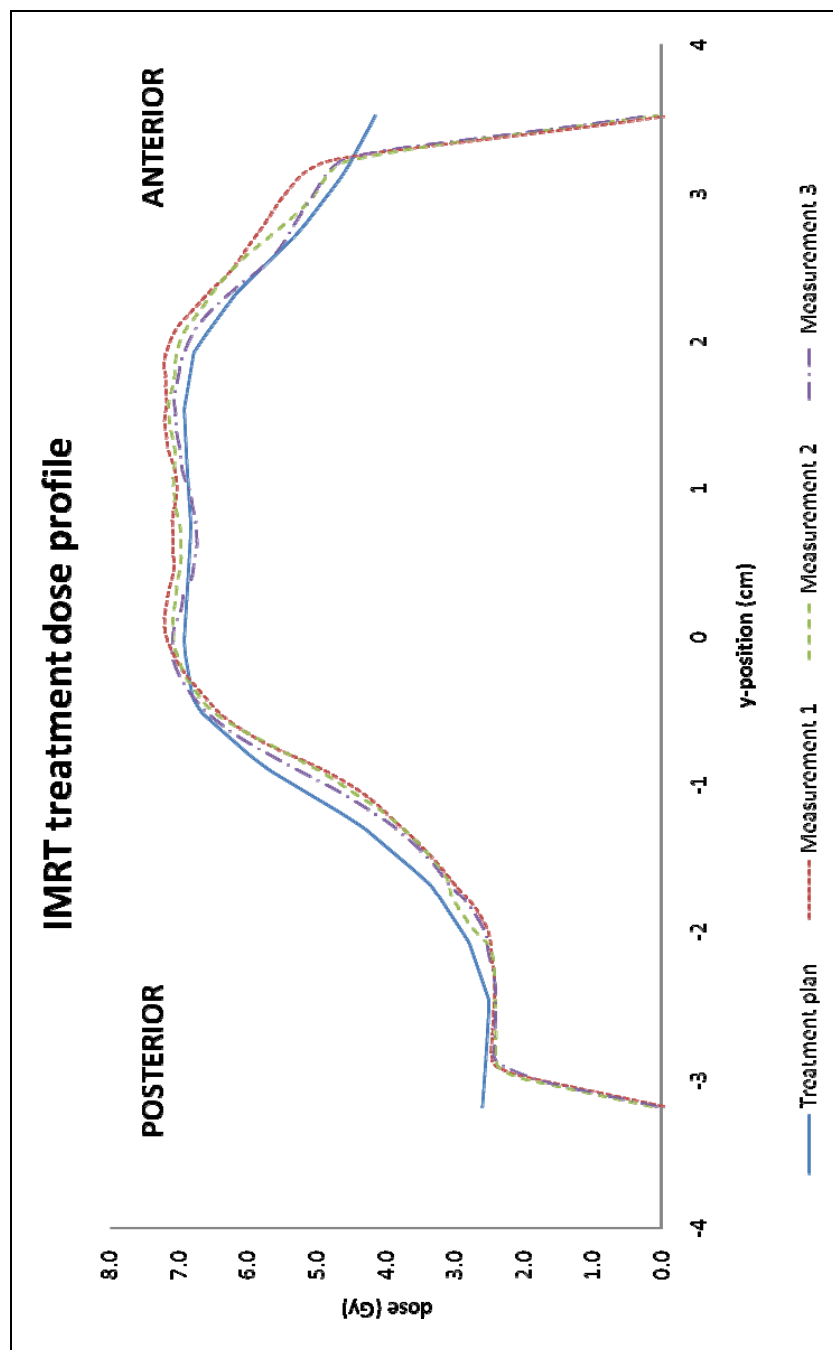


Figure 5-8 Posterior-to-anterior dose profile of the IMRT treatment

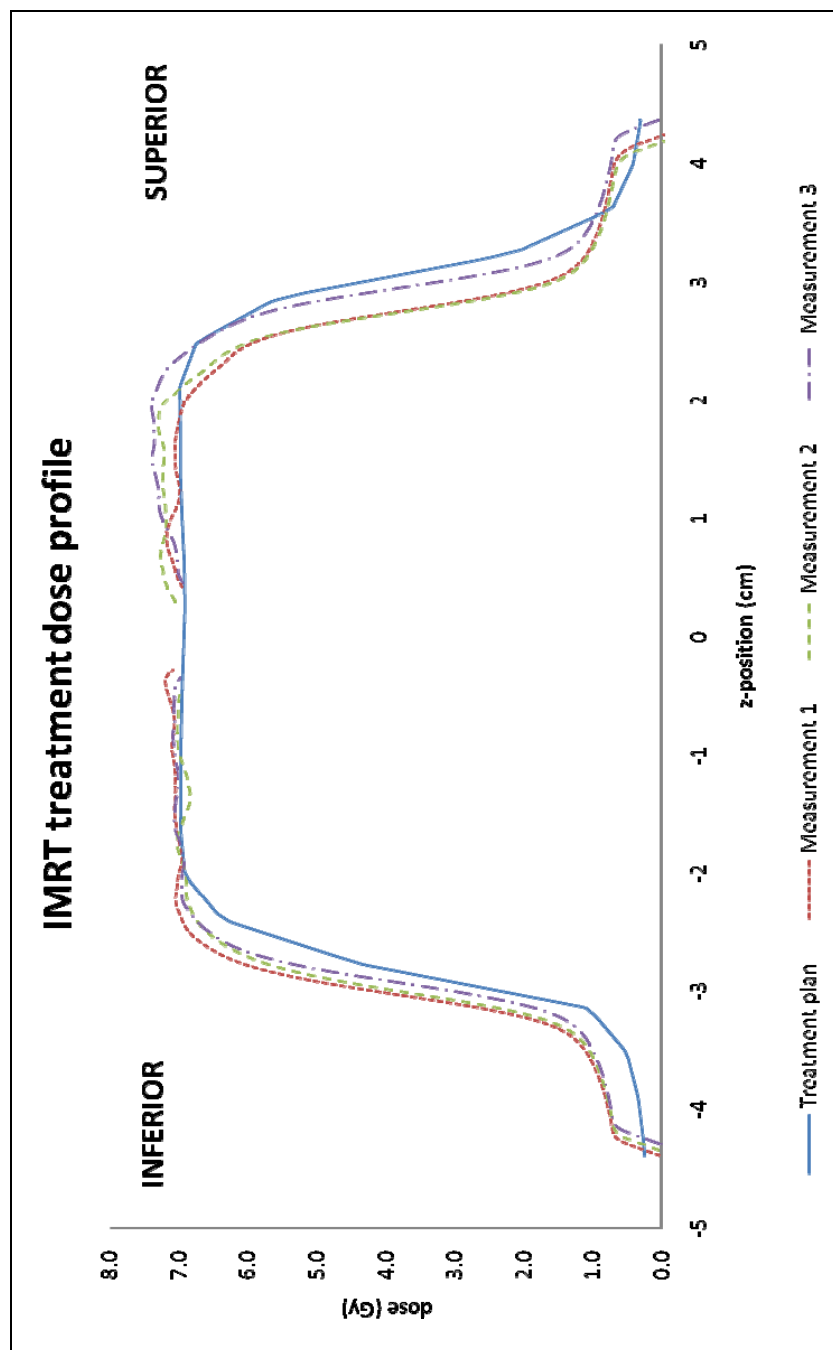


Figure 5-9 Inferior-to-superior dose profile of the IMRT treatment

### 5.3 Gamma analysis

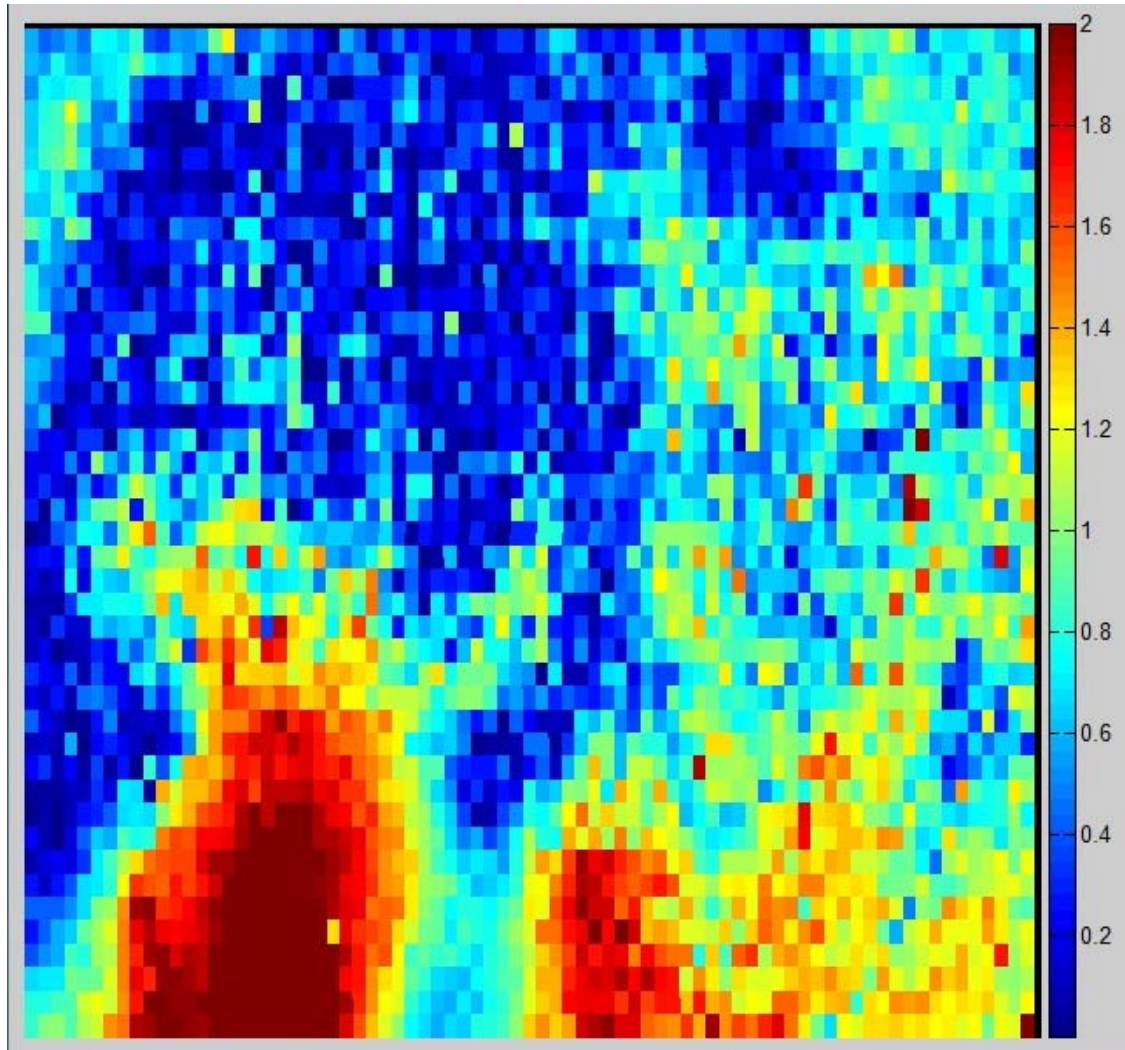


Figure 5-10 Axial gamma analysis (5%/3mm) of first Elekta VMAT treatment delivery

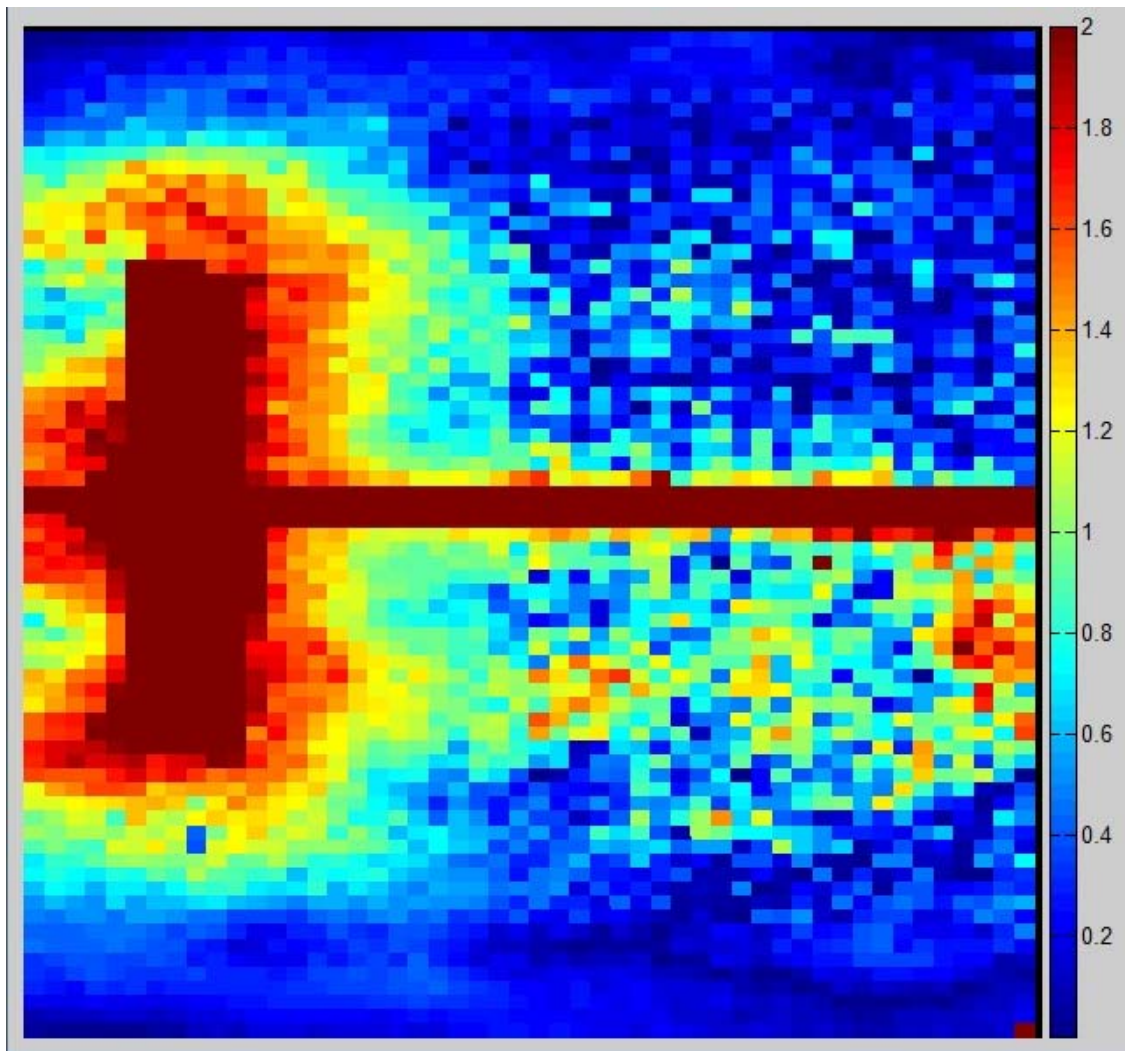


Figure 5-11 Sagittal gamma analysis (5%/3mm) of first Elekta VMAT treatment delivery



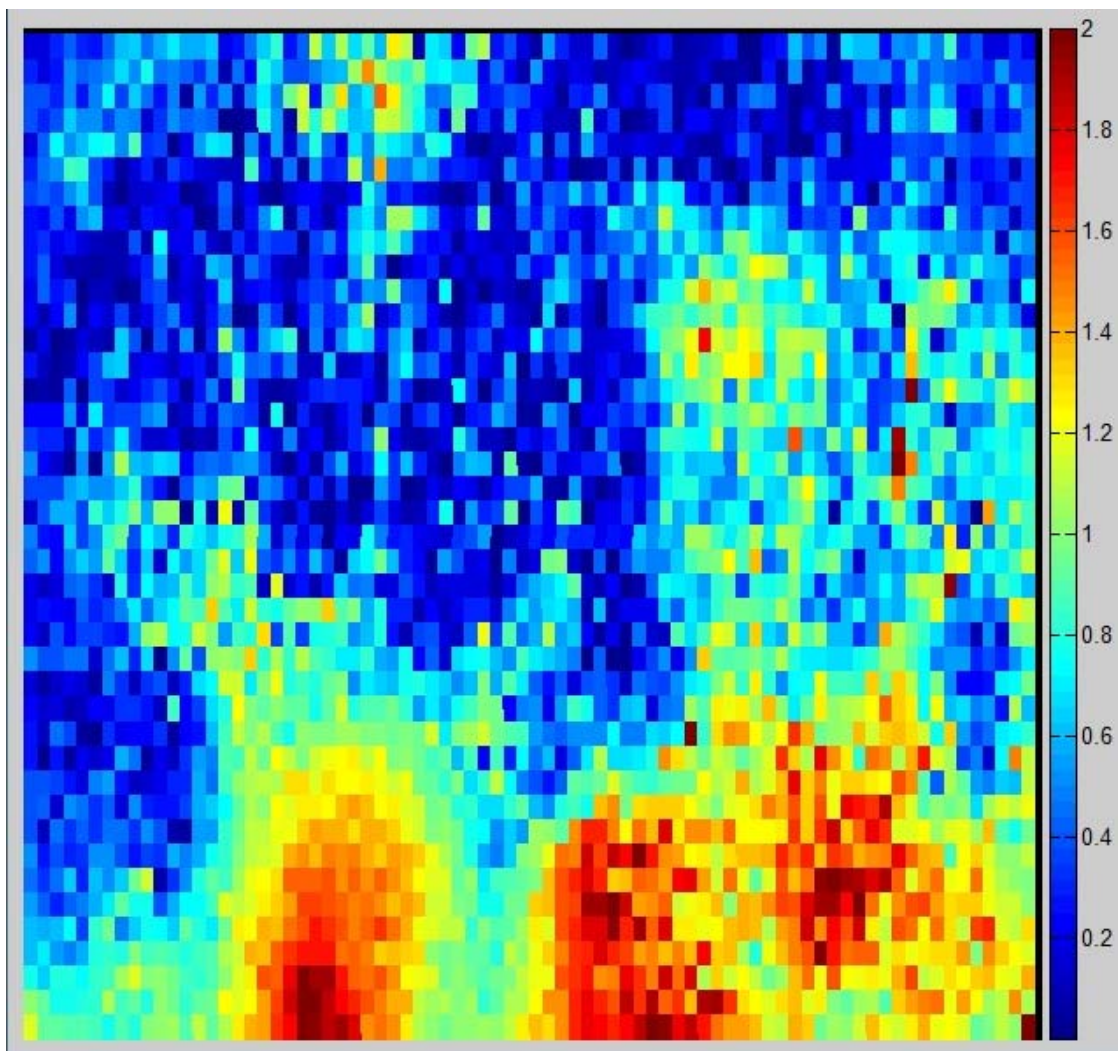
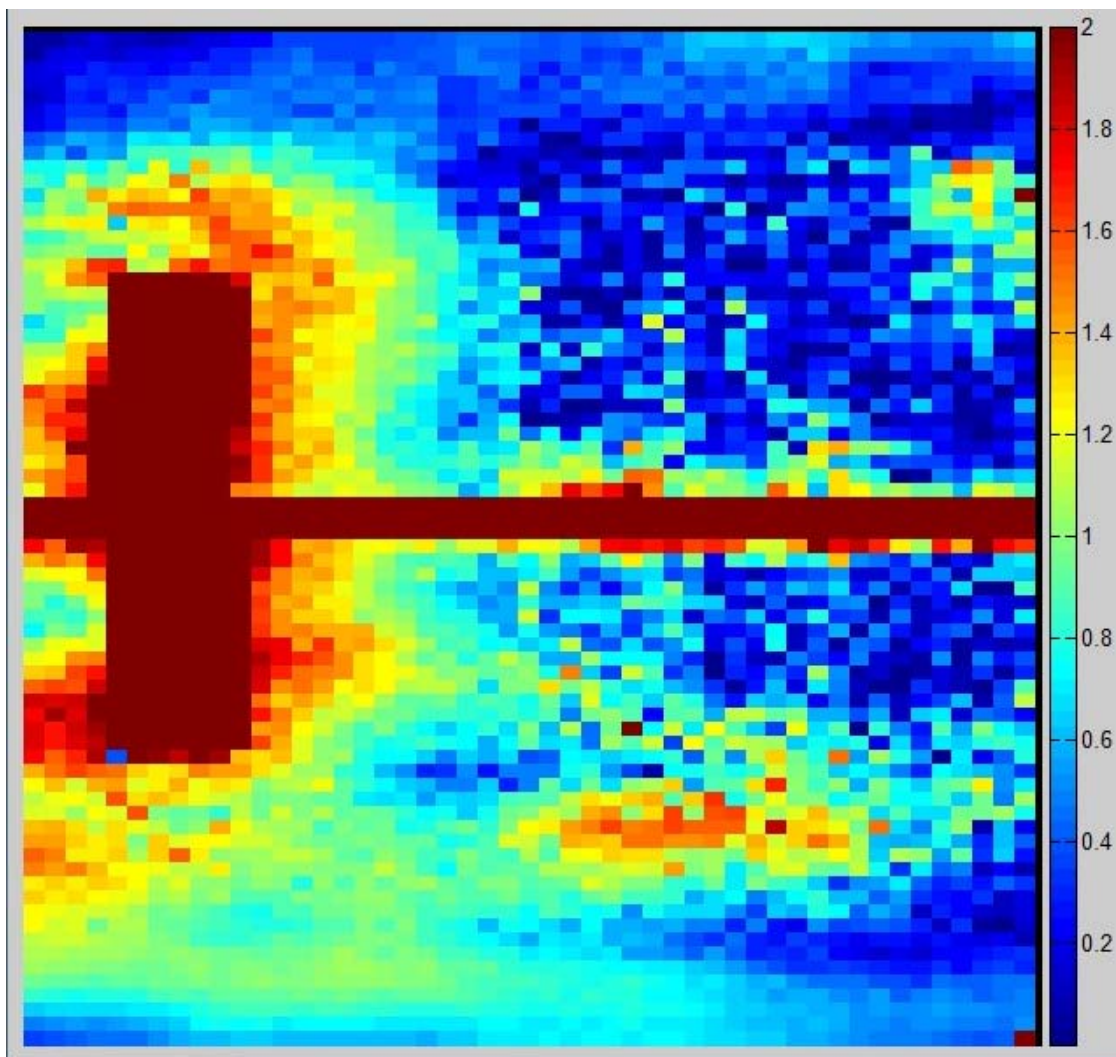
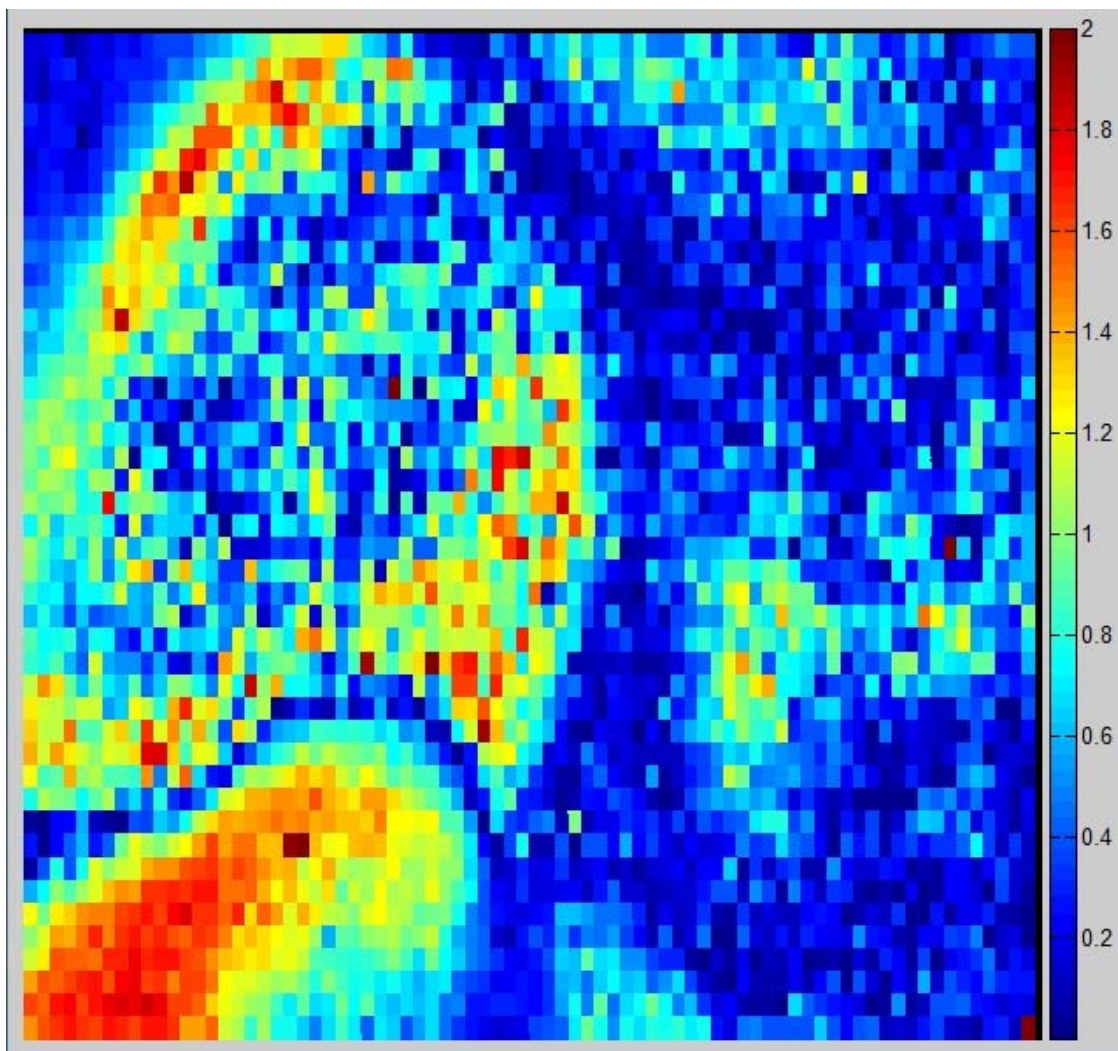


Figure 5-12 Axial gamma analysis (5%/3mm) of second Elekta VMAT treatment delivery



**Figure 5-13 Sagittal gamma analysis (5%/3mm) of second Elekta VMAT treatment delivery**





**Figure 5-14 Axial gamma analysis (5%/3mm) of second RapidArc treatment delivery**

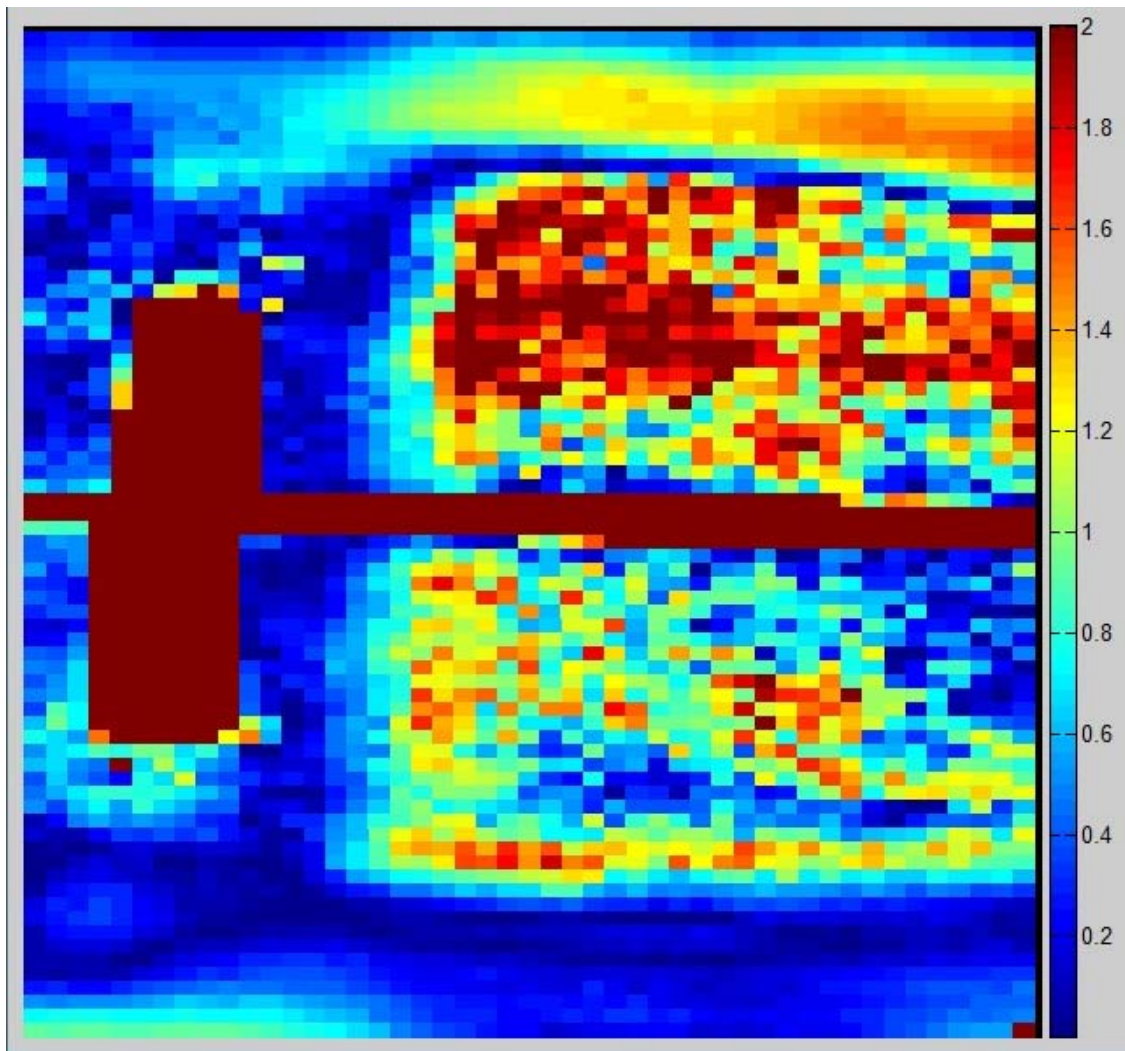


Figure 5-15 Sagittal gamma analysis (5%/3mm) of second RapidArc treatment delivery

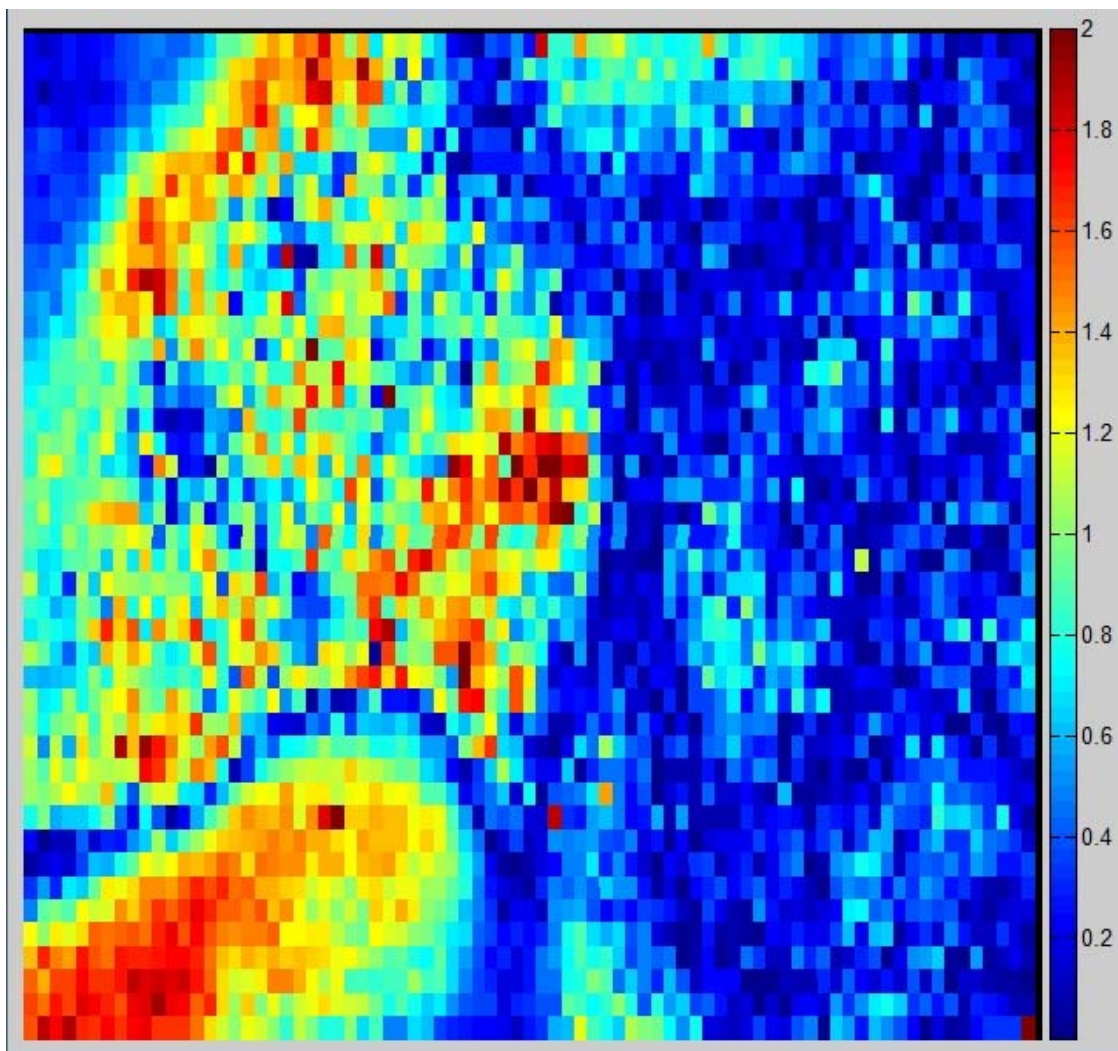
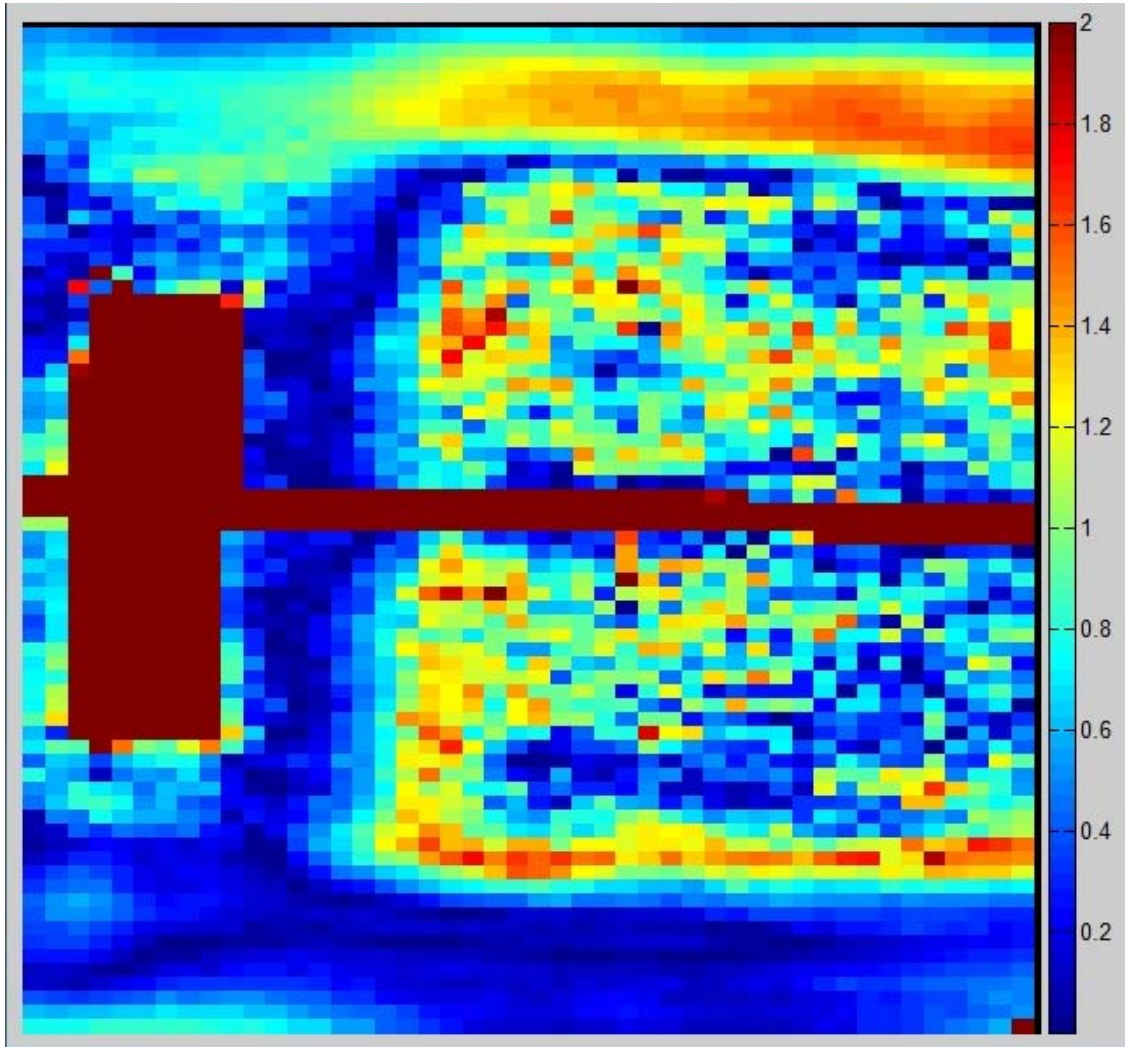


Figure 5-16 Axial gamma analysis (5%/3mm) of third RapidArc treatment delivery





**Figure 5-17** Sagittal gamma analysis (5%/3mm) of third RapidArc treatment delivery

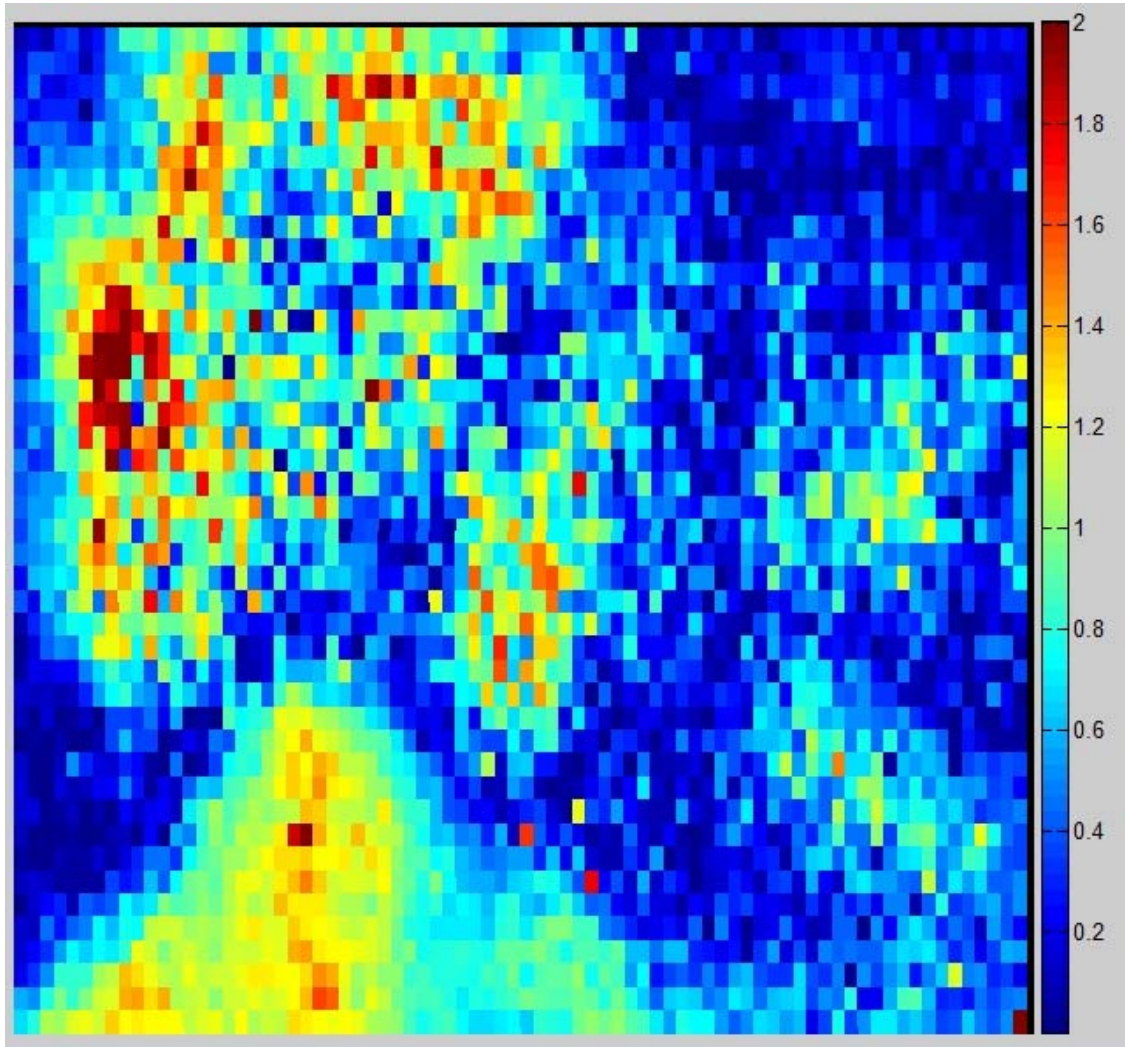


Figure 5-18 Axial gamma analysis (5%/3mm) of first IMRT treatment delivery

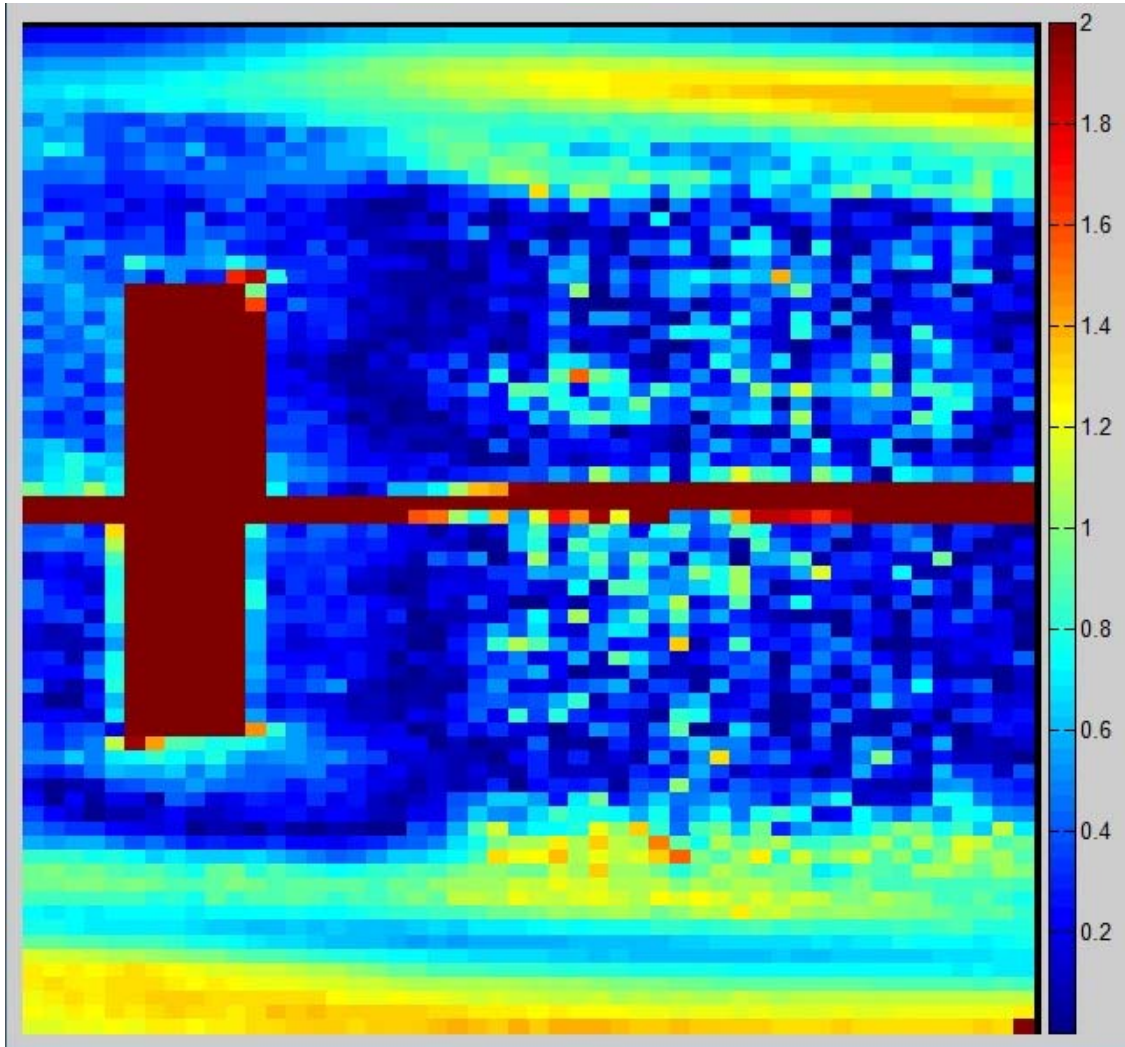
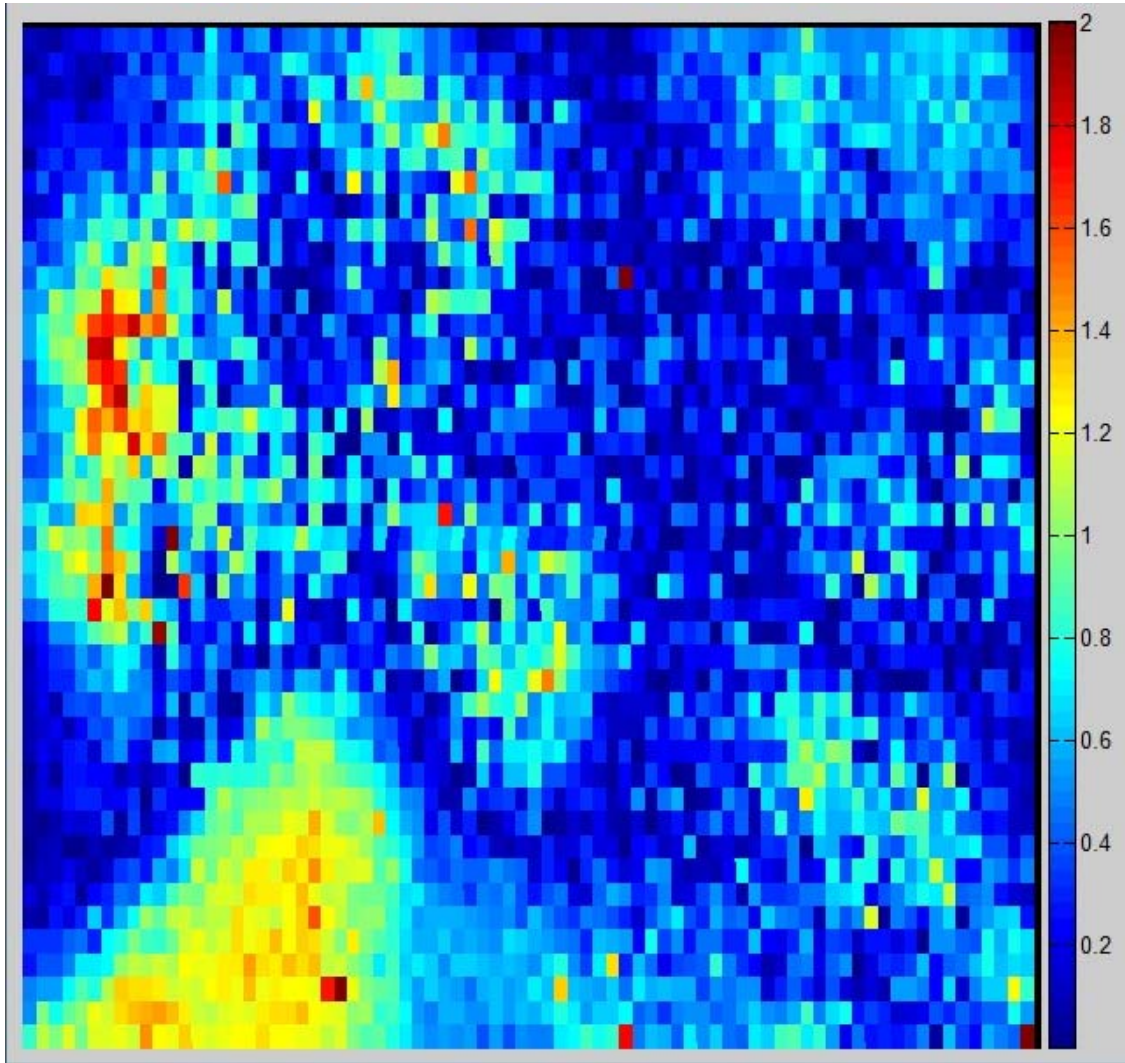
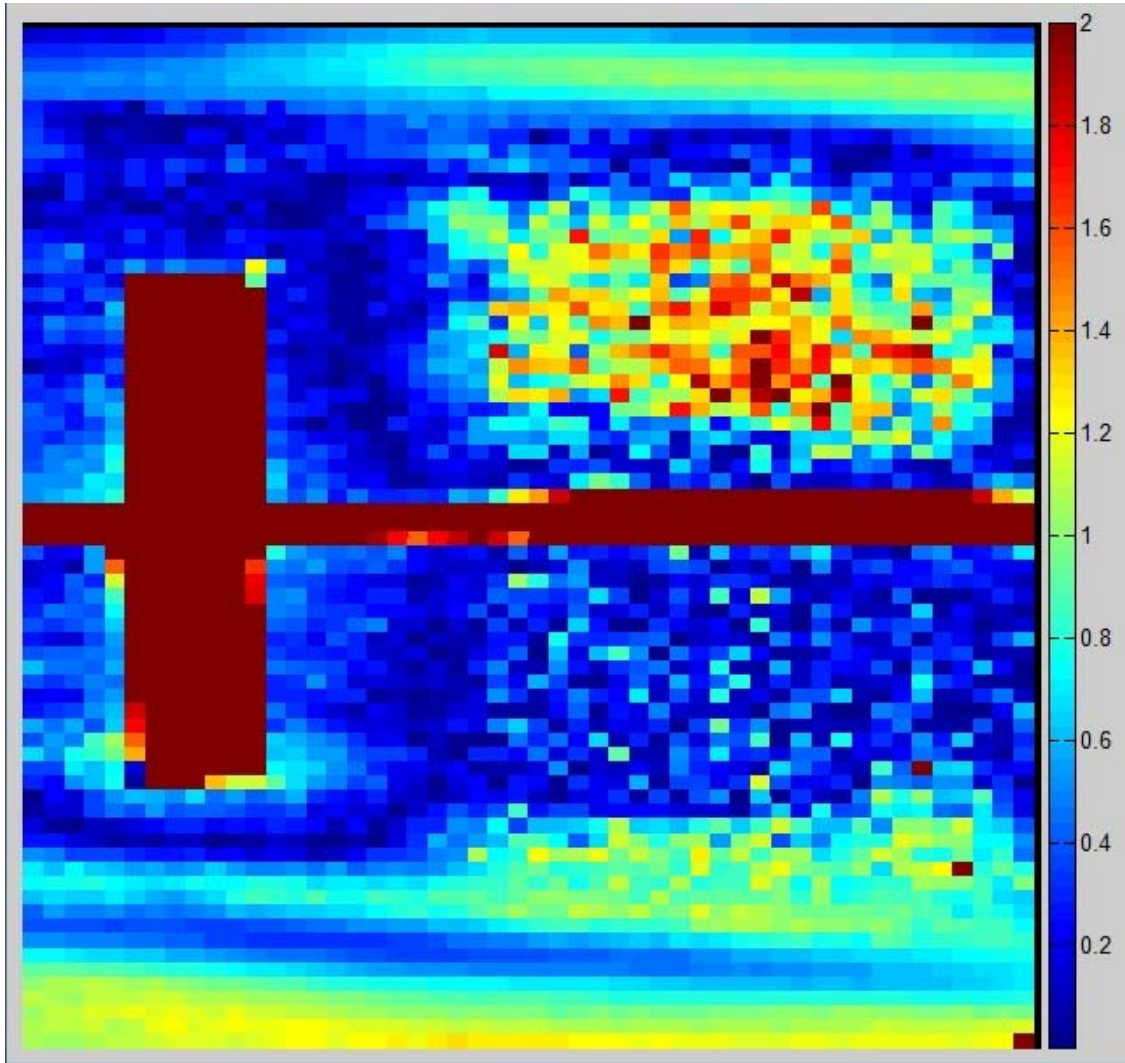


Figure 5-19 Sagittal gamma analysis (5%/3mm) of first IMRT treatment delivery





**Figure 5-20 Axial gamma analysis (5%/3mm) of third IMRT treatment delivery**



**Figure 5-21** Sagittal gamma analysis (5%/3mm) of third IMRT treatment delivery



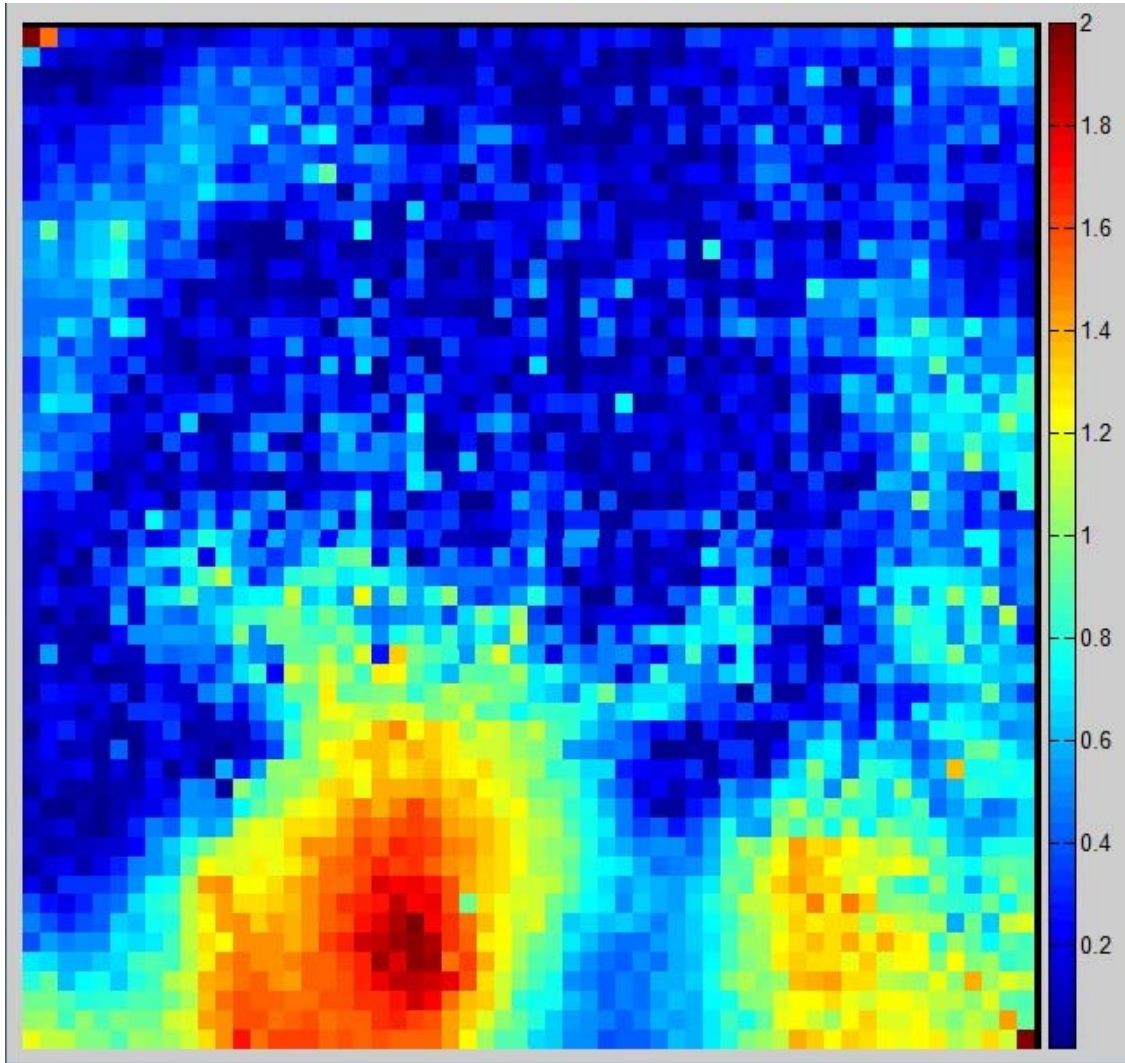


**Figure 5-22 Axial gamma analysis (7%/4mm) of first Elekta VMAT treatment delivery**

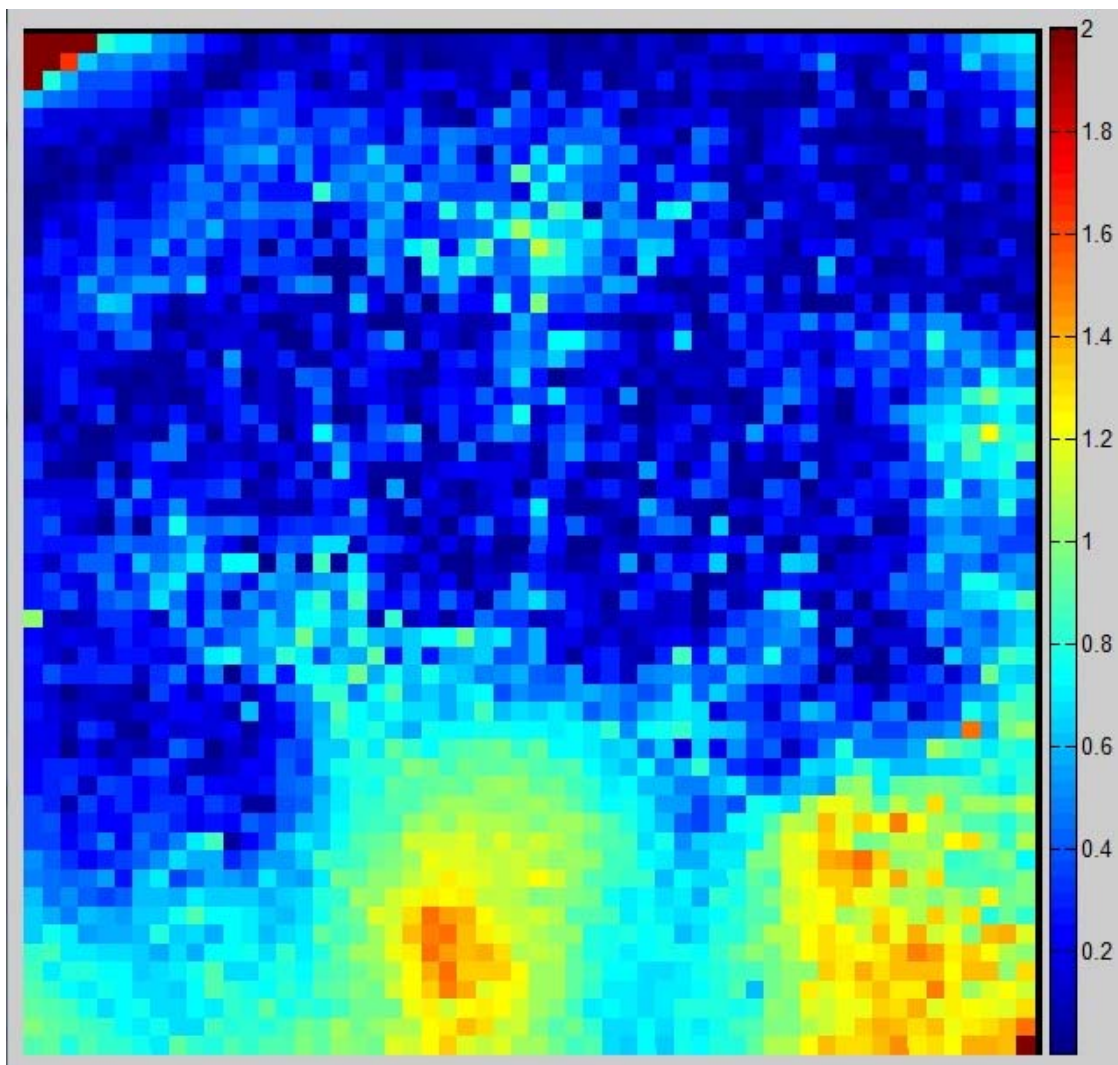
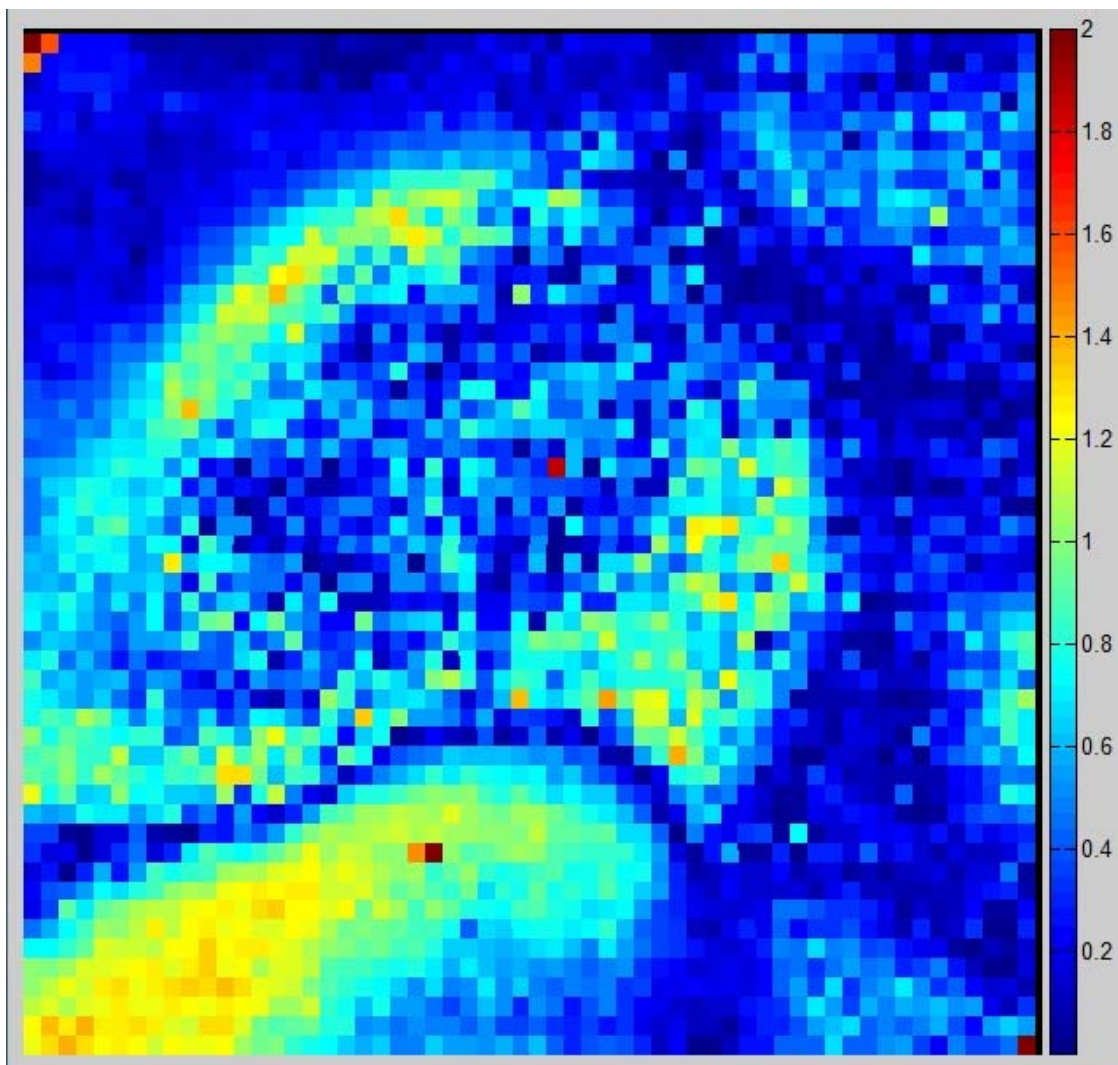


Figure 5-23 Axial gamma analysis (7%/4mm) of second Elekta VMAT treatment delivery



**Figure 5-24** Axial gamma analysis (7%/4mm) of second RapidArc treatment delivery



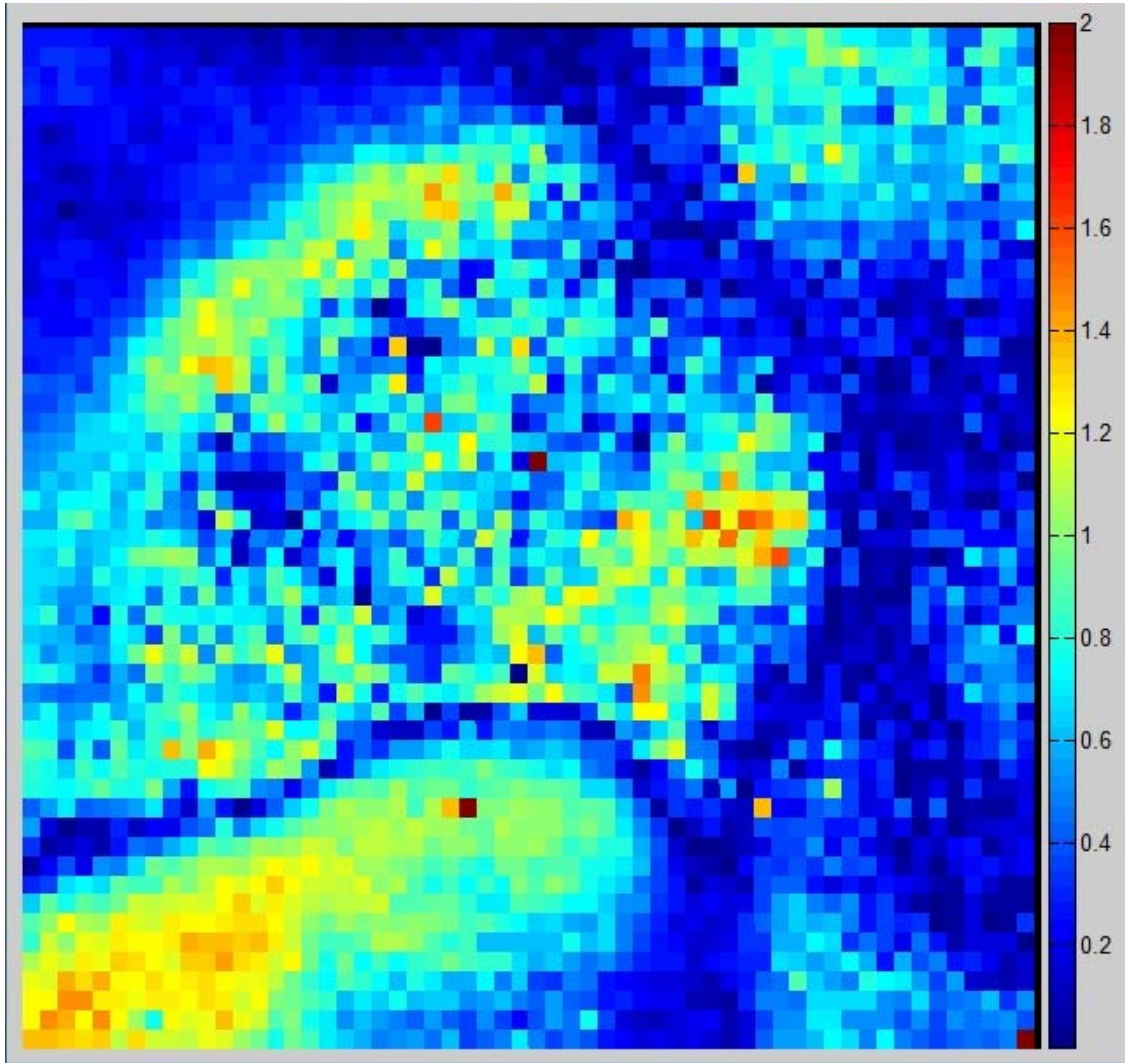


Figure 5-25 Axial gamma analysis (7%/4mm) of third RapidArc treatment delivery

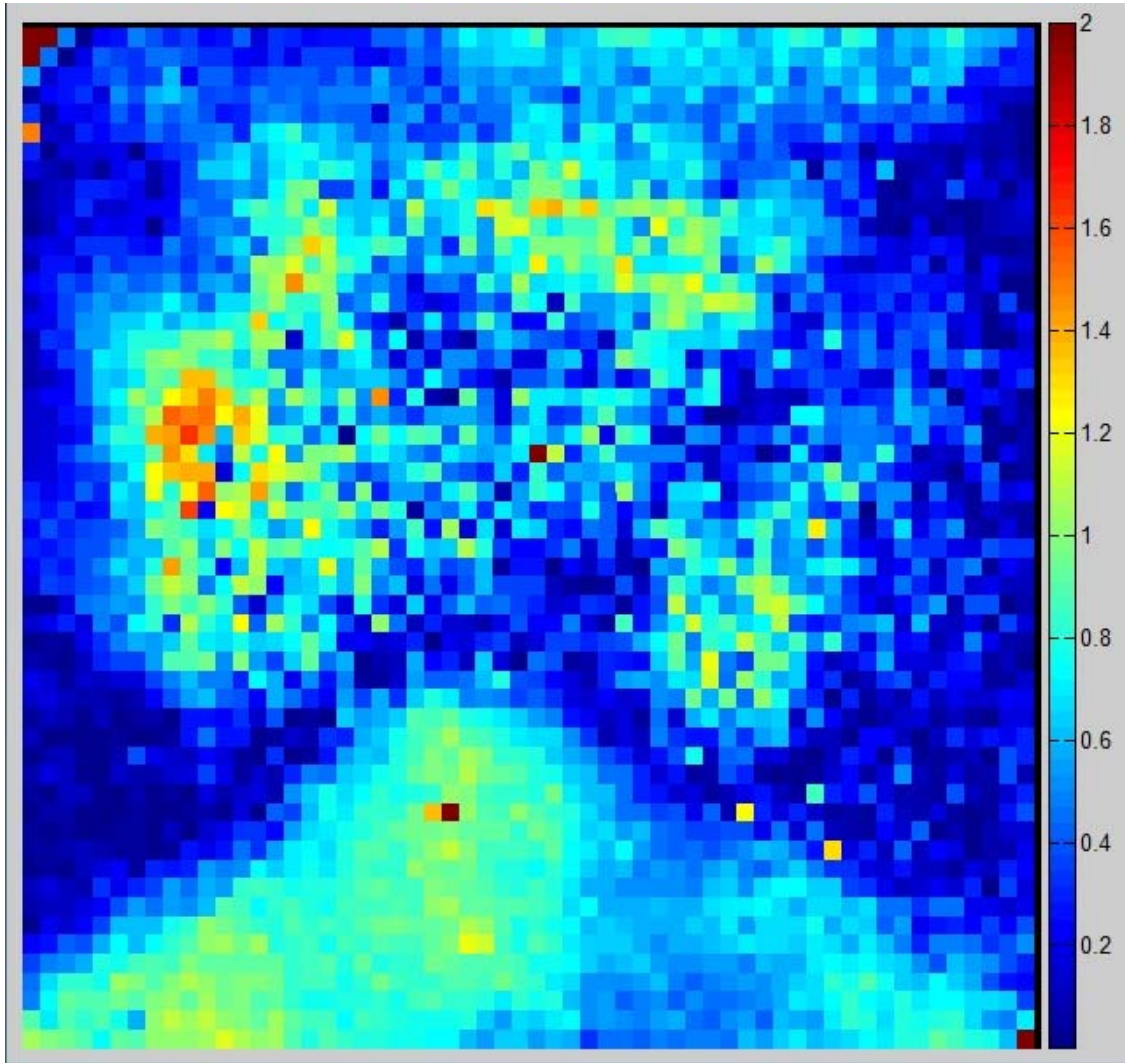
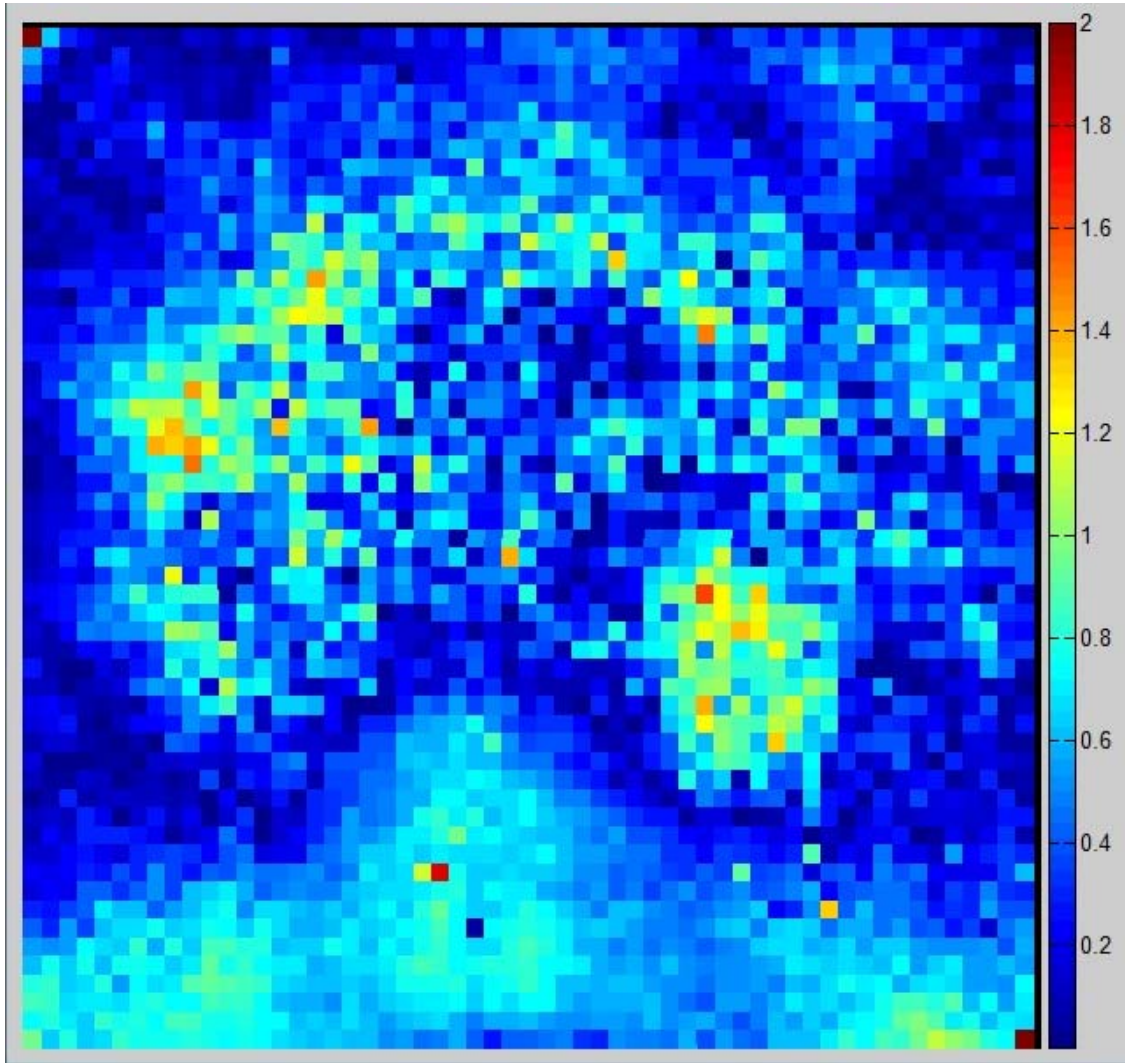


Figure 5-26 Axial gamma analysis (7%/4mm) of first IMRT treatment delivery



**Figure 5-27 Axial gamma analysis (7%/4mm) of second IMRT treatment delivery**

## 5.4 MLC Log File Results

**Table 5-1 The RMS values of leaf deviation (cm) for each moving leaf of both carriages for five deliveries of the first, clockwise arc of the RapidArc treatment**

Leaf	Delivery 1		Delivery 2		Delivery 3		Delivery 4		Delivery 5	
	Carriage A	Carriage B	Carriage A	Carriage B	Carriage A	Carriage B	Carriage A	Carriage B	Carriage A	Carriage B
23	0.027	0.024	0.027	0.024	0.027	0.024	0.026	0.024	0.026	0.024
24	0.044	0.041	0.044	0.041	0.044	0.041	0.043	0.041	0.044	0.041
25	0.051	0.038	0.051	0.038	0.051	0.038	0.051	0.038	0.051	0.038
26	0.043	0.041	0.043	0.041	0.043	0.041	0.043	0.041	0.043	0.041
27	0.047	0.044	0.046	0.043	0.047	0.044	0.046	0.043	0.047	0.044
28	0.044	0.037	0.044	0.037	0.044	0.037	0.044	0.037	0.044	0.037
29	0.043	0.038	0.043	0.038	0.044	0.038	0.043	0.038	0.043	0.038
30	0.043	0.046	0.043	0.046	0.043	0.046	0.043	0.046	0.043	0.046
31	0.046	0.051	0.046	0.051	0.046	0.051	0.046	0.051	0.046	0.051
32	0.036	0.045	0.036	0.044	0.037	0.045	0.036	0.044	0.036	0.044
33	0.035	0.041	0.035	0.04	0.035	0.04	0.035	0.04	0.035	0.04
34	0.038	0.047	0.038	0.047	0.038	0.048	0.038	0.047	0.038	0.048
35	0.04	0.052	0.041	0.052	0.041	0.052	0.04	0.052	0.04	0.052
36	0.031	0.045	0.031	0.045	0.031	0.045	0.031	0.045	0.031	0.045
37	0.031	0.043	0.031	0.043	0.031	0.043	0.031	0.043	0.031	0.043
38	0.024	0.024	0.024	0.023	0.024	0.024	0.023	0.023	0.024	0.024
Average	0.039	0.041	0.039	0.041	0.039	0.041	0.039	0.041	0.039	0.041
Maximum	0.051	0.052	0.051	0.052	0.051	0.052	0.051	0.052	0.051	0.052

**Table 5-2 The RMS values of leaf deviation (cm) for each moving leaf of both carriages for five deliveries of the second, counterclockwise arc of the RapidArc treatment**

Leaf	Delivery 1		Delivery 2		Delivery 3		Delivery 4		Delivery 5	
	Carriage A	Carriage B	Carriage A	Carriage B	Carriage A	Carriage B	Carriage A	Carriage B	Carriage A	Carriage B
23	0.021	0.024	0.022	0.024	0.021	0.024	0.022	0.024	0.021	0.024
24	0.036	0.051	0.036	0.051	0.036	0.051	0.036	0.051	0.037	0.051
25	0.035	0.044	0.035	0.044	0.035	0.044	0.035	0.044	0.035	0.044
26	0.041	0.051	0.041	0.051	0.041	0.051	0.041	0.051	0.041	0.051
27	0.048	0.051	0.048	0.051	0.048	0.051	0.048	0.051	0.048	0.051
28	0.043	0.052	0.043	0.052	0.043	0.052	0.043	0.052	0.043	0.052
29	0.049	0.056	0.049	0.056	0.049	0.056	0.049	0.057	0.049	0.056
30	0.043	0.048	0.043	0.048	0.043	0.047	0.043	0.048	0.043	0.048
31	0.049	0.04	0.049	0.04	0.049	0.04	0.049	0.04	0.049	0.04
32	0.044	0.048	0.044	0.048	0.044	0.048	0.044	0.049	0.044	0.049
33	0.046	0.04	0.046	0.04	0.046	0.041	0.046	0.041	0.046	0.04
34	0.051	0.031	0.051	0.032	0.051	0.032	0.051	0.032	0.051	0.032
35	0.046	0.034	0.046	0.034	0.046	0.034	0.046	0.034	0.046	0.034
36	0.047	0.032	0.047	0.032	0.047	0.032	0.047	0.032	0.047	0.032
37	0.041	0.03	0.041	0.03	0.041	0.03	0.042	0.03	0.041	0.031
38	0.028	0.027	0.028	0.027	0.028	0.027	0.028	0.027	0.028	0.026
Average	0.042	0.041	0.042	0.041	0.042	0.041	0.042	0.041	0.042	0.041
Maximum	0.051	0.056	0.051	0.056	0.051	0.056	0.051	0.057	0.051	0.056



## Chapter 6 Bibliography

1. Yu, C. X. 1995. Intensity-modulated arc therapy with dynamic multileaf collimation: an alternative to tomotherapy. *Physics in Medicine and Biology* 40:1435-1449.
2. Yu, C. X., X. A. Li, L. Ma, D. Chen, S. Naqvi, D. Shepard, M. Sarfaraz, T. W. Holmes, M. Suntharalingam, and C. M. Mansfield. 2002. Clinical implementation of intensity-modulated arc therapy. *International Journal of Radiation Oncology\*Biology\*Physics* 53:453-463.
3. Otto, K. 2008. Volumetric modulated arc therapy: IMRT in a single gantry arc. *Medical Physics* 35:310-317.
4. Oliver, M., W. Ansbacher, and W. A. Beckham. 2009. Comparing planning time, delivery time and plan quality for IMRT, RapidArc and Tomotherapy. *Journal of Applied Clinical Medical Physics*; Vol 10, No 4 (2009).
5. Bedford, J. L., and A. P. Warrington. 2009. Commissioning of Volumetric Modulated Arc Therapy (VMAT). *International Journal of Radiation Oncology\*Biology\*Physics* 73:537-545.
6. Verbakel, W. F. A. R., J. P. Cuijpers, D. Hoffmans, M. Bieker, B. J. Slotman, and S. Senan. 2009. Volumetric Intensity-Modulated Arc Therapy Vs. Conventional IMRT in Head-and-Neck Cancer: A Comparative Planning and Dosimetric Study. *International Journal of Radiation Oncology\*Biology\*Physics* 74:252-259.
7. Rao, M., W. Yang, F. Chen, K. Sheng, J. Ye, V. Mehta, D. Shepard, and D. Cao. 2010. Comparison of Elekta VMAT with helical tomotherapy and fixed field IMRT: Plan quality, delivery efficiency and accuracy. *Medical Physics* 37:1350-1359.
8. Gagne, I. M., W. Ansbacher, S. Zavgorodni, C. Popescu, and W. A. Beckham. 2008. A Monte Carlo evaluation of RapidArc dose calculations for oropharynx radiotherapy. *Physics in Medicine and Biology* 53:7167-7185.

9. Korreman, S., J. Medin, and F. Kj r-Kristoffersen. 2009. Dosimetric verification of RapidArc treatment delivery. *Acta Oncologica* 48:185 - 191.
10. RPC Website. 2008. Radiological Physics Center - RPC Website.
11. Bzdusek, K., H. Friberger, K. Eriksson, B. Hardemark, D. Robinson, and M. Kaus. 2009. Development and evaluation of an efficient approach to volumetric arc therapy planning. *Medical Physics* 36:2328-2339.
12. Molineu, A., D. S. Followill, P. A. Balter, W. F. Hanson, M. T. Gillin, M. S. Huq, A. Eisbruch, and G. S. Ibbott. 2005. Design and implementation of an anthropomorphic quality assurance phantom for intensity-modulated radiation therapy for the Radiation Therapy Oncology Group. *International Journal of Radiation Oncology\*Biophysics* 63:577-583.
13. Kirby, T. H., W. F. Hanson, and D. A. Johnston. 1992. Uncertainty analysis of absorbed dose calculations from thermoluminescence dosimeters. *Medical Physics* 19:1427-1433.
14. Arjomandy, B., R. Tailor, A. Anand, N. Sahoo, M. Gillin, K. Prado, and M. Vicic. Energy dependence and dose response of Gafchromic EBT2 film over a wide range of photon, electron, and proton beam energies. *Medical Physics* 37:1942-1947.
15. Niroomand-Rad, A., C. R. Blackwell, B. M. Coursey, K. P. Gall, J. M. Galvin, W. L. McLaughlin, A. S. Meigooni, R. Nath, J. E. Rodgers, and C. G. Soares. 1998. Radiochromic film dosimetry: Recommendations of AAPM Radiation Therapy Committee Task Group 55. *Medical Physics* 25:2093-2115.
16. Low, D. A., W. B. Harms, S. Mutic, and J. A. Purdy. 1998. A technique for the quantitative evaluation of dose distributions. *Medical Physics* 25:656-661.
17. Molineu, A. 2010. K. Kisling, editor, Houston, TX.
18. van Battum, L. J., D. Hoffmans, H. Piersma, and S. Heukelom. 2008. Accurate dosimetry with GafChromic[trademark sign] EBT film of a 6 MV photon beam in water: What level is achievable? *Medical Physics* 35:704-716

## **VITA**

Kelly Diane Kisling was born in Palm Beach Gardens, Florida on June 16<sup>th</sup>, 1986, the daughter of Karen and Douglas Kisling. In January 2001, she moved to Tolland, Connecticut where she attended Tolland High School and graduated in 2004. She then entered the Georgia Institute of Technology in Atlanta, Georgia. She received the degree of Bachelor of Science in Nuclear and Radiological Engineering in May 2008. In August 2008 she entered The University of Texas Health Science Center at Houston Graduate School of Biomedical Sciences.

Permanent address:  
123 Lakeshore Drive #1245  
North Palm Beach, FL 33408